Thermal Regulation of Human Mesenchymal Stem Cell Differentiation toward Bone and Cartilage Lineages

by

Jing Chen

A dissertation submitted to the Graduate Faculty in Biomedical Engineering in partial fulfillment of the requirements for the degree of Doctor of Philosophy

The City University of New York

2013

This manuscript has been read and accepted for the Graduate Faculty in Engineering in satisfaction of the dissertation requirement for the degree of Doctor of Philosophy.

Professor Sihong Wang

Date | Chair of Examining Committee

Professor Ardie D. Walser

Date | Executive Officer

Professor John M. Tarbell

Professor Luis Cardoso

Professor Susannah P. Fritton

Professor Steven B. Nicoll

Supervisory Committee

THE CITY UNIVERSITY OF NEW YORK

ABSTRACT

THERMAL REGULATION OF HUMAN MESENCHMAL STEM CELL DIFFERENTIATION TOWARD BONE AND CARTILAGE LINEAGES

by

Jing Chen

Adviser: Dr. Sihong Wang

In USA alone, osteoarthritis affects about 70 million people and over 65 billion dollars are spent each year to treat the disease and related conditions. The late stage of joint repair in arthritis patients usually requires to regenerate both cartilage and bone tissues. Human mesenchymal stem cells (hMSCs) are multipotent. Human MSCs seeded with bioengineered scaffolds, combined with growth factors and/or mechanical stress during osteogenesis and chondrogenesis have been intensively studied. However, despite these efforts, the osteoblasts and chondrocytes differentiated from hMSCs are still not as functionally mature as primary adult cells. Thermal regulation of hMSC differentiation may be one of the missing aspects that need to be investigated in terms of further maturation and optimization.

In this study, the direct effects of mild heat shock (HS) on the differentiation of hMSCs into osteoblasts and chondrocytes in self-assembling peptide hydrogel were investigated. Periodic HS at 41^{o}C for 1 hr significantly increased the alkaline phosphatase (ALP) activity and calcium deposition in osteogenic cultures and upregulated osteo-specific genes such as osterix, osteopontin, BMP2 and Runx2. Heat shock protein (HSP) 27, 70 and 90 were also evaluated during differentiation and HSP70

expression was upregulated via heat shock.

For chondrogenic cultures, biochemical analyses showed that periodic HS significantly increased sGAG content at early stage of differentiation in both 3D pellet and hydrogel cultures at Day 10 and 17 respectively. Immunohistochemical(IHC) analyses revealed a more intense staining of chondroitin sulfate proteoglycan in heat-shocked pellets than non heat-shocked pellets on Day 17, but weaker staining of collagen type II on Day 24 in heat treated samples. In summary, these results demonstrate that HS induced a faster differentiation of hMSCs and enhanced the maturation of osteoblasts and chondrocytes differentiated from hMSCs in the early stage. The further maturation of chondrocytes from hMSCs by HS might lead to hypertrophic chondrogenesis. The decrease of chondrogenic markers at late days might correlate with the phenomena similar to the process during endochondral ossification *in vivo*.

The potential of using low-intensity pulsed ultrasound (LIPUS) as a clinically relevant tool to deliver thermal stimulus to hMSCs was investigated. A custom-made LIPUS device with either focused or plane-wave ultrasound transducers was developed to apply heat to hMSCs cultured in a 12-well cell culture plate. A temperature measurement system with thermistors controlled by LabVIEW was built. A hydrophone was used to calibrate the ultrasound intensity distribution. Parameters such as, acoustic intensity (mW/cm^2), duty cycle, and pulse repetition frequency of the input signal were adjusted to achieve the temperature rise in cell culture wells. Further work will be conducted in the future to study thermal effects of ultrasound on hMSC osteogenesis and chondrogenesis. The study will guide the design of an US device for *in vivo* thermal treatments in bone and cartilage regeneration.

ACKNOWLEDGMENTS

First and foremost, I would like to sincerely thank my advisor, Dr. Sihong Wang for all her valuable guidance, endless support, and encouragement. Thank her for leading me into this challenging and interesting research field, and for helping me build the foundation of my future career. Also thank her for understanding and care, without which I would not be able to finish this dissertation. Her incredible enthusiasm and genuine curiosity in science, and her never-stop pursuit of high standards will continue to inspire me even after I leave City College.

Secondly, I would like to thank all my thesis committee members Dr. John Tarbell, Dr. Susannah P. Fritton, Dr. Luis Cardoso, and Dr. Steven B. Nicoll for their advice, guidance, and help along the way. Thank Dr. John Tarbell for his kindness in letting me use his Laboratory for molecular biology experiments. Thank Dr. Steven B. Nicoll for introducing me to his graduate student and providing Laboratory space and equipments for histology during the last year of my research. Thank Dr. Susannah P. Fritton for being my academic advisor in the first year of my study and providing me useful suggestions. Thank Dr. Luis Cardoso for collaboration in my ultrasound research project and valuable discussions. In addition, I want to thank Dr. Jeremy Mao and his lab students at Columbia Medical Center for introducing me hMSC isolation technologies. I also thank Dr. Mitchell B. Schaffler and Damien Laudier for guidance and helping on histology processes of some early samples.

Thirdly, I would like to give my special thanks to my Lab members, Zeynep Dereli Korkut, Pawan KC, Jingwei Zhang, Navneet Kaur, Kris Sunderic, Dr. Chenghai Li, and A.H. Rezwanuddin Ahmed. I also want to thank my colleagues from other lab, Dr. Zhong-Dong Shi, Dr. Xinying Ji, Michelle Gupta, and Dr. Jorge Morales. I enjoyed working with and learning from all of them. For all the technical assistance I received, I would like to thank Dr. Xinying Ji, Dr. Jorge Morales, and Michelle Gupta. I also would

like to thank A.H. Rezwanuddin Ahmed and Dr. Chenghai Li for their efforts in collaboration with some experiments.

Finally, I would like to dedicate this dissertation to my family members, especially thank my Mom for her unconditional love and company, my Dad back in China for love and support, my husband for love and always being there for me, through all these years of Ph.D. study, my baby for his beautiful smile and silent encouragement, and my grandparents who look down upon me from heaven for their everlasting love.

Contents

LIST OF FIGURES

LIST OF TABLES

CHAPTER 1 INTRODUCTION

1.1 Bone Tissue

Bone tissues are remarkable connective tissues. Their functions include providing mechanical supports and storing minerals, especially Ca^{2+} which is needed to maintain homeostasis in a body. Bone differs from other tissues in its greater stiffness and strength due to the deposition of minerals in the bone collagen matrix. There are two major types of bone tissues, namely cortical bone and cancellous (trabecular) bone (**Figure 1.1**). Cortical bone forms most of the outer shell of a bone with variable thickness. The external surface of bone is smooth and called periosteum. The periosteum is a vascularized structure covering most of the external surface of a bone. Cancellous bone generally exists only within the confines of the cortical bone and it is composed of short struts of trabeculae, so that it gives a spongy appearance. Main types of bone cells include osteocytes, osteoprogenitor cells, osteoblasts, and osteoclasts. Osteoprogenitor cells include preosteoblasts and preosteoclasts which respectively are precursors of bone-building osteoblasts and bone-resorbing osteoclasts. Osteocytes are terminally differentiated cells derived from osteoblasts, and are encased in the mineralized matrix with extended cytoplasmic processes interconnecting each other [1, 2].

Bone matrix proteins are composed of 90% of type I collagen and other noncollagenous proteins including osteocalcin, osteopontin, osteonectin, and bone sialoprotein which collectively have calcium-binding activity. And it is known that bone sialoprotein and osteopontin contain the Arg-Gly-Asp (RGD) peptide and thus can mediate attachments of both osteoblasts and osteoclasts to bone matrix [2].

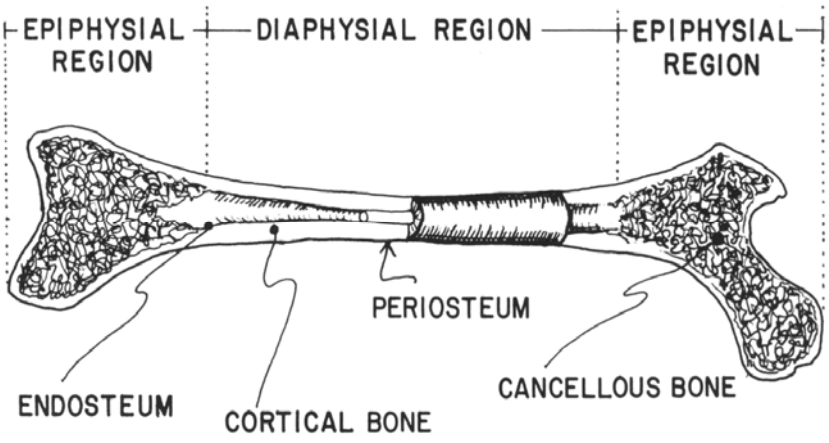

Figure 1.1 Longitudinal section of the femur illustrating two distinct bone types [1].

1.2 Cartilage Tissue

Cartilage is also a connective tissue of musculoskeletal systems. It is avascular and nutrients must be diffused through its extracellular matrix (ECM). Three most important types of cartilage are hyaline cartilage, elastic cartilage, and fibrocartilage. Hyaline cartilage is mostly found in joints covering long bones, typically called articular cartilage. Fibrocartilage can exist temporarily at bone fracture sites and where the hyaline cartilage was damaged. Chondrocytes are the only cells in cartilage tissues. It is sparsely distributed in articular cartilage, responsible for secretion and maintenance of the cartilage ECM. The cartilage matrix is composed of a dense network of type II collagen fibrils in a concentrated solution of proteoglycans (PGs) (**Figure 1.2**). Interactions between collagen II and proteoglycan networks enable cartilage to sustain a large load [1].

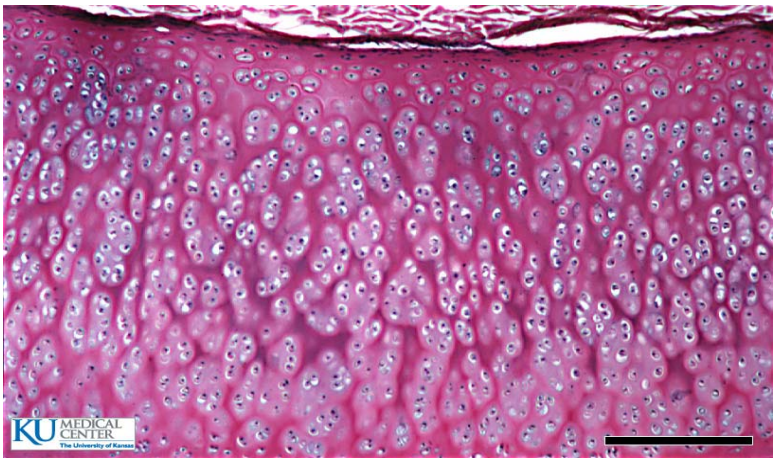

Figure 1.2 A histology picture showing the compositions of hyaline cartilage [1].

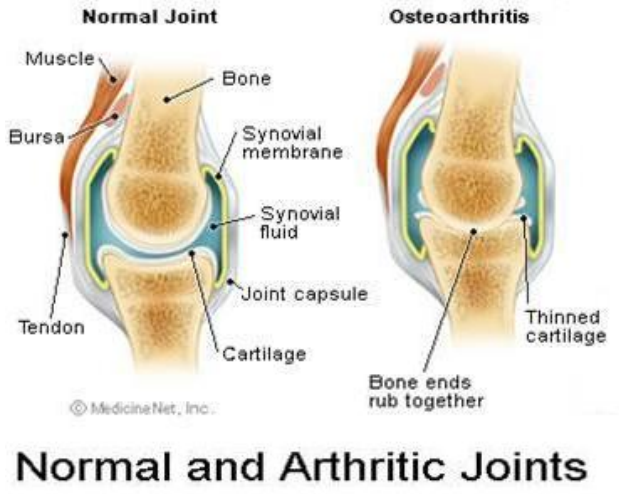

Figure 1.3 A comparison between normal joint and joints with osteoarthritis. Adapted from [1].

Synovial joints are fully articulated joints. They are covered with a thin layer of hyaline cartilage at two opposing bony surfaces. A joint cavity is filled with synovial fluid and lined with synovial membranes. A common disease that can affect cartilage is notably arthritis. One type of arthritis is osteoarthritis (OA) though its exact cause is unknown (**Figure 1.3**). In OA, cartilage breaks down in response to physical stress (wear and tear), and the ends of two bones in the joint may begin to rub together at the late stage of OA [1, 3].

Collagen II molecules in articular cartilage are inhomogeneously distributed, resulting in a layered characteristic. A zonal distribution for the collagen network is shown schematically in **Figure 1.4**. There are four zones, surface, middle, deep and tidemark zones. The tidemark zone is the interface between articular cartilage and calcified cartilage beneath. The amount of collagen decreases in each zone moving closer to bone, and the inhomogeneity of fiber orientation appears to function in a manner to distribute the stresses more uniformly across loaded regions of the joint [1].

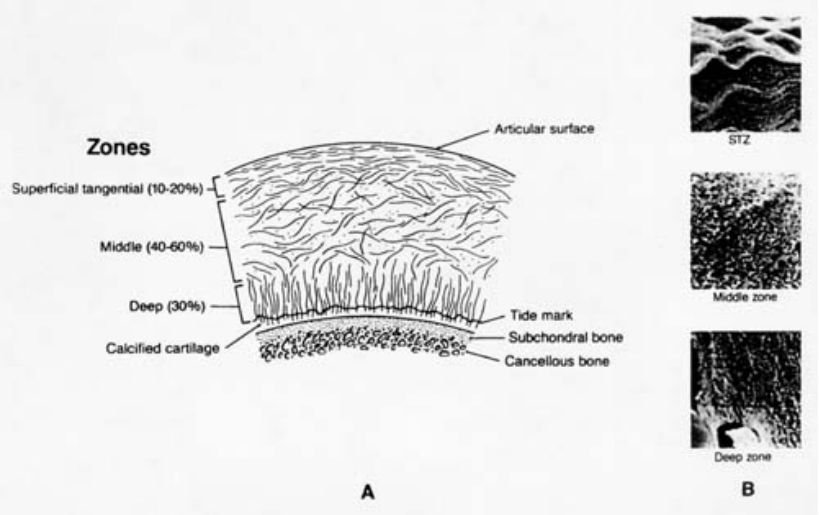

Figure 1.4 The zones contain different collagen organization [1].

1.3 Mesenchymal Stem Cells

"A stem cell is a cell that, when it divides, can produce a copy of itself as well as a differentiated cell progeny" [4]. Stem cells can be classified by their origins into embryonic stem cells (ESCs) and adult stem cells. An adult stem cell is defined as "an undifferentiated cell that is found in a specialized tissue" [5]. Mesenchymal stem cells (MSCs) are one form of adult stem cells and defined as self-renewable, multipotent progenitor cells with a capacity to differentiate into several distinct mesenchymal lineages [6]. MSCs can be easily explanted ex vivo and current protocols for expansion of MSCs have been adequately optimized to generate sufficient

cell numbers for therapeutic applications. Nevertheless, the major inherent disadvantage of MSCs is their limited life-span and proliferative potential especially seen in elder patients. Another disadvantage is the heterogeneity of the putative MSCs population, and the scarcity of distinguishing markers that would identify them as true stem cells [7].

MSCs have been isolated from bone marrow (BM) and other tissues, such as periosteum, trabecular bone, adipose tissue, synovium, skeletal tissue, and deciduous teeth [8]. They can be differentiated into several tissue-forming cells like osteoblasts, chondrocytes, myoblasts, adipocytes, and fibroblasts. They also express some of key markers typically existing in endothelial cells, neuron-like cells, and cardiomyocytes [9] (**Figure 1.5**). Currently bone marrow is a rich and the most characterized source of MSCs, MSCs from bone marrow represent a very small fraction (0.001-0.1%) of the total population of nucleated cells and they play a supporting role for hematopoietic stem cells (HSCs) [8, 10].

The first successful isolation of fibroblast-like colonies from bone marrow, i.e., MSCs, was described about 4 decades ago by Friedenstein et al. [11, 12]. Human mesenchymal stem cells (hMSCs) are generally isolated from an aspirate of bone marrow harvested from the superior iliac crest of pelvis. An isolation was based on the adherence of fibroblast-like cells to plastic (polysterene) cell culture plates, and non-adherence of hematopoietic cells. To date, this procedure is considered as a widely-used standard protocol to isolate BM MSCs. However, only part of the adherent cells are indeed MSCs if they are demonstrated to differentiate into multiple cell lineages. Since the adherent population tends to form colonies of spindle-shaped cells, this procedure was called colony-forming unit-fibroblast (CFU-F) assay.

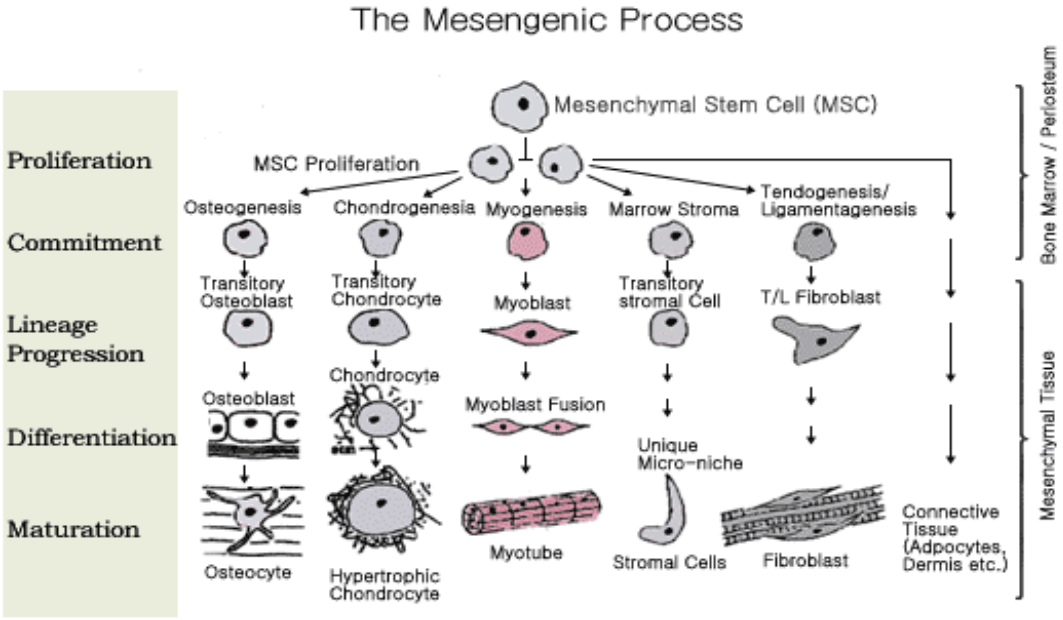

Figure 1.5 Multilineage potential of adult mesenchymal stem cells (MSCs) [13].

Other isolation protocols were based on the process of negative selection, in which cells lacking expressions of endothelial (CD31) and hematopoietic cell markers (CD14, CD34, CD45 etc.) are sorted out by flow cytometry and maintained as primary cultures. Besides, the first antibody (Stro-1) capable of providing positive identification of BM-derived MSCs was available [14]. The phenotypic identity of MSCs is not unique, sharing features of multiple cell lineages. Initial cultures of adherent MSC population have been labeled by a panel of antibodies targeting a wide range of cell-surface antigens and peptides such as SH2 (CD105), SH3, SH4 (CD73), SB-10, and so forth [8].

MSCs-based therapeutic approaches may circumvent the deficiencies associated with autograft as for providing enough cell sources. Its multilineage differentiation ability makes it possible to heal many tissues as well. MSCs or MSCs-derived cells can alternatively be seeded into biocompatible scaffolds, shaped into the anatomical structure of target tissues and consequently the construct can be implanted to repair damaged or diseased tissues [9].

1.4 Osteoblastic and Chondrogenic Differentiation of MSCs

Osteogenic differentiation requires a well-explored cocktail containing dexamethasone, β-glycerophosphate, and ascorbic acid-2-phosphate (AsAP) [8]. Dexamethasone is a glucocorticoid steroid capable of stimulating osteogenic differentiation of MSCs at lower doses; AsAP further facilitates osteogenic differentiation in which ascorbic acid is the bioactive component; β-glycerophosphate is critical to stimulate calcium deposition [9]. In the presence of all these, MSCs acquire an osteoblastic morphology with upregulation of alkaline phosphatase (ALP) activity as an early indicator, and deposition of a mineralized matrix can be histologically verified using von Kossa (silver nitrate) stain. Type I collagen is a non-specific marker as well, while bone sialoprotein, osteocalcin, osteopontin, and osteonectin are useful late osteogenic differentiation markers. Chondrogenic differentiation occurs when MSCs are grown under conditions (1) 3D culture, (2) serum-free medium, and (3) one of the transforming growth factor-β (TGF-β) family supplemented [8]. Also, selected bioactive factors and chemicals are added. MSCs lose their fibroblastic morphology and begin to initiate synthesis of cartilage-specific ECMs like glycosaminoglycan (GAG) detectable using a histological stain Safranin O. Chondrogenic differentiation markers include collagen type II, and various proteoglycans such as aggrecan [8, 9] (**Figure 1.6**). In 2D culture, there is a tendency for differentiated chondrocytes to dedifferentiate and/or transdifferentiate into fibroblasts. Thus approaches such as pellet culture, or 3D scaffolds culture using alginate, agarose, or poly (ethylene glycol) diacrylate (PEGDA) hydrogel are frequently used. Mechanical testing of either tissue-engineered bone or cartilage is of paramount importance. Because they are designed to withstand mechanical stresses, the proper mechanical properties are much needed besides the “right ingredients” as well as the “right” structural characteristics [9].

Lineage-specific gene expression is ultimately under the regulation of transcription factors. They act as the key switching mechanisms to induce gene transcription. Transcription factors Cbfa-1/Runx-2, osterix, and TAZ are all absolute requirements for osteoblast differentiation. TAZ, mediates the osteoblastic commitment of MSCs; while Cbfa-1/Runx-2 and osterix both occur late in the osteoblast lineage scheme [2]. Chondrogenic differentiation is also driven by transcription factors from the SOX family. Sox-9 expression is required for chondrogenic differentiation and it is expressed in differentiating chondrocytes. Sox-5 and Sox-6 are also expressed during chondrogenic differentiation [9].

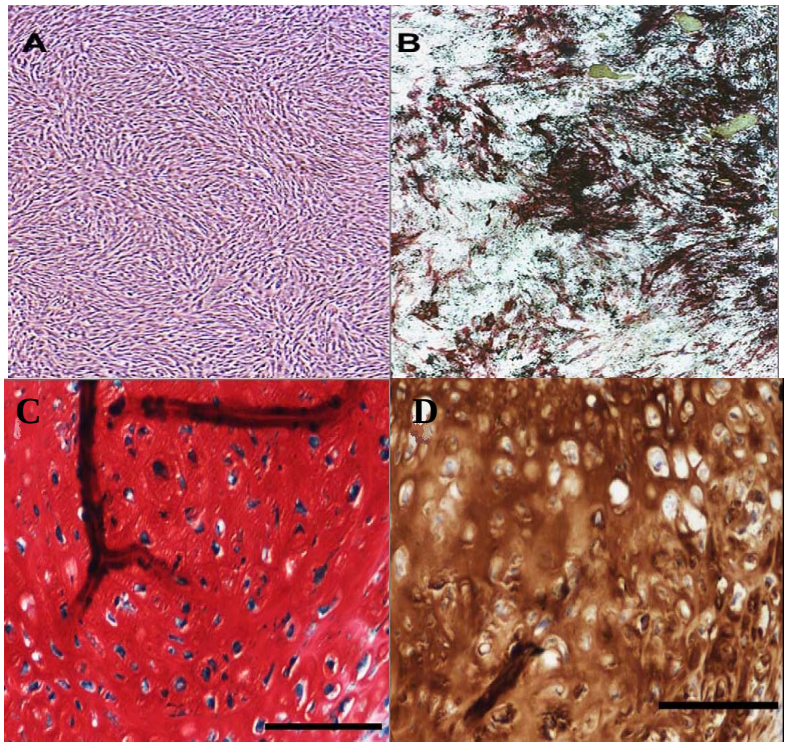

Figure 1.6 (A) Undifferentiated MSCs grown in culture; **(B)** Differentiation along the osteogenic lineage; **(C) & (D)** Differentiation along the chondrogenic lineage; Differen-tiation was observed following staining with von Kossa **(B)** Safranin O **(C)** immuno-staining for type II collagen **(D).** Adapted from [8].

1.5 PuraMatrix™

For mesenchymal cells (e.g. osteoblasts, chondroblasts) that use proteolysis for migration, a multi-layer network provided by hydrogel would likely be most representative of the 3D environment experienced by these cells *in vivo* [15]. The reason of using synthetic hydrogel instead of natural product-based hydrogel (e.g. collagen, Matrigel) in this project is that collagen or Matrigel has considerable batch-to-batch property variations and unknown growth factors. In addition, Matrigel, which is derived from sarcoma grown in mice, has potential tumorigenicity and immunogenicity. Those factors limit their use for therapeutic applications.

Therefore, we used a well-defined synthetic hydrogel biomaterial known as PuraMatrix^{TM} that can promote cell attachment and migration for the MSC differentiation studies. PuraMatrix™ is a new synthetic material discovered by Dr. Zhang in 1992 [16]. It is a self-assembling synthetic peptide scaffold, consisting of a 16-amino acid sequence (AcN-RADARADARADARADA-CNH2). Four RADA (arginine-alanine-aspartate) repeats in PuraMatrix™ are similar to the ubiquitous integrin receptor binding site RGD (arginine-glycine-aspartate) sequence. Cell attachment has been studied across a number of cell types using PuraMatrix. PuraMatrix™ self-assembles in the presence of cation to form beta-sheet polymers, and further to form hydrogel containing ≥ 99% water. The fiber and pore sizes of PuraMatrix™ are 10-20 nm and 50-200 nm, respectively, which are similar to those of the *in vivo* extracellular matrix [17]. There have been reports on the applicability of PuraMatrix™ on cultured cells such as the nerve [18, 19], cartilage [20], liver [21, 22], heart [23, 24], and vascular endothelial cells [24].

Recently, the osteoconductive ability of PuraMatrix™ was investigated on bone regeneration in a mouse calvaria defect model. The expression of bone-related genes was higher

in the tissues at the site of defects treated with PuraMatrix™ than that with Matrigel™. The bone defect treated with PuraMatrix™ was uniformly filled with the newly formed bone tissues showing higher density and strength [17]. Osteogenic and chondrogenic differentiation potentials of MSCs in PuraMatrix™ were also studied in two newly published papers. However, the findings from the first incomplete study only showed that rat MSCs can be viable, differentiate into osteoblasts and form mineralized matrices within the hydrogel scaffold [25]. In the latter study, preliminary studies using hMSCs embedded in PuraMatrix™ demonstrated a pronounced chondrogenic differentiation compared to control pellet culture. The chondrogenesis was enhanced in PuraMatrix™ and marked increase in mechanical properties was observed in long-term culture [26]. In summary, it was shown that PuraMatrix™ can serve as an excellent scaffold to promote differentiation and functions of many types of cells. PuraMatrix™ provides a nanofibrous 3D scaffold for cell encapsulation. Therefore, it can be considered as an attractive synthetic biomaterial for bone and cartilage tissue engineering.

1.6 Heat Shock Proteins (HSPs)

Heat shock proteins are major stress proteins which are upregulated in response to stresses. Main heat shock proteins include HSP90, HSP 70, HSP 60 and the group of small heat shock proteins. HSPs serve as a defense for cells against sub-lethal stresses including hyperthermia, and also function as molecular chaperones in unstressed cells. Endogeneous HSPs can be upregulated by externally controlled stresses so that chaperon functions are enhanced. HSPs can also be induced by a mild stress to provide protection to cells and tissues against subsequent severe or lethal stress. The overexpression of HSPs is a transient phenomenon with a time constant (~several days) and the process consists of a progressive rise to maximum, followed by a temporary period of elevation, and subsequently a decline to normal levels [27]. Heat shock

transcription factors (HSFs) are essential for induction of the heat shock response (HSR). Upon stress, HSF is released from inactive state, translocates to the nucleus and binds to heat shock elements (HSE) finally resulting in transcription of HSPs [28]. HSPs may then bind to the surfaces of adjacent cells and initiate signal transduction as well as the transport to distant immune cells [29].

1.7 Previous Studies on Heat Shock Effects on Cell Differentiation

Temperature is a crucial physical factor in general growth processes. Early studies have indicated that heat (1.5-3^{o}C above normal) stimulates bone growth and embryonic development of animals. Local temperature rise at bone fracture sites was observed to be closely related with new bone formation. Hyperthermia may improve blood supply and therefore influence bone metabolism. Local bone diathermy to repair bone injury has been investigated in animals but their mechanisms are unclear. Thus, direct effect of temperature on the differentiation of human bone marrow-derived stromal cells (BMSCs) in culture conditions was investigated in a pioneering study. Cells were exposed to either mild heat shock conditions (1h at 39-45^{o}C), or continuous 96-h exposure to 39-41^{o}C. Differential heat shock effects on cell differentiation were found at different temperatures. Results showed that a mild heat shock induces the differentiation of osteoprogenitor cells. HSPs may also have important roles in osteoblast physiology [30]. Following this study, two more recent studies further investigated the heat shock effects on osteoblastic differentiation of MSCs. One of them used a telomerase-immortalized hMSC line (hMSC-TERT). Cells were exposed to 1h HS at 41 ^{o}C, 42.5 ^{o}C, or 44 ^{o}C using a water bath prior to further experiments. The results suggest that an 1-h HS of 42.5 ^{o}C is the most beneficial pretreatment to the hMSC-TERT cells as it enhances the differentiation of hMSCs. The exact mechanisms are still in a progress to be elucidated [31]. Interestingly, another study used

conditioned media from heat shock-treated (42^{o}C for 1h) human fetal osteoblast (hFOB) cells to promote the osteogenesis of rabbit MSCs, without exposing the MSCs directly to heat shock. It provides clear evidence of a synergistic effect of conditioned media, heat shock and chemical stimuli on the osteogenesis of MSCs [7].

CHAPTER 2 ENHANCED OSTEOGENESIS OF HUMAN MESENCHYMAL STEM CELLS BY PERIODIC HEAT SHOCK IN SELF-ASSEMBLING PEPTIDE HYDROGEL

2.1 Introduction

In USA alone, osteoarthritis (OA) affects about 70 million people and over 65 billion dollars are spent each year to treat the disease and related conditions [32]. In clinical therapy for bone diseases, bone graft is often used to fill bone defects and promote bone regeneration. An autograft represents the current "gold standard" of bone graft; however, it is associated with problems such as, limited number of donors and donor site trauma and morbidity [9]. Allograft is used as an alternative but also has inherent risks including disease transmission, and altered biomechanical strength [33]. Ceramic artificial bones can offer good strength, but they cannot provide adequate environment for cell penetration and settlement deeply inside of the bone defects [17]. In addition, the drawback of both is a lack of physiological remodeling that must take place over postsurgical years [3]. Therefore, for functional bone tissue engineering, cells seeded with bioengineered scaffolds that are biodegradable, biocompatible, osteoconductive and osteogenic are being investigated [25, 34-37].

Human mesenchymal stem cells (hMSCs) have the potential to differentiate into a variety of cell types including osteoblasts, chondrocytes, and adipocytes, and they can also express key markers of endothelial cells and cardiomyocytes [9, 14]. Intensive studies have been done on influences of growth factors [38], cytokines [2], or mechanical loading [39] on MSC differentiation into osteoblasts. However, the osteoblasts differentiated from MSCs are still not as functionally mature as primary adult cells. Further maturation and optimization of

differentiation is needed. Temperature has an important impact on bone growth *in vivo*. It may be one of the missing factors in the regulation of the MSC differentiation.

Local diathermy can promote the bone repair after injury *in vivo*. Local hyperthermia (38^oC-41^oC) treatment induced the new bone formation in rats following mechanical expansion at the sagittal suture [40]. Hyperthermia is used as a thermotherapy for musculoskeletal diseases. It improves blood supply, therefore may influence bone metabolism and accelerate local bone formation [41]. Microwave heating on the joints of animal osteoarthritis models inhibited the progress of cartilage damage [42]. The localized heat that applied to articular joints likely involves the direct heating of chondrocytes, osteoblasts and osteoprogenitor cells. Early studies have indicated that heat (1.5~3^oC above regular body temperature) stimulates bone growth and embryonic development of the animals [43, 44]. In addition, local temperature rise at bone fracture site was observed to be closely related with new bone formation [45]. However, very few studies have been conducted to investigate thermal effects on bone marrow stem cell differentiation into osteoblasts, and their results in terms of alkaline phosphatase activities and calcium deposition varied from time to time during differentiation [30]. In another study, conditioned media from heat shock-treated human fetal osteoblast (hFOB) cells were able to promote the osteogenesis of rabbit MSCs [7]. Most of previous studies focused on the effects on cell lines such as telomerase-immortalized hMSC line (hMSC-TERT) [31] or osteosarcoma-derived cell lines [46]. All the previous studies were performed using 2-dimensional (2D) culture configurations. The exact mechanism of thermal-induced bone growth is unclear. Whether thermal-regulation plays a role in adult stem cell differentiation is also not well studied, especially in 3D culture environment.

In this study of hMSC osteogenesis under the thermal stimulation, synthetic peptide hydrogel, 0.25% PuraMatrix with storage modulus of 2.5 kPa [47] at 0.5%, and conventional 2D tissue culture plates with Young's modulus of 3.5 GPa [48] were chosen as 3D culture matrix and 2D culture substrates respectively. These two substrates would better mimic the mechanical environment that bone marrow MSCs experience *in vivo* while they migrate from bone marrow niche (storage modulus of 0.2 kPa [49]) and differentiate into osteoblasts for bone (Young's modulus of 9 GPa [48]) repair. The peptide of PuraMatrix consists of a 16-amino acid sequence (RAD16-I, AcN-RADARADARADARADA-$CONH_2$) and can self-assemble in the presence of cations in physiological solutions to form 3D interweaving nanofiber scaffold containing over 99% of water [16]. The fiber diameter and pore sizes in the hydrogel are about 10 nm and 50-200 nm respectively. PuraMatrix promotes cell attachment and migration across a number of cell types [19, 50]. Cellular phenotypes have been studied in PuraMatrix culture using hepatocytes [21, 22], chondrocytes [20], osteoblasts [51], and MSCs [52, 53]. In addition, the osteoconductive ability of PuraMatrix was investigated on bone regeneration in a mouse calvaria defect model [17]. It was also shown to be a potential biomaterial to fill in the bone defect through injection *in vivo* [54].

Our preliminary study using only one heating cycle did not show significant HS-enhancement on osteogenesis. Therefore, periodic heat shock was used to have prolonged thermal effects on the MSC differentiation during 4 weeks. Considering the elevated body temperature (~39^{o}C) during exercise [55] and knowing a common recommendation to OA patients from Arthritis Foundation is to take a daily hot shower, once-a-week heating at 41ºC was chosen in this study to provide enough heat stimulation. Osteogenesis was measured by alkaline phosphatase activities, quantitative calcium deposition, and gene expressions of

osteogenic markers. Results of this study would validate a suitable heating protocol for MSC osteogenesis and thus benefit further investigations of using thermal treatments for bone regeneration *in vivo*.

2.2 Materials and Methods

All reagents and chemicals without manufacture labels were purchased from Sigma-Aldrich (St Louis, MO). hMSCs were isolated from human bone marrow and then characterized by FACS analysis. Cells were seeded in 2D culture plates or 3D PuraMatrix gel, and exposed to 1hr HS at 41 ^{o}C once a week during osteogenic differentiation. Cell morphology and cell-cell as well as cell-matrix interactions on hydrogel scaffold were analyzed by SEM, and calcium deposits from the cells were localized by calcium x-ray spectrum. The analysis of induction of osteogenic differentiation and the extent of mineralization was also performed using quantitative alkaline phosphatase(ALP) and calcium assays, respectively. The gene expression of the osteo-specific markers was measured by real-time PCR and heat shock proteins (HSP27, HSP70, HSP90) expression was further determined by Western blot analysis.

Isolation and Culture of Bone Marrow hMSCs

Human bone marrow (BM) from the iliac crest of a 27-year-old donor was purchased (AllCells LLC, Berkeley, CA). Mononuclear cells were enriched and retrieved with RosetteSep MSC enrichment cocktail (StemCell Technologies, Vancouver, Canada) according to manufacturer's instructions, then cultured in tissue culture flasks with MSC growth medium (MSCGM) consisting of Dulbecco's modified Eagle's medium-low glucose, 10% fetal bovine serum (FBS) (Atlanta Biologicals, Lawrenceville, GA), and 1% penicillin-streptomycin (Invitrogen, Carlsbad, CA) in an incubator at 37^{o}C with 5% CO_2. Subculture was performed at a density of 5000 cells/cm^2. Passage 4 MSCs were used in this study.

Characterization of hMSCs by Surface Markers and Flow Cytometry

Isolated hMSCs at the concentration of 10^6 cells/ml in MSCGM were incubated with mouse anti-human antibodies (BD Biosciences, San Jose, CA). Samples were either double stained with a pair of antibodies such as the negative control pair of IgG-PE (phycoerythrin)&IgG-FITC (fluorescein isothiocyanate), CD45-FITC&CD44-PE, CD147-FITC&CD29-PE, CD147-FITC&CD34-PE, or single stained with CD146-PE for 20 min at room temperature. The cells were analyzed on a FACSCalibur flow cytometer (BD Biosciences) with adjusted fluorescence compensation setting and processed on the same machine. Negative control samples were used to set up the thresholds of quadrant markers.

Assembling of Peptide Hydrogel and Cell Seeding

PuraMatrix (BD Biosciences) was assembled using MSCGM following the manufacturer's protocol in 24-well plates, 300 μL of 0.25% (w/v) gel per well. Cell seeding densities were 10^4 hMSCs per well for 2D culture and 4×10^4 hMSCs per well for 3D PuraMatrix culture using surface seeding. Osteogenic differentiation was induced with osteogenic medium the day (Day 0) after seeding and was used for control cultures. Osteogenic medium consists of MSCGM supplemented with 50 μM ascorbic acid phosphate (AsAP) (Wako Chemicals USA, Richmond, VA), 0.1 μM dexamethasone and 10 mM β-glycerol phosphate. The medium was changed every 3-4 days.

Heat Exposure

Human MSCs in osteogenic(OS) cultures were exposed to mild heat shock (HS) periodically on Day 3, 10, 17, and 24. The transient 1 hour heating at 41^oC was performed using a cell culture incubator pre-calibrated with an accuracy of $\pm 0.2^oC$. Choosing 41^oC as the heating temperature was based on a previous study that repeated 1-hr exposure to 41^oC once every 3

days generated highest ALP activities and calcium deposition in hMSC 2D culture compared to 39^{o}C or 42.5^{o}C [30]. The medium was changed after heating and the cells were back to the 37^{o}C incubator. The control samples stayed in the 37^{o}C incubator while the medium was changed at the same time as the heat shocked samples.

Differentiation and Visualization of Minerals

The morphology changes of hMSCs in different culture conditions were observed by phase microscopy using a Zeiss Axio Observer Z1 Inverted microscope. Von Kossa staining was used to visualize mineralization on Day 24 [56]. Briefly, hMSCs were rinsed with Tyrode's balanced salt solution, fixed with 10% buffered formalin (Fisher Scientific, Pittsburgh, PA) for 30 min, incubated with 2% silver nitrate solution for 10 min in the dark, rinsed with ddH_2O, and exposed to light for 15 min. Bright-field images of stained samples were captured with a Zeiss Axiovert 40 CFL inverted microscope.

Surface Morphology of 3D Culture and Calcium Localization

To study the detailed surface morphology of hMSCs on PuraMatrix, Scanning Electron Microscopy (SEM) was used. Lab-Tek chambered coverglass (Thermo Fisher, Rochester, NY) was used to culture hMSCs (4×10^4 cells/well) on 0.25% PuraMatrix for SEM analysis. On Day 26, samples were fixed in 4% glutaraldehyde (Electron Microscopy Sciences, Hatfield, PA) overnight at 4^{o}C, followed by ethanol dehydration, and critical point drying. Samples were then sputter-coated with 10 nm of gold-palladium or carbon coated with a carbon thread evaporator. The gold-coated samples were examined under Supra 55 VP (Carl Zeiss MicroImaging, Thornwood, NY) using the in-lens detector at 5 kV to collect secondary electron (SE) images [57]. The carbon-coated samples were analyzed by Energy Dispersive x-ray Spectrometry (EDS) at 15 kV using the Apollo 40 EDAX detector to generate calcium X-ray spectrum.

Quantitative Alkaline Phosphatase (ALP) Assay

Samples were lysed with 300 µl of ALP lysis buffer, 0.5% Triton X-100 (Bio-Rad Laboratories, Hercules, CA), on Day 6 and 12 during differentiation. The hydrogel samples were homogenized with pipetting and sonicated for 10 min. The samples were vortexed and incubated with Alkaline Buffer solution and phosphatase substrate solution at 37^{o}C for 15 min [58]. The ALP activity in nmol/min was calculated by comparing samples' absorbance of p-nitrophenol product at 405 nm with that of p-nitrophenol standards using SpectraMax M2e microplate reader (Molecular Devices, Silicon Valley, CA). The statistical comparison was drawn between heat shocked and non-heat shocked osteogenic samples.

Calcium Quantification

Samples for calcium deposition assay were collected on Day 19 and 27 during differentiation using 0.5N HCl. Calcium was extracted from the cells by shaking the samples on an orbital shaker for 4 hours at 4^{o}C, followed by centrifugation at 500g for 2 min. The supernatant was collected for calcium determination according to instructions provided in Calcium Liquicolor kit (Stanbio Laboratory, Boerne, TX). Absorbance was read at 550 nm. Total calcium amount in µg/well was calculated by comparing to the standard curve.

Gene Expression Measured by Real-time Reverse Transcription-Polymerase Chain Reaction (RT-PCR)

Total RNA was extracted from hMSC samples on Day 11, 19, and 25 during osteogenesis using TRIzol Reagent (Invitrogen, Carlsbad, CA) and RNeasy Mini kit (Qiagen, Valencia, CA) following manufacturer's instructions, and used to synthesize cDNA with Cells-to-cDNA II kit (Ambion, Austin, TX), followed by real-time PCR analysis in ABI Prism 7000 Sequence Detection System (Applied Biosystems, Foster City, CA). **Table 2.1** includes RT-PCR

primers of osteogenic genes, bone morphogenetic protein 2 (BMP2), osteopontin (OP), Runx2, osterix (OSX) ordered from Integrated DNA Technologies (Coralville, Iowa). Glyceraldehyde-3-phosphate dehydrogenase (GAPDH) was used as an internal control. The thermal profile for all reactions was 95^{o}C for 10 min, followed by 45 cycles at 95^{o}C for 15s, 55^{o}C for 35s, and 72^{o}C for 35s. Relative expression levels in heat shocked or non-heat shocked osteogenic samples were calculated as an average of the ratio, to the value of that of undifferentiated cells for a specific gene on individual days after normalization with GAPDH.

Table 2.1. Primer sequences for real-time RT-PCR.

Gene		5' to 3' sequence	Amplicon size (bp)
BMP2	Forward Reverse	CATGCCATTGTTCAGACG TGTACTAGCGACACCCACA	172
Osteopontin	Forward Reverse	ACCCTTCCAAGTAAGTCC TGTCCTCGTCTGTAGCAT	349
Runx2	Forward Reverse	AAATCGCCAGGCTTCATA CTGCCAGGAGTGGTCAAA	447
Osterix	Forward Reverse	CCTGCGACTGCCCTAATT GCGAAGCCTTGCCATACA	123
GAPDH	Forward Reverse	GGATTTGGTCGTATTGGG GGAAGATGGTGATGGGATT	205

Heat Shock Protein (HSP) Detection by Western Blot and ELISA

Samples were lysed at 24 hrs after heat shock on Day 4, 11, 18 and 25 during differentiation. Cells in PuraMatrix culture were extracted first from gel following the manufacturer's instruction before cell lysis. Lysis buffer for 3D culture contains 1% SDS, 50 mM Tris-HCl, 5 mM EDTA, and protease inhibitors, while 2D culture samples were lysed with 1X extraction buffer of HSP70 EIA kit (Assay Designs, Ann Arbor, MI) supplemented with protease inhibitors. Cell lysate of 3D culture was briefly sonicated. The cell lysate was then centrifuged at 21,000g for 10 min at 4^{o}C and supernatant was collected for Western blot or ELISA. Total protein concentration was determined by Bio-Rad protein assay kit. 10% Tris-

HCl Ready Gel and polyvinylidene fluoride (PVDF) membranes (Bio-Rad Laboratories) were used. The primary antibodies were monoclonal mouse anti-human HSP27 (Assay Designs), HSC70&HSP70, HSP90 (Santa Cruz Biotechnology, Santa Cruz, CA), and actin (Millipore, Billerica, MA). The secondary antibody was horseradish peroxidase (HRP) conjugated goat anti-mouse IgG (Assay Designs). Tetramethylbenzidine (TMB) substrate kit (Vector Laboratories, Burlingame, CA) was used to visualize the protein bands. Membranes were dried and scanned into digital images. Protein bands were analyzed quantitatively using Quantity One software (Bio-Rad Laboratories). The HSP expression was presented as a ratio of total intensity of HSPs normalized by that of actin after global background subtraction to equalize the total protein loading for each sample.

The concentrated protein samples of 2D culture were also used for inducible HSP70 measurement. The 3D protein samples collected were buffer-exchanged using both Amicon Ultra-4 and Ultra-0.5 Centrifugal Filter columns (Millipore) so that SDS concentrations in the final lysate would be compatible with commercial HSP70 EIA kit. HSP70 ELISA was performed following the manufacturer's instruction. HSP70 expression in ng/mg was presented as a ratio of the HSP70 concentration normalized by the total protein concentration of the same sample.

Statistical Analysis

All values were expressed as mean ± standard deviation (SD) and analyzed statistically using a two-tailed Student's t-test. The level of significance was set at $p<0.05$.

2.3 Results

Expression of Surface Markers in Isolated hMSCs

In **Figure 2.1**, flow cytometric analysis shows that passage 4 of isolated hMSCs was over 80% positive for surface markers of CD44 (hyaluronan receptor), CD29 (integrin β1), and

CD147 (extracellular matrix metalloproteinase inducer), slightly positive for CD146 (melanoma cell adhesion molecule), and more than 90% negative for CD45 (leukocyte common antigen) and CD34 (lipopolysaccharide receptor). CD34 and CD45 are surface markers of the hematopoietic lineage, and CD146 is the surface marker of endothelial cell lineage, an epitope suggested as a biomarker for MSCs.

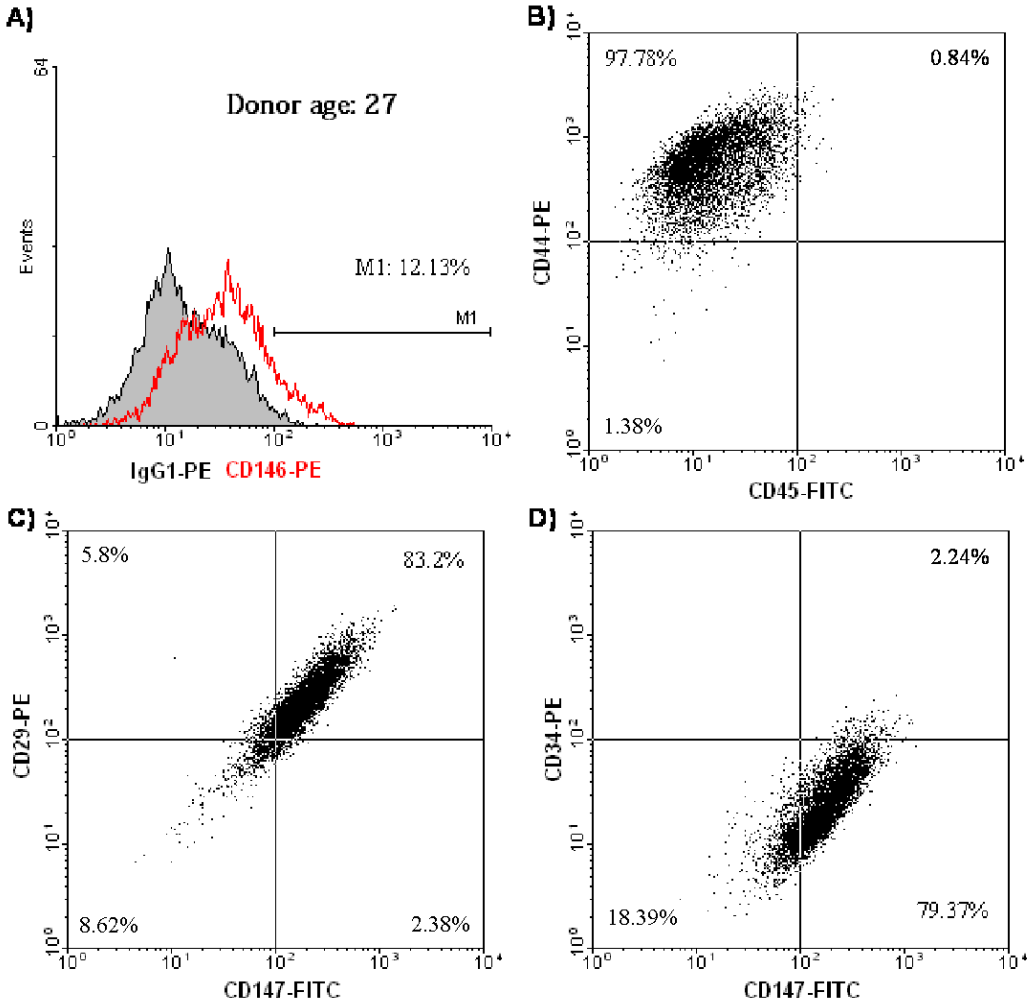

Figure 2.1. Characterization of hMSCs by flow cytometric analysis. Isolated hMSCs were positive to surface markers CD146, CD44, CD29, and CD147, and negative to CD45 and CD34.

Morphological Changes during Differentiation of hMSCs

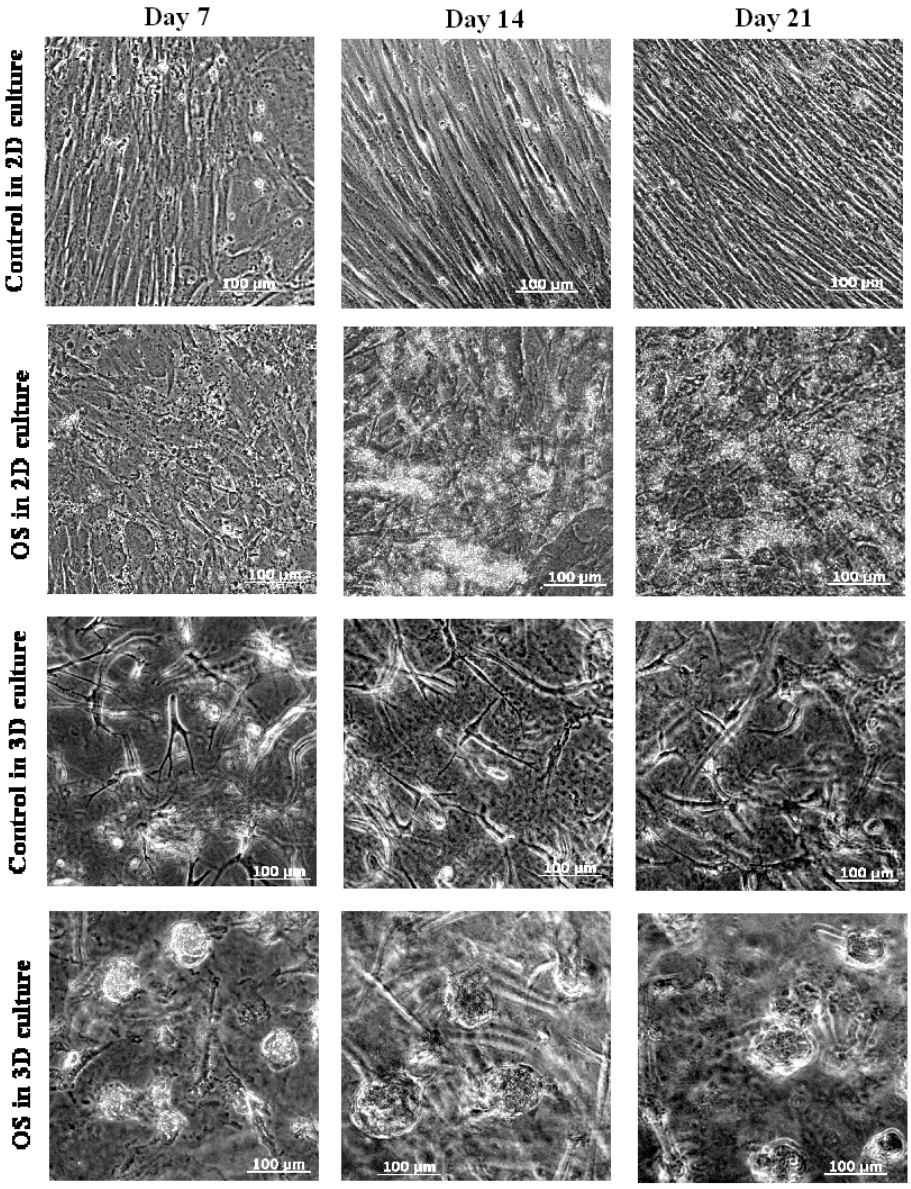

Figure 2.2. Phase-contrast images showing the morphology of hMSCs cultured on 0.25% PuraMatrix™ or in 2D culture plates in osteogenic or growth medium on Day 7, 14, and 21 during differentiation

Human MSCs underwent a dramatic morphology change with osteogenic (OS) medium, while obvious cell proliferation was only observed in undifferentiated (Ctrl) hMSCs. **Figure 2.2** shows phase-contrast images of different culture conditions on Day 7, 14 and 21 during differentiation. In 2D Ctrl culture, hMSCs were spindle-shaped with better alignment when cell

numbers increased. For 3D Ctrl culture on 0.25% PuraMatrix, hMSCs remained in fibroblast-like morphology and migrated inside PuraMatrix. In OS 2D culture, abundant secretions of extracellular matrix (ECM) and small nodular aggregates were detected on Day 14 and 21 respectively. In contrast, small cell aggregates were formed in OS 3D PuraMatrix culture on Day 7, and their sizes increased in Day 14 and 21 cultures along with dark regions of mineral confirmed by von Kossa staining of mineral deposits on Day 24 shown as black nodules in **Figure 2.3**. No mineral was detected in 2D Ctrl culture. However, in 3D Ctrl culture, there was mineral staining but much less intensive than that in OS 3D culture.

.

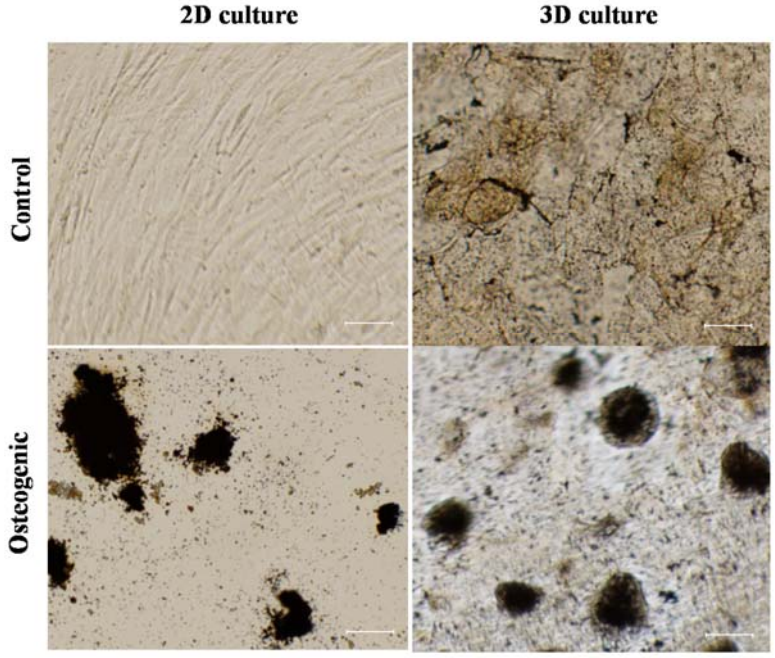

Figure 2.3. Von Kossa staining for mineral deposits from hMSCs cultured in 2D plates and on 3D PuraMatrix in the normal growth condition and osteogenic condition at Day 24 after differentiation. Scale bar = 50 μm.

Surface Morphology of hMSCs on PuraMatrix and Localization of Calcium Deposition

Figure 2.4 includes SEM images revealing detailed surface morphology of hMSCs on PuraMatrix and cell-hydrogel interactions. **Fig. 2.4(A) & (B)** are SEM images from gold-coated

samples. Undifferentiated hMSCs remained as fibroblast-like (**Fig. 2.4(A)**), while differentiated hMSCs formed aggregates (**Fig. 2.4(B)**). The network composed of cell protrusions into PuraMatrix nanofibers was observed in both growth and differentiation conditions. The inset picture in **Figure 2.4(C)** is an SEM image of a carbon-coated hMSC sample in the growth condition. Calcium X-ray spectrum of the same specimen showed that there was no significant amount of calcium deposition in the hMSC growth culture on PuraMatrix (**Fig. 2.4(C)**). As a

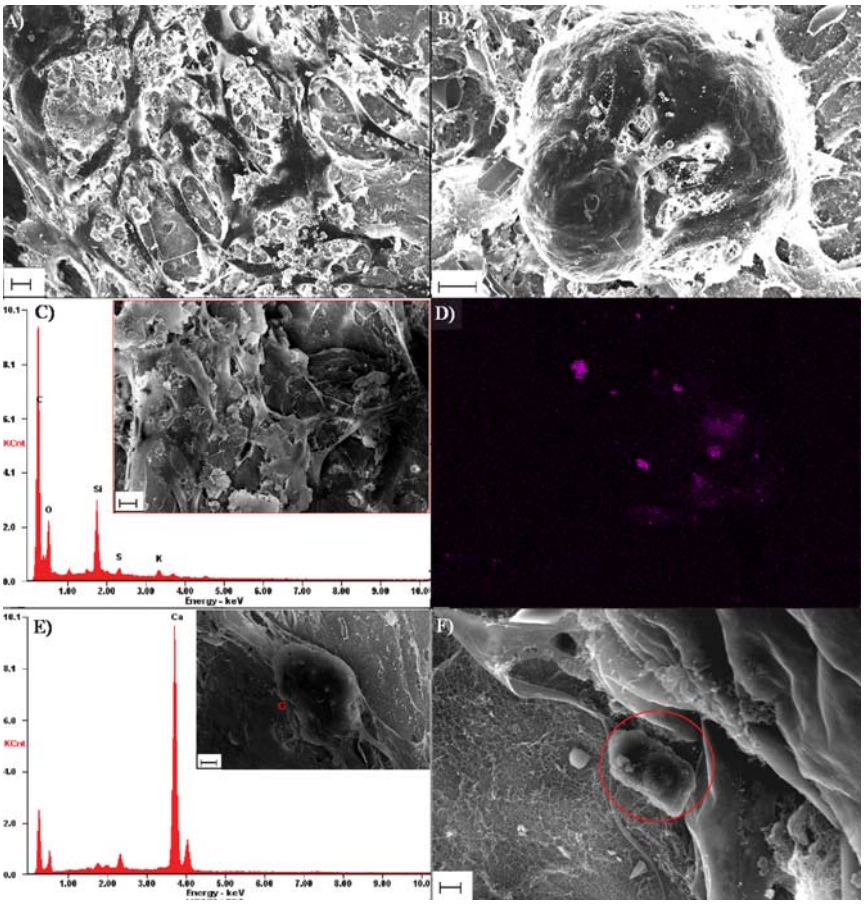

Figure 2.4. The morphology of **(A)** undifferentiated hMSCs and **(B)** differentiated hMSCs on PuraMatrix analyzed by SEM; **(C)** Calcium X-ray spectrum of hMSCs on PuraMatrix in the growth condition with an inset SEM image of the same sample; **(D)** Calcium X-ray map of heat-shocked & differentiated hMSCs on PuraMatrix with purple areas indicating calcium locations; **(E)** Calcium X-ray spectrum of a specific spot in its SEM inset image circled in red color; **(F)** A zoom-in SEM image showing a calcium crystal indicated by a red circle, the same spot highlighted in the SEM inset in **(E)**. All scale bars are 20 μm except one, which is 2 μm in **(F)**.

contrast, mineralization sites were largely detected and distributed in and around differentiated hMSCs with variant density and calcium intensity shown by the calcium X-ray intensity map (**Fig. 2.4(D)**). The inset picture in **Figure 2.4(E)** is the SEM image of the same specimen used to obtain **Figure 2.4(D)**. In particular, a crystal structure was located under a high magnification of SEM shown in **Figure 2.4(F)**, which is a zoom-in SEM image of areas around the small red circle in the inset of **Figure 2.4(E)**. The high peak of calcium at the corresponding location in the calcium X-ray spectrum (**Fig. 2.4(E)**) confirmed that the crystal structure indicated by the red circle in **Figure 2.4(F)** was made of calcium.

Alkaline Phosphatase Activity

Alkaline phosphatase (ALP) activity is one marker of early stage osteogenic (OS) differentiation. The significant increase of ALP activities by heat shock (HS) was observed on Day 6 in 2D OS culture, while there was no significant ALP increase comparing between HS and non-HS 2D OS conditions on Day 12 (**Fig. 2.5(A)**). In 3D PuraMatrix culture, the heat shock effect was less significant on the increase of ALP activities on Day 6. Interestingly, heat shock significantly reduced ALP activities on Day 12 in 3D OS culture (**Fig. 2.5(B)**). The 1-hr heat exposure at 41^{o}C resulted in a 1.24-fold increase of ALP activities in 2D OS culture and 1.35-fold in 3D OS hydrogel culture on Day 6.

Enhanced Mineralization by Heat Shock

Calcium deposition was used as an indicator of late stage osteogenesis and maturation of osteoblasts differentiated from MSCs. As shown in **Figure 2.6**, periodic heat shock at 41^{o}C significantly enhanced the mineralization in 2D OS culture on Day 19 and 3D OS PuraMatrix culture on Day 19 and 27, while the enhancement effect of heat shock was less remarkable in 2D OS culture on Day 27. Calcium deposition was increased by 1.64-fold and 1.49-fold in heat

shocked osteogenic samples compared to non-heat shocked osteogenic ones in 2D culture and 3D culture respectively on Day 19 and 1.34-fold in 3D culture on Day 27.

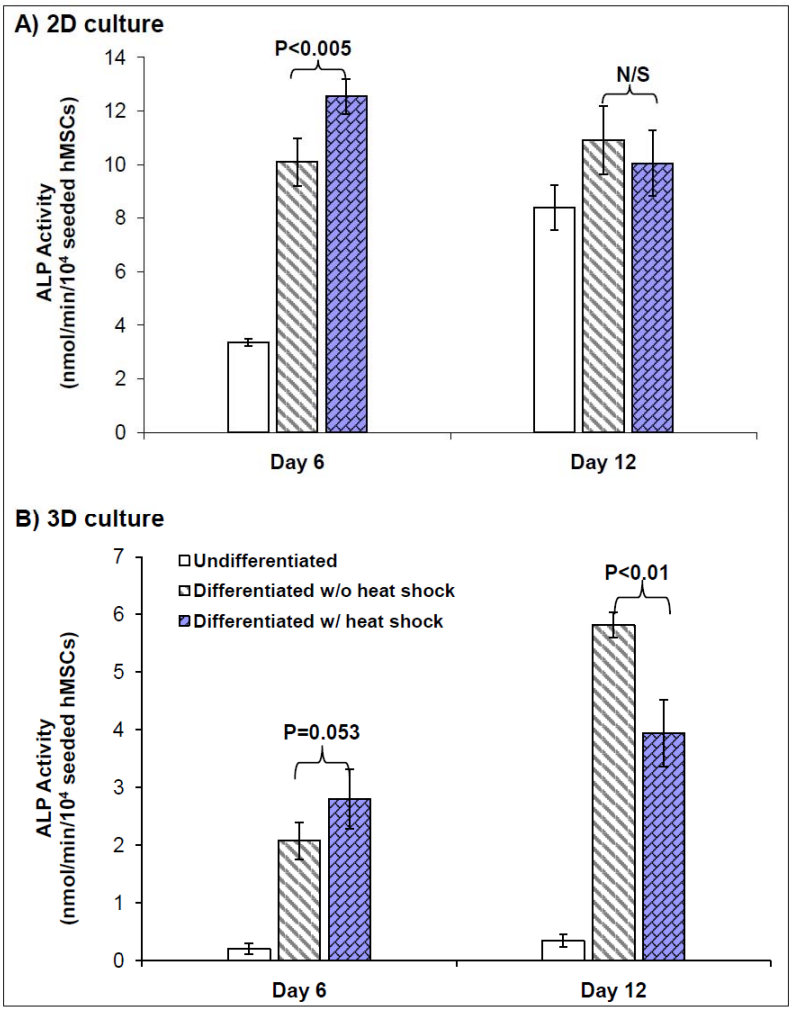

Figure 2.5. Heat shock effects on alkaline phosphatase (ALP) activity measured by quantitative ALP assay in **(A)** 2D and **(B)** 3D culture at Days 6 and 12 during osteogenesis.

Dynamic Expression of Osteo-specific Genes

Gene expression of osteogenic lineage was assessed by real-time RT-PCR on Day 11, 19 and 25 during differentiation. **Figure 2.7** shows that in 2D culture, osteogenic genes BMP2, osteopontin (OP), Runx2, OSX were all up-regulated in osteogenic samples compared to 2D

control samples at growth conditions. Furthermore, the expression levels of these osteo-specific genes were increased in the late differentiation stage than that of early stage, which indicated the progression of MSC osteogenesis in 2D culture. Heat shock further enhanced the expression of

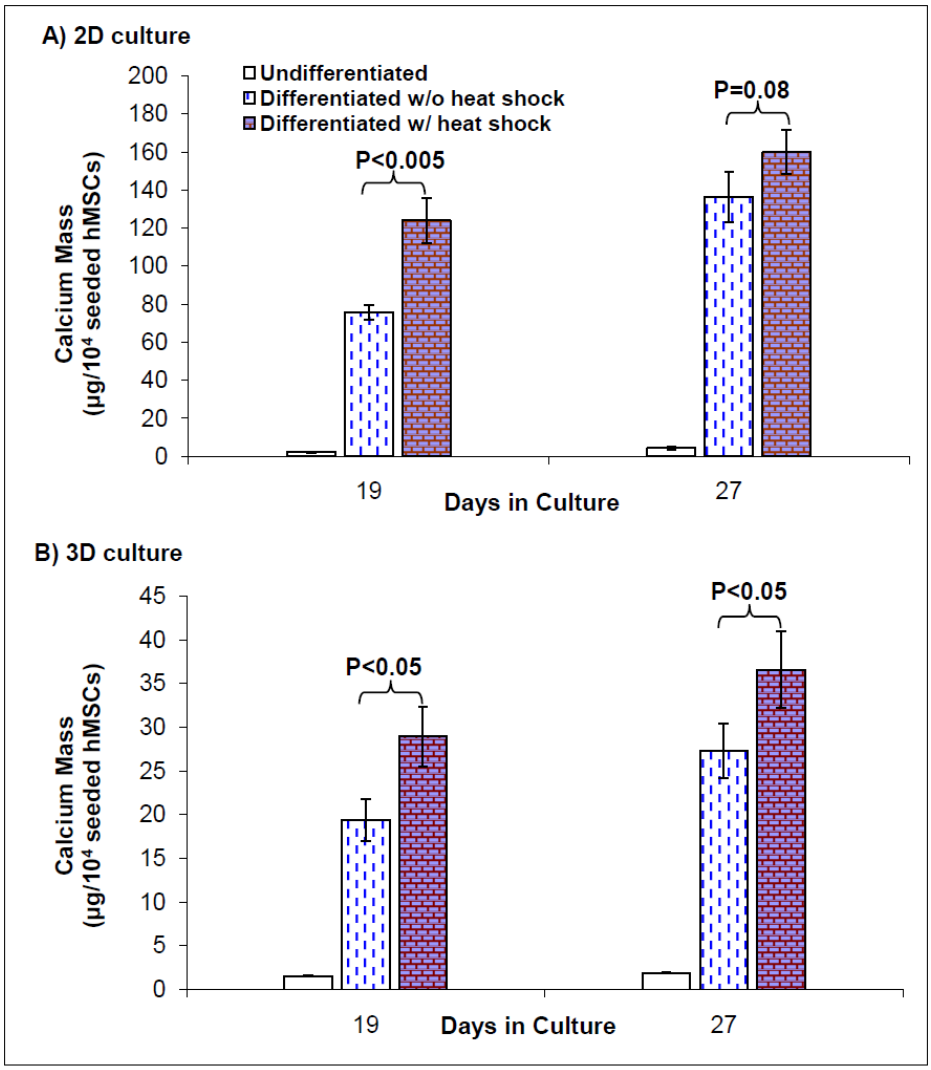

Figure 2.6. Heat shock effects on calcium deposition during hMSC osteogenesis in **(A)** 2D culture and **(B)** 3D culture at Day 19 and 27.

OSX on Day 11, OP on Day 19, BMP2 and Runx2 on Day 25. BMP2 and Runx2 were down-regulated by heat shock in 2D culture on both Day 11 and Day 19. **Figure 2.8** shows the real time RT-PCR results of four genes in 3D PuraMatrix culture. BMP2, Runx2 and OP had the

similar gene expression patterns as that of 2D culture under the periodic thermal stimulation. However, OSX gene had an opposite expression pattern under thermal stimulation in 3D PuraMatrix culture compared to the 2D culture. Interestingly, for 3D PuraMatrix culture, osteogenic medium did not induce the upregulation of four genes except for Runx2.

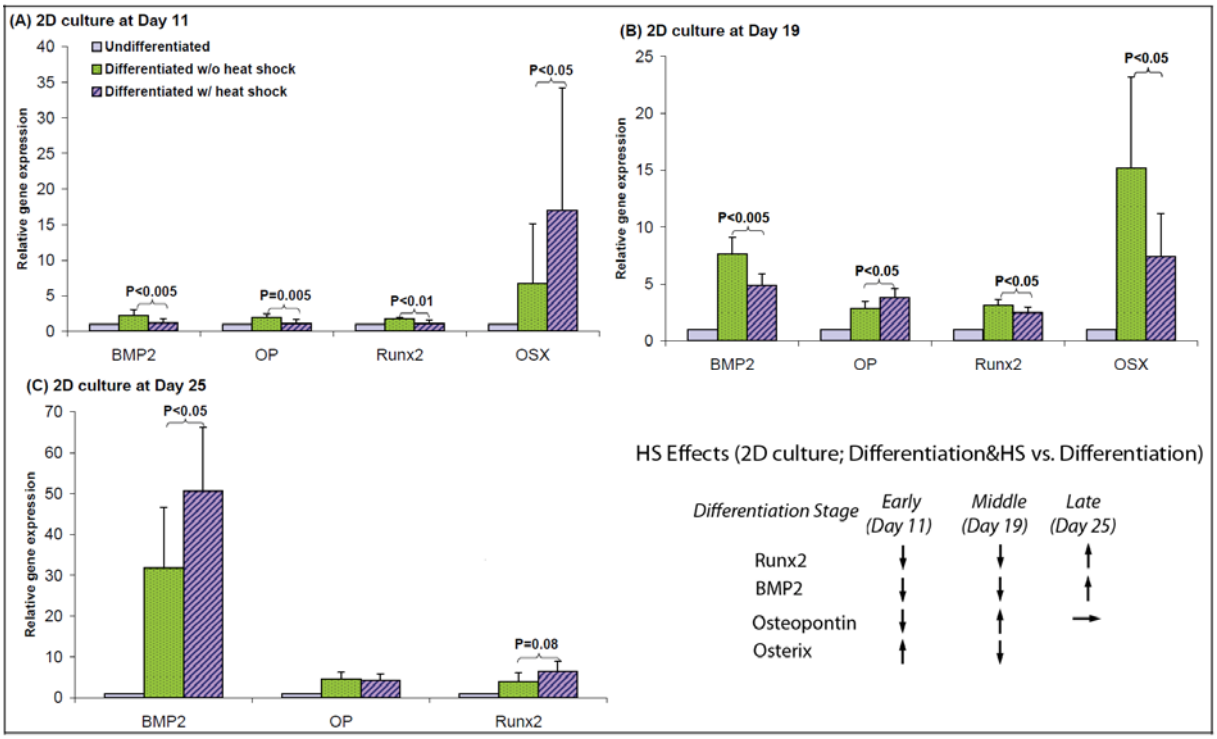

Figure 2.7. Gene expression of osteo-specific markers (BMP2, OP, Runx2, OSX) assessed by real-time RT-PCR in 2D culture at **(A)** Day 11 **(B)** Day 19 **(C)** Day 25 after differentiation. Comparison was between differentiated hMSCs with and without the effect of heat shock. Undifferentiated hMSCs were used as control (mean ± SD, N=6-16).P values were calculated using student t-test.

Expression of Heat Shock Proteins

The expression of heat shock proteins (HSP27, HSC70+HSP70, and HSP90) was investigated at 24 hrs after heat shock on Day 4, 11, 18, and 25 during differentiation. **Table 2.2** lists the HSP expression data quantified from the western blot membranes. It shows that HSP27 expression was significantly up-regulated in osteogenic (OS) samples compared with undifferentiated control (Ctrl) samples while there was no significant increase of HSP27 in heat

shocked osteogenic (HS) samples compared with OS samples in both 2D and 3D cultures. In contrast, the expression of HSC70+HSP70 was significantly down-regulated in OS samples compared with Ctrl samples but heat shock significantly increased its expression in HS samples

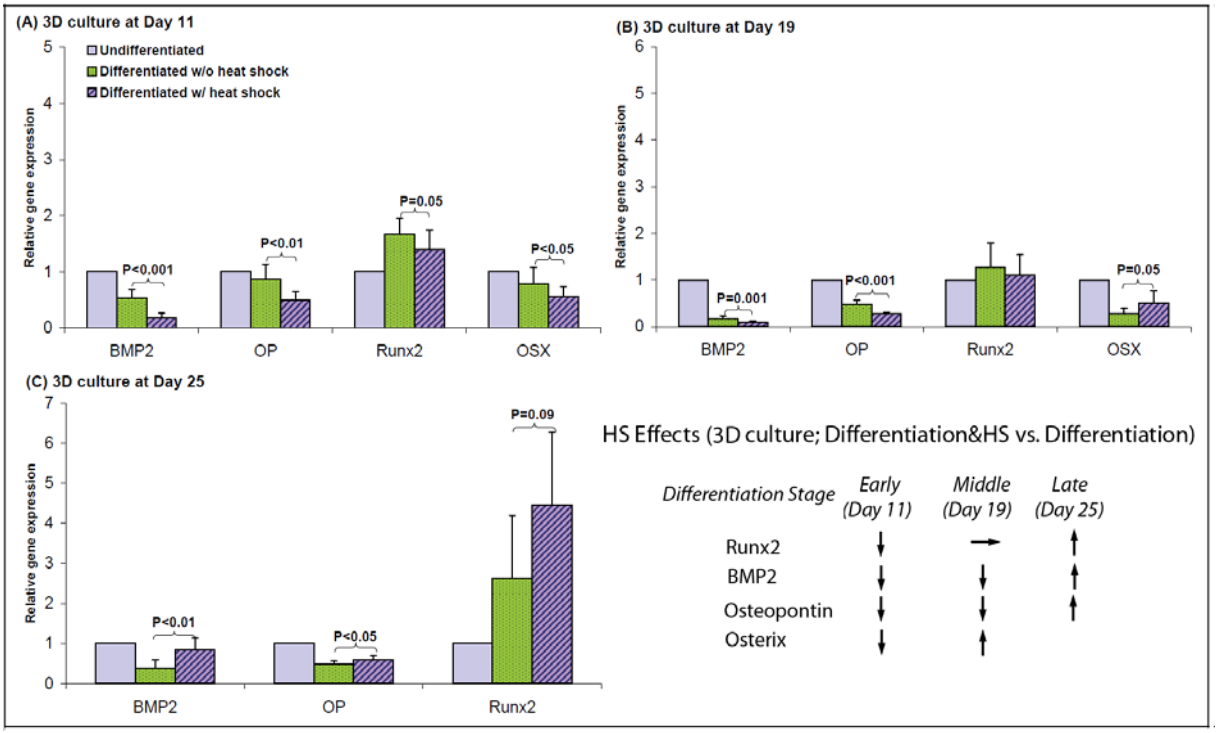

Figure 2.8. Gene expression of osteo-specific markers (BMP2, OP, Runx2, OSX) assessed by real-time RT-PCR in 3D culture at **(A)** Day 11 **(B)** Day 19 **(C)** Day 25 during differentiation. Comparison was between differentiated hMSCs with and without the effect of heat shock. Undifferentiated hMSCs were used as control (mean ± SD, N=6-12).P values were calculated using student t-test.

compared to OS samples in 2D culture. For HSP90 expression, up-regulation was observed in OS samples compared to Ctrl samples and down-regulation in HS samples compared with OS samples in 2D culture with the only significance on Day 4. In general, the HSP expression levels in 3D PuraMatrix culture were lower than that of 2D culture, and too low to be detected using Western blot except for HSP27 on Day 11 and beyond. The expression patterns of individual HSPs in different conditions (Ctrl, OS, HS) on one sample collection day and their

corresponding western blot membranes were displayed in **Figure 2.9**. In 2D culture, HSP27 expression was much higher than HSC70+HSP70 or HSP90. The expression pattern of inducible

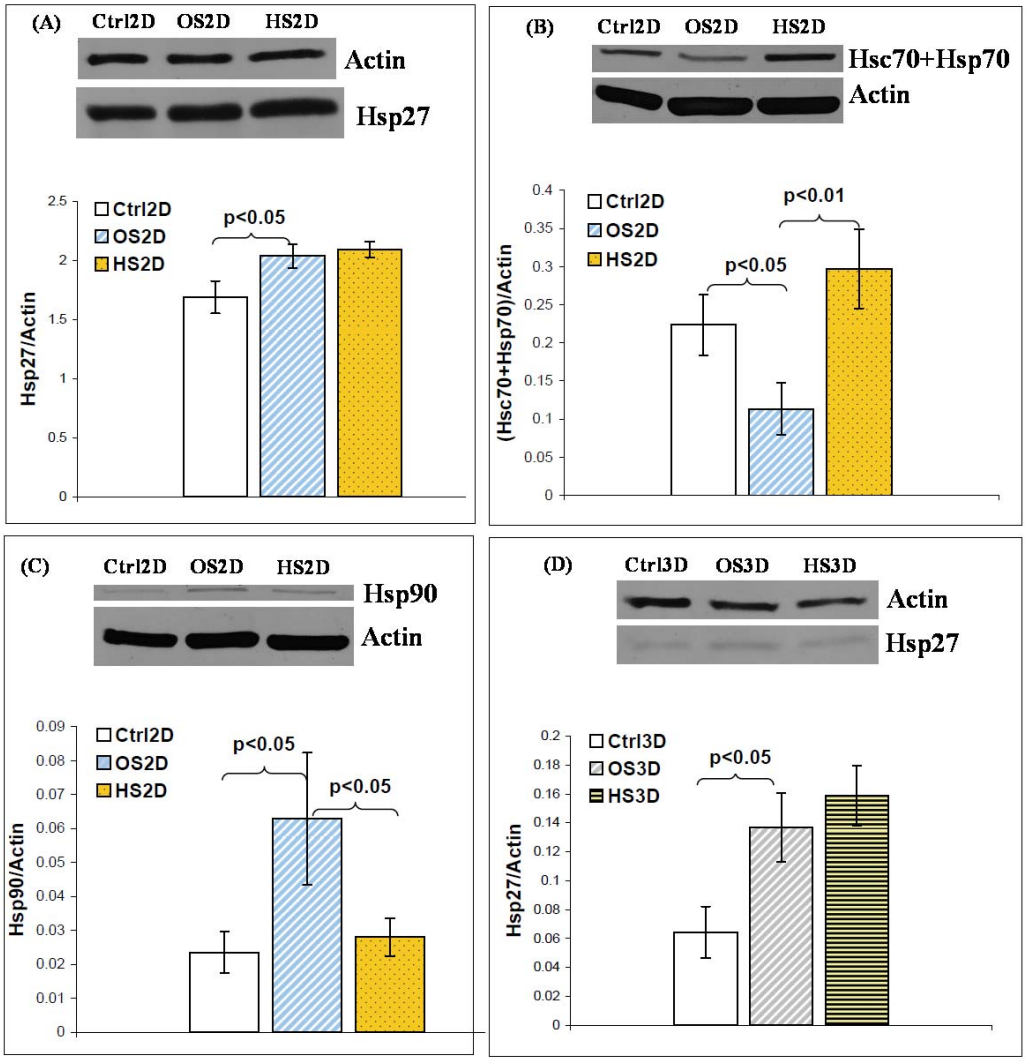

Figure 2.9. The representative western blot membrane followed by a corresponding bar graph of **(A)** HSP27 expression in 2D culture on Day 11 during differentiation, **(B)** HSC70+HSP70 expression in 2D culture on Day 11 during differentiation, **(C)** HSP90 expression in 2D culture on Day 4 during differentiation and **(D)** HSP27 expression in 3D culture on Day 11 during differentiation. (Ctrl: undifferentiated hMSCs, OS: differentiated hMSCs, and HS: differentiated hMSCs with heat shock).

HSP70 measured by ELISA was similar to that of HSC70+HSP70 (constitutive+inducible), and

inducible HSP70 expression in 3D culture was also significantly lower than that of 2D culture shown in **Figure 2.10**.

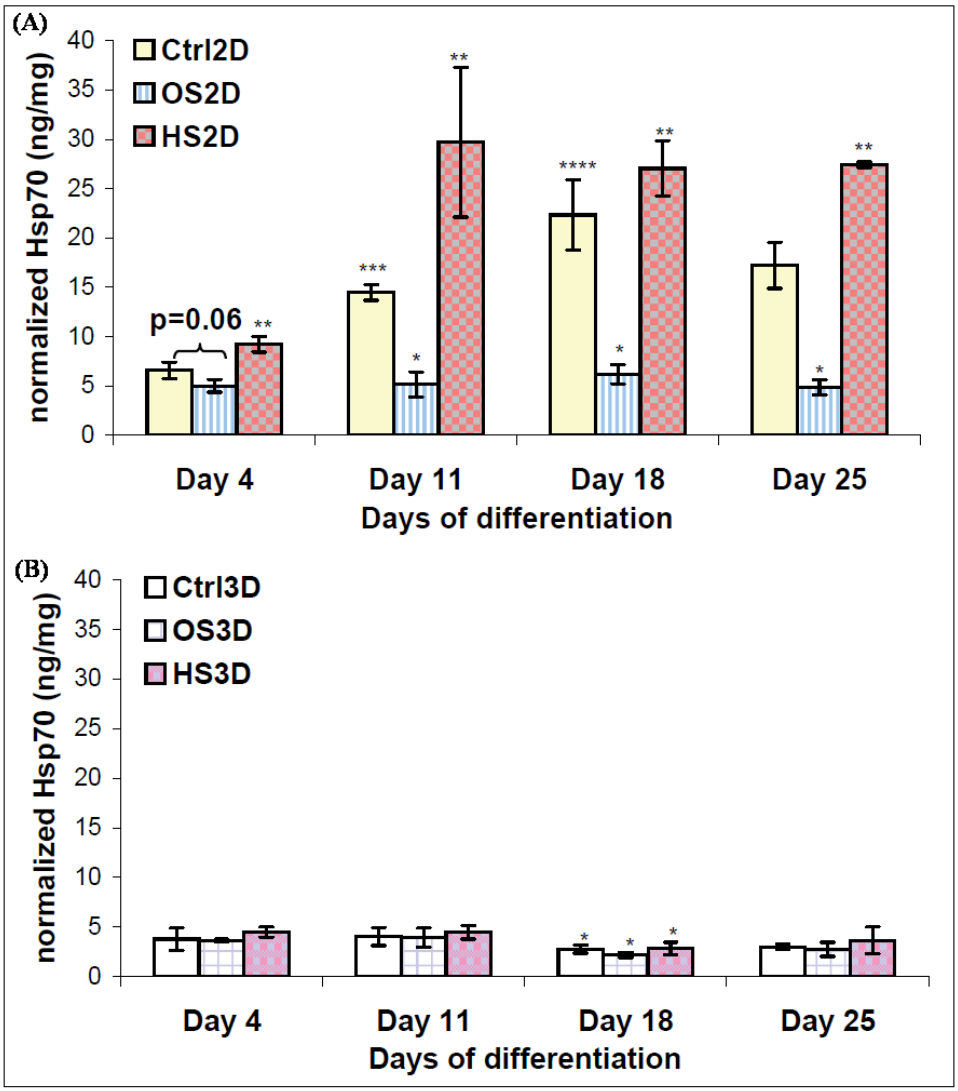

Figure 2.10. Inducible HSP70 expression measured by ELISA in **(A)**2D culture and **(B)**3D culture on Days 4, 11, 18 and 25 during differentiation. (Ctrl: undifferentiated hMSCs, OS: differentiated hMSCs without heat shock, and HS: differentiated hMSCs with heat shock). In panel **(A)**, *p<0.05(OS culture compared to the corresponding Ctrl culture on the same day), **p<0.05(HS culture compared to the corresponding OS culture on the same day), ***p<0.05(Day 11 Ctrl culture compared to Day 4 Ctrl culture), ****p<0.05(Day 18 Ctrl culture compared to Day 11 Ctrl culture). In panel **(B)**, *p<0.05(The corresponding conditions (Ctrl, OS, HS) compared between Day 18 and Day 11).

Table 2.2. Expression of heat shock proteins (HSP27, HSC70+HSP70, HSP90) on Day 4, 11, 18 and 25 during differentiation in hMSC cultures (n=3, mean ± SD, C [growth], O[osteogenic], H[osteogenic & heat shocked], *p<0.05 [O vs. C], **p<0.05 [O vs. H], ND [not detected])

Days / HSP/Actin		Day 4	Day 11	Day 18	Day 25
2D					
HSP 27	C	1.339±0.107	1.690±0.137	1.244±0.109	1.211±0.037
	O	1.554±0.069*	2.037±0.099*	3.168±0.385*	1.378±0.071*
	H	1.703±0.105	2.094±0.066	3.412±0.545	1.555±0.133
HSC70 +HSP70	C	0.126±0.002	0.224±0.040	0.201±0.005	0.297±0.015
	O	0.097±0.008*	0.113±0.035*	0.075±0.017*	0.129±0.022*
	H	0.196±0.005**	0.297±0.052**	0.279±0.022**	0.322±0.067**
HSP90	C	0.024±0.006	0.083±0.017	0.046±0.004	0.078±0.030
	O	0.063±0.019*	0.102±0.016	0.055±0.010	0.069±0.017
	H	0.028±0.006**	0.098±0.012	0.048±0.016	0.090±0.017
3D					
HSP 27	C	ND	0.064±0.018	0.054±0.017	0.070±0.022
	O	ND	0.137±0.024*	0.092±0.018*	0.199±0.022*
	H	ND	0.159±0.021	0.100±0.025	0.206±0.058

2.4 Conclusion and Discussion

In this study, effects of periodic heat shock (41^{o}C once a week for 1 hr) on hMSC osteogenic differentiation were investigated in both 2D conventional culture and 3D PuraMatrix (peptide hydrogel) culture. In-house isolated hMSCs in osteogenic medium formed mineralized aggregates in 2D culture plates and 3D peptide hydrogel (**Fig. 2.2&2.3**). Largely distributed calcium deposits were detected in differentiated hMSCs on PuraMatrix (**Fig. 2.4**). Meanwhile,

mild heat shock was able to significantly facilitate the early osteogenic differentiation indicated by the ALP activity (**Fig. 2.5**) and enhance the maturity of differentiated osteoblasts in the late stage shown by the calcium deposition in both 2D and 3D cultures (**Fig. 2.6**). In addition, thermal effects on osteo-specific genes were highly dynamic with a pattern of down-regulated gene expression of BMP2, Runx2 and osteopontin in the early stage of osteogenic differentiation but upregulation of these genes in the late stage in both 2D and 3D cultures. Overall, our results demonstrate that periodic mild heat shock can be a potential simple approach to enhance hMSC differentiation into osteoblasts and promote earlier differentiation, and thus may have a significant impact on future *in vivo* applications.

Our results of enhanced ALP activities in the early osteogenic differentiation and calcium deposition by periodic heat shock at 41^{o}C for 1 hr in both 2D and 3D cultures are consistent with an early study of heat shock effects on hMSC osteogenic differentiation in 2D culture [30]. In that study, Shui et al showed that both ALP activities and calcium deposition in differentiated hMSCs linearly increased with temperatures ranging from 33^{o}C to 41^{o}C after multiple 1-hr heat exposure once every 3 days up to 21 days. Heat shock seems to speed up the differentiation process by shifting the peak of ALP activities much earlier than normal. ALP expression is a dynamic process and its activity usually peaks between Day 9 and Day 12 during osteogenesis, varying from donor to donor [56]. The decrease of ALP activities in 2D and 3D cultures on Day 12 may be an indicator of the shifting of the ALP peak time. Heat shock also induced an earlier mineralization in differentiated hMSCs and further enhanced the maturation of osteoblasts in the late stage. This earlier maturation may have significance for bone regeneration *in vivo*, as it will shorten the waiting time required to obtain differentiated and mature osteoblasts from hMSCs,

which normally takes about 30 days for *in vitro* differentiation, for clinical bone repair using stem cell therapy.

Effects of mild hyperthermia on osteogenic gene expression during hMSC differentiation were not well studied. Cbfa1/Runx2 is an essential transcription factor for osteoblastic differentiation [59]. Osterix is a downstream gene of Runx2 [60], and a necessary transcription factor for osteopontin expression [59, 61]. Osteopontin is an ECM protein that mediates cell attachment in osteoprogenitor cells and osteocytes [62], and considered as a late bone marker for osteoblast differentiation and mineralization [59]. BMP2 plays an important role in embryonic bone development [63]. We observed that heat shock dynamically upregulated these osteogenic genes in a time-dependent manner during about 4 weeks of hMSC osteogenesis. In 2D hard surface culture, it seems that heat shock could upregulate late osteogenic genes much faster than the early ones (**Fig. 2.7**), demonstrated by upregulation of osterix gene at early stage (Day 11), osteopontin at intermediate stage (Day 19), but BMP2 and Runx2 at late stage (Day 25) only. Considering the gene expression pattern under heat shock, upregulating of late osteogenic genes and depressing the early ones during early to intermediate osteogenic differentiation stages, together with our data of enhanced early ALP activities and calcium deposition, we can speculate that heat shock may bypass some early osteo-specific genes but turn on a few late osteo-specific genes directly. Since the basal production of ECM is likely regulated by Runx2 [64] and BMP2 expression may be required for terminal differentiation into osteocytes, the upregulation of these two genes by heat shock in the late stage of hMSC osteogenesis is consistent with the results of enhanced mineralization in differentiated hMSC culture under thermal stimulation.

In 3D PuraMatrix culture, the up/down-regulation patterns of four genes (i.e. BMP2, Runx2, OP and OSX) comparing between osteogenic and osteogenic&heat-shock conditions

were similar to that of 2D culture. Interestingly, BMP2, OP and OSX were not upregulated in differentiated hMSCs comparing to the control (**Fig. 2.8**) despite the definite hMSC differentiation confirmed by cell morphology (**Fig. 2.2)**, ALP activities (**Fig. 2.5B**) and calcium deposition (**Fig. 2.6B**). Other osteo-specific genes must be turned on in this case. DNA microarray technology could be used to identify those genes. On the other hand, the lower expression of four osteogenic genes in 3D soft PuraMatrix culture are consistent with the delay of differentiation reflected by lower ALP activities or calcium deposition in 3D culture compared with 2D (**Fig. 2.5&2.6**). The hard polystyrene surface of 2D culture plates (Young's modulus of 3.5 GPa) is much stiffer than the soft substrate, 0.25% PuraMatrix (storage modulus of 2.5 kPa at 0.5%). In general, matrix elasticity, or the stiffness of the substrate could significantly affect the stem cell differentiation directions [65]. Apparently, the 3D soft hydrogel seemed to delay the hMSC osteogenesis compared to tissue culture plates, while the hard surface of 2D culture plate itself actually facilitates osteogenesis [65]. This may be one of reasons that the heat-induced higher calcium deposition was still very significant in 3D culture even on Day 27, but not very significant in 2D culture (**Fig. 2.6**). Heat shock may have forced hMSCs in osteogenic medium on soft hydrogel more toward osteo-lineage. In addition, 3D culture environment enables intercellular contacts from different layers. Whether or not the 3D culture configuration itself triggers the different differentiation signals needs to be investigated more.

To further study the mechanisms in the HS-enhanced osteogenic differentiation of hMSCs, HSP expression including HSP27, HSC70+HSP70, HSP70 alone and HSP90 was investigated. Heat shock proteins (HSPs) are chaperon proteins which are upregulated in response to stresses. HSP27 is a multifunctional protein with a molecular weight of 27kDa. It is an important regulator in almost all cellular processes such as migration, proliferation,

differentiation, and apoptosis due to its close association with actin. HSP27 overexpression during different stages of cell differentiation and development was reported [66]. In this study, significantly increased HSP27 expression in differentiated cells (**Fig. 2.9A&D**) may be due to cytoskeleton reorganization during differentiation, resulting in the morphological changes of differentiated cells. Despite this, exposure of differentiated hMSCs to heat shock did not further stimulate the expression of HSP27, which is consistent with no observable morphological differences between heated&differentiated hMSCs and non-heated ones. However, the subtle change of phosphorylated HSP27 needs to be studied in the future.

Heat shock protein 70 (MW: 70 kDa) have two types, constitutive HSC70 and inducible HSP70 [67]. HSP90 also has two isoforms, inducible form HSP90α and constitutive form HSP90β, and the level of expression is usually lower in the former than the latter. Both HSC70/HSP70 and HSP90 are involved in various cell processes, such as proliferation, differentiation and apoptosis [67, 68], by correcting misfolded proteins under stresses or helping to fold newly synthesized proteins during normal physiological conditions. The reduced expression of heat shock protein 70 in differentiated hMSCs (**Fig. 2.9B**) may be a result of extremely low cell proliferation during differentiation. Mild hyperthermia increased biochemical reaction rates in hMSCs, which induced overexpression of HSC70 and HSP70 in differentiated plus heat shocked hMSCs. The elevated HSP70 expression was also reported in a previous study using hMSC 2D culture and hyperthermia [30]. In contrast, HSP90 was up-regulated in differentiated cells compared to undifferentiated cells, and heat shock down-regulated its expression (**Fig. 2.9C**), but significance was only seen in the early stage of differentiation. The mechanisms remained unclear, but studies on different lineage also confirmed the importance of HSP90β overexpression from early to late stage of germ cell differentiation and also for early

embryonic development [69, 70]. Both HSP70 and 90 are molecular chaperones but it seems that they modulate cell differentiation through their own and maybe different signaling pathways. There was no similar study reporting the HSP90 expression in differentiated hMSCs toward bone lineage with heat shock. The underlying mechanisms of its downregulation remain unclear. The upregulation of HSP90 may not be a must-need to sustain an enhanced differentiation due to the fact that HSP70 is upregulated. Further experiments will be required to find out what specific roles it plays. In 3D PuraMatrix culture, the expression of three heat shock proteins was significantly lower, which may be correlated with the less stresses cells experienced on the peptide hydrogel during growth or differentiation.

In summary, this is the first comprehensive study of heat shock effects on hMSC differentiation into osteoblasts in 3D hydrogel scaffold. Our results showed that periodically mild heat shock was able to facilitate MSC differentiation into osteoblasts and enhance their maturity. In addition, this study provided a 3D MSC culture model *in vitro* to mimic *in vivo* environment surrounding bone marrow. Altogether, our data may have a significant impact on the development of a therapeutic thermal treatment protocol to enhance stem cell differentiation during cell transplantation. For bone regeneration *in vivo*, differentiated osteoblasts from hMSCs can be transplanted into bone defects, by injection using PuraMatrix as carrying medium coupled with a heating device developed according to the results of this study. Future studies will use siRNAs/shRNAs targeting HSP70 and HSP90 to investigate the role of HSPs during hMSC differentiation with or without heat shock. Other heating patterns and temperatures (e.g. 39^{o}C, known as the elevated body temperature during exercise [55]) will be evaluated in further studies to optimize the heating protocol for hMSC differentiation. Other biomaterials with different stiffness for bone and cartilage regeneration will be evaluated in the future using the similar

experimental protocol described in this study. Given the fact that osteoarthritis (OA) greatly affects the elderly people, and it requires regeneration of both bone and cartilage at late stage, hyperthermia (via ultrasound and microwaves etc.) may represent a less invasive and simple therapy for clinical joint repair, and thus potentially be a promising approach in bone and cartilage regenerative medicine.

CHAPTER 3 HEAT SHOCK ENHANCED THE MATURATION OF CHONDROCYTES DIFFERENTIATED FROM HUMAN MESENCHYMAL STEM CELLS IN PELLET AND HYDROGEL CULTURES

3.1Introduction

Articular cartilage is an avascular connective tissue that has limited capacity for self-repair. Partial thickness of articular lesion, which affects only the superficial cartilage, does not heal spontaneously [71]. Injuries that affect deep into the subchondral bone, exhibit a repair process leading to the formation of a fibrocartilage, however is inferior to native articular cartilage [72]. Autologous chondrocyte implantation (ACI), the first cell therapeutic approach introduced in 1994, is currently used in clinical cartilage repair, but it has disadvantages such as limited cell availability, and donor site morbidity [71-73]. Thus tissue engineering approaches using biodegradable and biocompatible scaffolds with cells and/or growth factors [73-75] may hold a great promise for functional cartilage regeneration. They may also provide curing solutions to the challenging diseases such as osteoarthritis (OA) which occurs frequently in the aging population.

Due to the low chondrocyte density in articular cartilages and the fact that they tend to dedifferentiate when expanded in 2D culture, there is a shift of cell sources from chondrocytes to adult stem cells for cartilage tissue engineering applications [71, 76]. Human mesenchymal stem cells (hMSCs) isolated from a well-known source, i.e. bone marrow, have multilineage differentiation potential and can be differentiated towards chondrogenic lineage *in vitro* [8, 9]. In addition, they have been tested for cartilage repair potential by mixing with biomaterials like type I collagen in studies in rabbits [77-80] with promising results and further in some clinical

studies [81-83]. A lot of recent research has focused on effects of growth factors [84, 85], scaffold materials [52, 86], or mechanical loading [87, 88] on MSC differentiation into chondrocytes. However, the extracellular matrix (ECM) content produced by MSCs and mechanical properties of constructs formed by them are inferior to those functional cartilaginous properties of mature primary chondrocyte-seeded constructs [53, 89]. These suggest that methods for inducing MSC chondrogenesis have yet to be optimized to enhance the maturation of cells differentiated from MSCs and generate tissue-engineered cartilage that matches native cartilage. Temperature has an important impact on tissue development in general. It may be one of the missing factors in the regulation of the MSC differentiation.

Hyperthermia has been widely used as a thermotherapy for the musculoskeletal diseases, such as the treatment of articular cartilage with OA [42]. Heat stimulation was known to relieve the pain in OA patients, however, the effect has not been sufficiently investigated in clinical studies and the mechanism remains unknown. The direct effect of heat on metabolism and repair of the articular cartilage, the mainly affected tissue of OA, is also unknown. Furthermore, a few studies have shown that heat shock protein HSP70 has a protective effect on the cartilage as it inhibits apoptosis of chondrocytes as well as increases the cartilage metabolism [90-96], and thus induction of HSP70 by hyperthermia may help slow down the progression of OA and further prevent cartilage degeneration. Besides, in one study, proteoglycan metabolism in chondrocyte was found to be increased using heat at 41^{o}C [97]. In addition, effect of hyperthermia on the articular cartilage *in vivo* has been studied in a rabbit model [98]. Microwave applied on rabbit knee joint has increased the joint temperature to 40 ^{o}C and also increased the proteoglycan and type II collagen expression in the articular cartilage and meanwhile, HSP70 was upregulated in the chondrocytes and confirmed to be partially responsible for the increase in the matrix

production [98]. However, no studies have been conducted to investigate thermal effects on bone marrow stem cell differentiation into chondrocytes.

A large variety of both synthetic and natural biomaterials with different properties including poly(ethylene glycol) (PEG) [3], agarose [86, 89], alginate [86], type I collagen[52], have been employed as scaffold in cartilage tissue engineering. Among all scaffolds, hydrogel scaffolds as the most commonly explored ones, have proven satisfactory in cartilage repair [72]. Hydrogels are favorable as they can be mixed with cells homogeneously while providing a 3D microenvironment, injected non-invasively, and fill any shapes of defect easily [73]. Therefore in this study, we used a well-defined synthetic peptide hydrogel PuraMatrix to study the heat shock effects on hMSC chondrogenesis. This RAD16-I ($[RADA]_4$) hydrogel scaffold is a 16-amino acid peptide that self-assembles to form a scaffold with pore sizes ranging from 50 nm to 200 nm [16]. It has been shown to support the culture of numerous cell types including cartilage [20, 99, 100], liver [21, 22], and cardiovascular cells [23, 24]. Also, several studies have demonstrated the potential of PuraMatrix to allow *in vitro* chondrogenesis of MSCs [52, 53, 85, 101] and *in vivo* cartilage repair through injection with MSCs in a rabbit joint model [102].

Recently we have shown in an *in vitro* study, periodic heat shock at 41 ^{o}C enhanced osteogenic differentiation of hMSCs in 2D culture plates and 3D peptide hydrogel [103]. On the basis of this finding and the fact that heat treatment of knee joint usually involves both cartilage and bone in OA patients, we hypothesize that the effect of heat on bone and cartilage may be closely correlated with each other. Therefore, the aim of this work was to further investigate direct heat shock effects on hMSC chondrogenesis in both 3D pellet and peptide hydrogel culture. Conventional 3D pellet culture was used as a control. The synthesis of sulfated glycosaminoglycans (sGAGs) was assessed biochemically. Immunohistochemical analyses were

used to determine the type of ECM produced including collagen type II and aggrecan. Results of this study would help elucidate the mechanism of heat stimulation on articular cartilage regeneration *in vivo* and guide the design of a thermotherapy protocol potentially for OA treatments.

3.2 Materials and Methods

All reagents and chemicals without manufacture labels were purchased from Sigma-Aldrich (St Louis, MO).

hMSC Isolation and Characterization

Human MSCs were isolated from bone marrow (BM) of a 28-year-old donor (AllCells LLC, Berkeley, CA) as described previously [103]. Briefly, the BM was mixed with RosetteSep MSC enrichment cocktail (StemCell Technologies, Vancouver, Canada) and incubated for 20 minutes at room temperature. Afterwards, the sample was layered on top of the Ficoll-Paque (StemCell Technologies) density gradient solution and centrifuged for 25 minutes at 300×g. Enriched mononuclear cells were then removed and cultured as passage 0 in tissue culture flasks with hMSC growth medium consisting of Dulbecco's modified Eagle's medium (DMEM)-low glucose, with 10% fetal bovine serum (FBS) (Atlanta Biologicals, Lawrenceville, GA), and 1% penicillin-streptomycin (Invitrogen, Carlsbad, CA)). The adherent cells were further expanded at 5000 cells/cm^2 until passage 4. Prior to the following study, hMSCs were characterized using surface markers by flow cytometry as previously described [103]. Briefly, the cells were stained with antibodies against human CD45, CD44, CD147, CD29, CD34, or CD146 (BD Biosciences, San Jose, CA) and analyzed on a FACSCalibur flow cytometer (BD Biosciences).

Chondrogenic Differentiation in 3D Pellet Culture

Passage 5 hMSCs were used for chondrogenic differentiation. For forming each pellet, aliquots of 2.5×10^5 hMSCs in 0.5 ml medium were centrifuged down in a 15 ml conical tube at 150×g for 5 minutes at room temperature [104]. Chondrogenic differentiation was induced by chondrogenic medium composed of DMEM-high glucose, supplemented with 1% ITS+Premix (BD Bioscience), 1% penicillin-streptomycin, 100 µg/ml sodium pyruvate (Invitrogen), 50 µg/ml ascorbic acid-2-phosphate, 40 µg/ml L-proline, 0.1 µM dexamethasone, and 10 ng/ml recombinant human transforming growth factor-beta3 (TGF-β3) (Lonza, Walkersville, MD). Undifferentiated hMSC (Ctrl) pellets were maintained in hMSC growth medium. Pellets were cultured at 37°C, 5% CO_2 with medium changes every 2-3 days for 24 days.

Encapsulation of hMSCs in PuraMatrix™ Hydrogel

PuraMatrix™ stock solution (1% w/v) (BD Biosciences) was sonicated for 30 mins to decrease its viscosity before use. Human MSCs were encapsulated in 0.5% PuraMatrix™ hydrogel at a concentration of 10^7 cells/ml following the manufacturer's protocol in 24-well cell culture inserts. Briefly, mixture of PuraMatrix and cells in a total volume of 100 µl was loaded into the insert. The gelation was initiated with 250 µl of media in the lower chamber and promoted with 400 µl of media on top. The media were changed twice in both the inserts and the wells to equilibrate the pH of the PuraMatrix. 250 µl of media was finally placed on top of the gel and 750 µl into the well. Chondrogenic differentiation was induced in encapsulated hMSCs in hydrogel, and they were fed on the same schedule as those for pellet cultures.

Heat Exposure

Human MSCs in chondrogenic(Chon) cultures were exposed to mild heat shock (HS) periodically on Day 2, 9, 16, and 23. The transient 1 hour heating at 41°C was performed using a cell culture incubator pre-calibrated with an accuracy of ± 0.2°C as described in previous study

[103]. The medium was changed after heating and the cells were back to the 37^{o}C incubator. The control samples stayed in the 37^{o}C incubator while the medium was changed at the same time as the heat shocked samples.

Histology and Immunohistochemistry

Chondrogenic pellets or 3D hydrogel samples were harvested for histological analyses on Day 17 and 24 during differentiation. They were fixed using 10% acid-formalin with 70% ethanol [105] for 45 minutes at 4 ^{o}C, and embedded in 2% agarose for easier handling, followed by dehydration in a graded ethanol series. The samples were then embedded in paraffin, and sectioned at a thickness of 5 μm using a Microm Rotary Microtome (Thermo Scientific, Walldorf, Germany). Thin sections were mounted in slides, stained for glycosaminoglycans (GAGs) with Safranin O and cell nuclei were counterstained with Weigert's iron hematoxylin. In addition, immunohistochemical analyses of collagen type I/II or aggrecan were performed to visualize collagen matrix distribution and confirm the aggrecan synthesis. Briefly, sections were deparaffinized, endogenous peroxidase was quenched by 3% H_2O_2 in methanol for 10 minutes at room temperature, and nonspecific antibody binding was blocked by incubation with 10% normal horse serum (for COLI&II) or goat serum (for aggrecan) for 20 minutes at room temperature. Monoclonal mouse anti-human antibodies to collagen type I (Sigma) &II (Developmental Studies Hybridoma Bank, University of Iowa, Iowa City, IA) (1:5800 & 1:43 dilutions in 10% horse serum in phosphate-buffered saline (PBS)) or chondroitin sulfate proteoglycan (CSPG) (Sigma) (1:100 dilution in 10% goat serum in PBS) were applied to sections as primary antibody at 4^{o}C overnight. Samples were then incubated with biotinylated horse anti-mouse IgG (for collagens) or goat anti-mouse IgM (for CSPG) secondary antibody (Vector Laboratories, Burlingame, CA) (1:50 dilution), for 30 minutes at room temperature

followed by a peroxidase-based Vectastain ABC kit (Vector Laboratories). Samples were stained with diaminobenzidine (DAB) substrate kit (Vector Laboratories) and mounted with Clear-Mount aqueous mounting medium (Electron Microscopy Sciences, Hatfield, PA) before viewing. Images were captured with a Zeiss Axiovert 25 C inverted microscope.

Biochemistry

Pellet and hydrogel samples (n=4) harvested on Day 10, 17 and 24 during chondrogenesis were weighed wet, lyophilized overnight, and then weighed dry. Following that, samples were homogenized and digested in 13.22 mg/ml pepsin in 0.05N acetic acid at 4^{o}C for 48 hrs. The reaction was neutralized by 10X tris buffered saline (pH: 8). Total sulfated glycosaminoglycan (sGAG) content was then determined using quantitative 1.9-dimethylmethylene blue (DMMB) assay based on a chondroitin-6 sulfate standard curve. Absorbance was read at 595 nm using a BioTek Instruments microplate reader (Synergy 4, Winooski, VT). sGAG content was normalized to wet weight of each sample.

Statistical Analysis

All values were expressed as mean ± standard deviation (SD) and analyzed statistically using analysis of variance (ANOVA) test and a two-tailed Student's t-test. The level of significance was set at $p<0.05$.

3.3 Results

Expression of Surface Markers in Isolated hMSCs

Passage 4 of isolated hMSCs was characterized by staining for a set of surface markers including CD44 (hyaluronan receptor), CD29 (integrin β1), CD147 (extracellular matrix metalloproteinase inducer), CD146 (melanoma cell adhesion molecule), CD45 (leukocyte common antigen) and CD34 (lipopolysaccharide receptor). CD34 and CD45 are surface markers

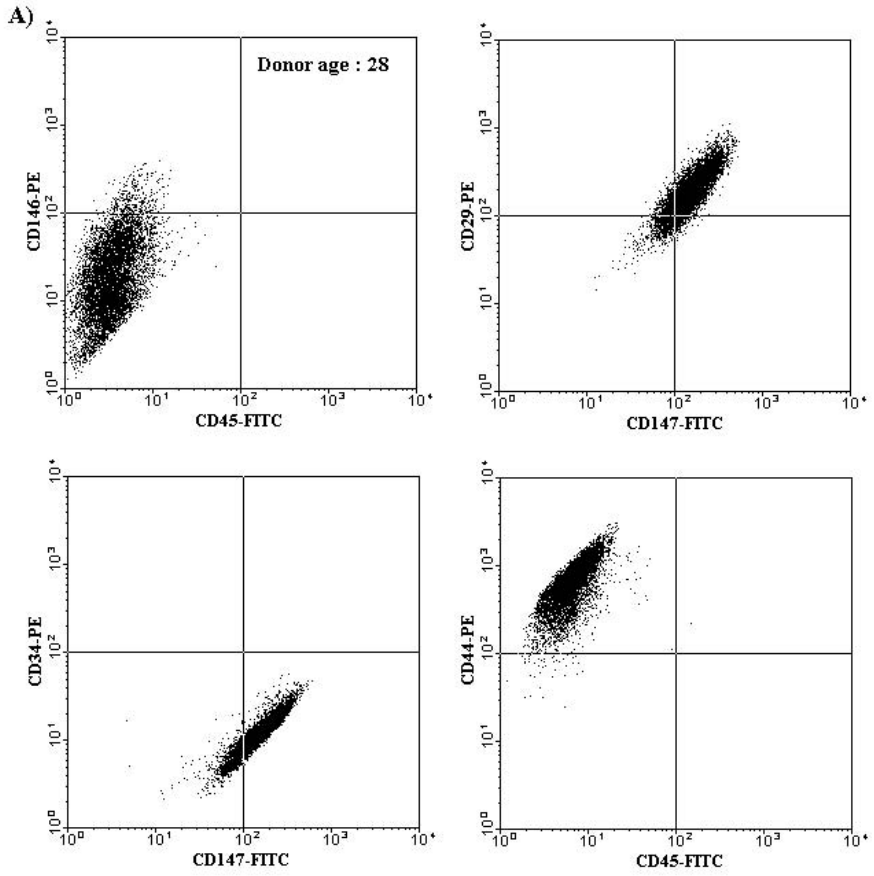

B)

FACS analysis				
hMSCs, 28 yr	**CD146+**	**CD29+**	**CD147+**	**CD44+**
	3.85% ± 0.64%	88.03% ±0.57%	81.65% ±2.29%	99.52% ±0.13%
	CD45-		**CD34-**	
	0% ± 0.01%		0% ± 0%	

Figure 3.1. Characterization of hMSCs by flow cytometric analysis. **(A)** Isolated hMSCs were positive for surface markers CD146, CD29, CD147 and CD44, and negative for CD45 and CD34. **(B)** The individual percentages of each surface marker expressed in these cells from the quantitative FACS analysis. Data represent the mean ± SD (n=3).

of the hematopoietic lineage, and CD146 is the surface marker of endothelial cell lineage, an epitope suggested as a biomarker for MSCs. Flow cytometric analysis showed that isolated hMSCs were slightly positive for surface marker CD146, positive for CD29, CD147 and CD44,

and negative for CD45 and CD34 (**Fig. 3.1(A)**). Quantitative results from FACS analyses of these cells were shown in **Fig. 3.1(B)**. The individual percentages for surface markers CD146, CD29, CD147, CD44 expressed in these hMSCs were 3.85 ± 0.64%, 88.03 ±0.57%, 81.65 ±2.29%, and 99.52 ±0.13%, respectively, and none of cells were revealed to express CD45 and CD34 (0%).

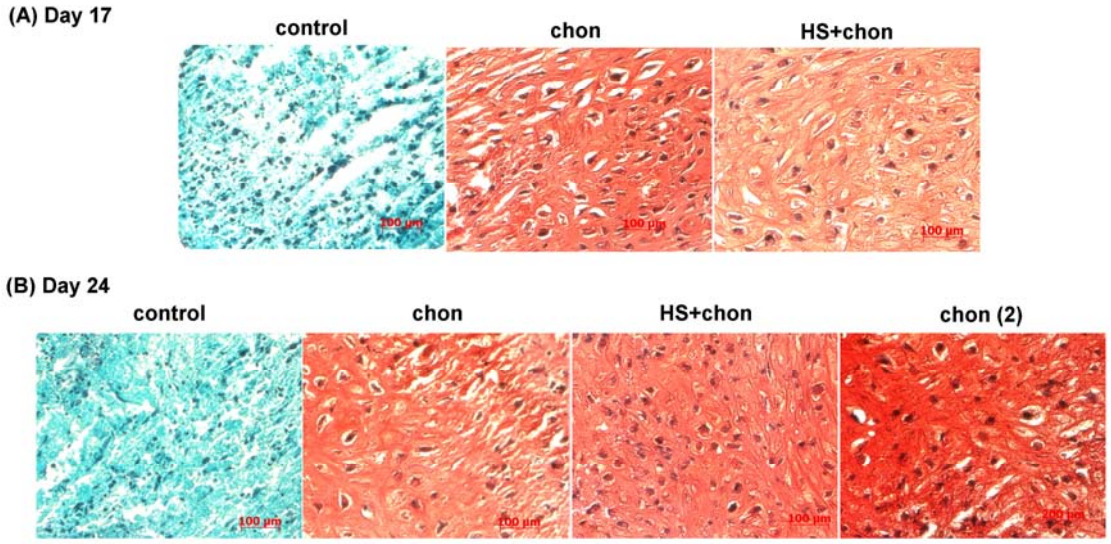

Figure 3.2. Representative images of Safranin O staining of GAGs in pellet culture samples on **(A)** Day 17 **(B)** Day 24. Scale bar: 100 μm. (control: undifferentiated hMSCs, chon: chondrogenic differentiated hMSCs, and HS+chon: chondrogenic differentiated hMSCs with heat shock).

Accumulation of GAGs and sGAG Content

As shown in **Figure 3.2**, GAGs were abundantly synthesized in the pellet samples treated with chondrogenic medium compared with control samples on both Day 17 and 24. However, Safranin O staining of GAGs did not show a consistently increased or decreased GAG synthesis by periodic heat shock in 3D pellet culture as visualized by the intensity of the staining.

Biochemical analyses demonstrated that periodic heat shock stimulated a ~1.5-fold increase in sulfated GAG (sGAG) content in 3D pellet culture on Day 10 (**Fig. 3.3(A)**, $p<0.05$)

and a ~2-fold increase in 3D hydrogel culture on Day 17 (**Fig. 3.3(B)**, $p<0.005$) relative to non heat-shocked controls. sGAG content increased with time in chondrogenic culture in pellets through Day 24 (**Fig. 3.3(A)**); in contrast, a nearly constant amount of sGAG was retained in 3D hydrogel culture by Day 24 compared with Day 17 (**Fig. 3.3(B)**). In addition, significantly lower (~1.5-fold) sGAG content was found in heat-shocked pellets compared with sGAG amount in non heat-shocked pellets on Day 24 (**Fig. 3.3(A)**, $p<0.05$).

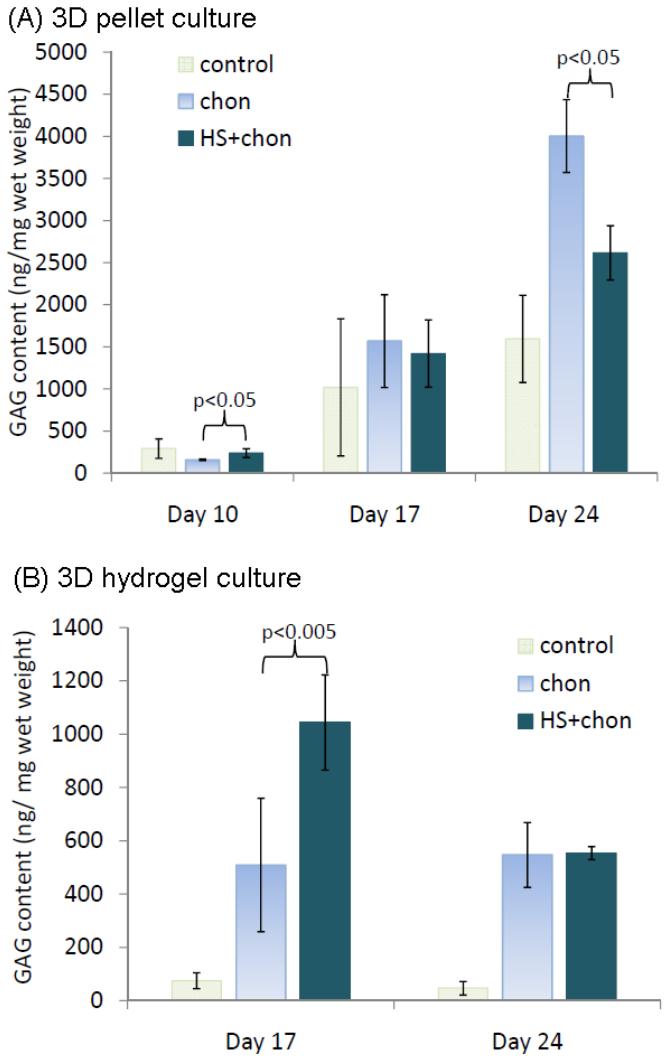

Figure 3.3. Sulfated GAG (sGAG) content normalized to wet weight in **(A)** 3D pellet culture on Day 10, 17 and 24, and **(B)** 3D hydrogel culture on Day 17 and 24, with and without HS. Data represent the mean ± SD (n=4). P values were calculated using ANOVA and Student t-test.

Distribution of Collagen Type I/II

Immunohistochemical (IHC) analyses revealed a weaker staining of collagen type II in heat-shocked pellets than non heat-shocked pellets on both Day 17 and 24 (**Fig. 3.4**), whereas almost no difference was observed in the staining of collagen type I with the effects of periodic heat shock throughout the culture period (**Fig. 3.5**). Also, chondrogenic pellets exhibited a more intensely stained collagen type II matrix with even more on Day 24 than Day 17, but for collagen type I, staining was primarily confined to the pericellular regions and it was less intense and uniform compared with collagen type II (**Figs. 3.4&3.5**). Little or no staining was seen in all the negative control samples.

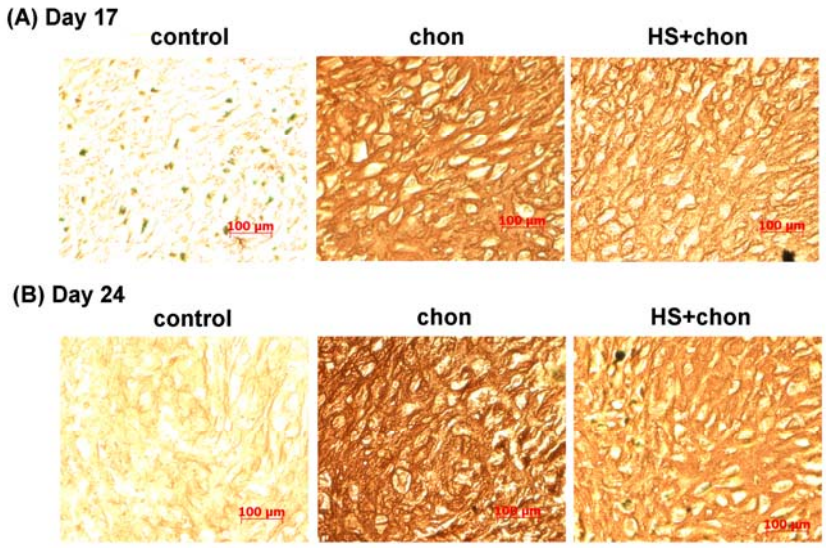

Figure 3.4. Representative images of immunohistochemical staining of collagen type II in pellet culture samples on **(A)** Day 17 **(B)** Day 24. Scale bar: 100 µm. (control: undifferentiated hMSCs, chon: chondrogenic differentiated hMSCs, and HS+chon: chondrogenic differentiated hMSCs with heat shock).

Aggrecan Synthesis

A modestly more intense staining of chondroitin sulfate proteoglycan (CSPG) by heat shock on Day 17 was observed .The staining for aggrecan was uniformly distributed and densely localized in the cell-associated regions (**Fig. 3.6**).

3.4 Conclusion and Discussion

This study is the first to investigate the direct heat shock (HS) effects on chondrogenic differentiation of hMSCs in the pellet and 3D hydrogel cultures. It was shown that in-house isolated hMSCs that undergo chondrogenesis produced cartilage-like matrix rich in GAGs, aggrecan and type II collagen, meanwhile, periodic HS at 41^{o}C for 1 hr once per week, was able to increase the sulfated GAG content (**Fig. 3.3**) in both 3D pellet and hydrogel cultures, as well as enhance the aggrecan synthesis in pellet culture (**Fig. 3.6**) on early differentiation days. These results support the hypothesis that mild HS may facilitate the earlier differentiation of hMSCs into mature chondrocytes, and thus it could be a simple and non-invasive approach for enhancing the regeneration of articular cartilage using stem cells.

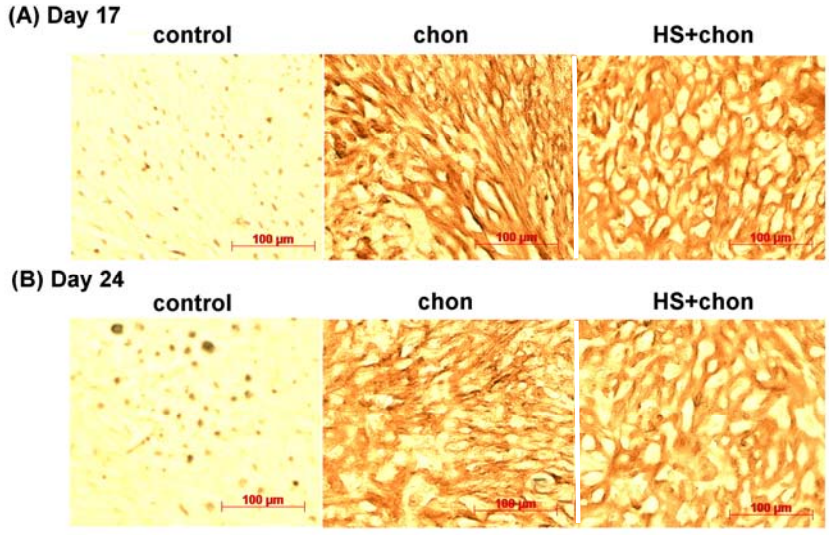

Figure 3.5. Representative images of immunohistochemical staining of collagen type I in pellet culture samples on **(A)** Day 17 **(B)** Day 24. Scale bar: 100 µm. (control: undifferentiated hMSCs, chon: chondrogenic differentiated hMSCs, and HS+chon: chondrogenic differentiated hMSCs with heat shock).

MSCs have been shown to differentiate into chondrogenic lineage *in vitro* using a high cell density pellet culture system [106], which mimics the mesenchymal condensation in embryonic development of cartilage tissue, with transforming growth factor β (TGF-β) superfamily members, TGF-β1 or TGF-β3 [104, 107]. Typical protein or gene markers used for the chondrocyte phenotype identification include type II collagen and aggrecan [73], which are the two major extracellular matrix (ECM) components of cartilage. The effects of periodic HS on hMSC chondrogenesis in both conventional 3D pellet culture and peptide hydrogel culture were evaluated through ECM accumulation and compared between samples treated with or without HS.

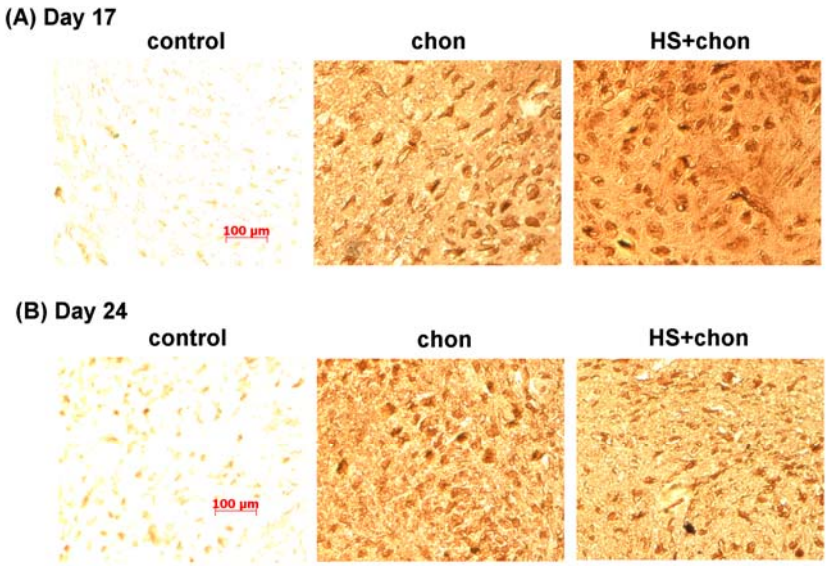

Figure 3.6. Representative images of immunohistochemical staining of aggrecan in pellet culture samples on **(A)** Day 17 **(B)** Day 24. Scale bar: 100 µm. (control: undifferentiated hMSCs, chon: chondrogenic differentiated hMSCs, and HS+chon: chondrogenic differentiated hMSCs with heat shock).

The production of a cartilaginous matrix in the chondrogenic pellets after 2 weeks in culture was verified by histological staining with Safranin O for sulfated GAGs (sGAGs) (**Fig. 3.2**). There were some variations within the group of chondrogenic pellet samples with or

without effects of HS. In addition, the central region of all chondrogenic pellets was stained more intensely for sGAGs than the periphery (data not shown). Therefore, a quantitative sGAG assay was used to better evaluate the differences of sGAG production between heat shocked and non-heat- shocked pellet or hydrogel samples. Biochemical analyses revealed that periodic HS significantly increased sGAG content at early stage of differentiation in both 3D pellet and hydrogel cultures on Day 10 and 17 respectively (**Fig. 3.3**). Hydrogel seemed to slow down the differentiation process compared with pellets and thus the enhancement effects from HS were still significant in hydrogel a week later than that in pellets, which was similarly observed in our previous study of heat shock effects on osteogenesis [103]. Consistent with earlier reports on chondrogenesis of hMSCs in pellet culture [104], abundant accumulation of sGAGs was found after 2 weeks and increased over time to 3-4 weeks in pellet culture. In contrast, the level of retained sGAGs was maintained in peptide hydrogel in the final week of culture without much increase. This is different from results of a previous study in which chondrogenesis of MSCs was investigated also using PuraMatrix [101]. This study showed an increase of sGAG content from 2 to 3 weeks in culture. And PuraMatrix was shown to retain sGAGs in the hydrogel compared to other types of materials. The differences may be due to: (1) Bovine MSCs were used in their study and hMSCs were used in this study, and the different cell type may behave differently; (2) Their sGAG content has not been normalized while normalization to wet mass was used in this study. Besides, sGAGs produced and lost to the medium were not quantified in this data reported, whether they are negligible compared with the total sGAGs is to be determined. Interestingly, HS decreased the sGAG content in pellets on Day 24 (**Fig. 3.3A**), which was possibly because that HS speeded up the chondrogenic differentiation of hMSCs in pellet culture and enhanced the earlier maturation which resulted in hypertrophic chondrocytes with less sGAGs at late days.

Another possible reason may be that one more cycle of periodic heating enhanced sGAG solubility in the surrounding medium, which needs further investigation.

Immunohistochemical (IHC) staining was used to investigate HS effects on the protein expression of other ECM molecules present in chondrogenic pellet cultures of hMSCs, including type II collagen, type I collagen, and aggrecan. In agreement with other studies [104, 108] , type II collagen showed an increase in protein expression over time from 2 to 3 weeks in pellet cultures (**Fig. 3.4**). However, as shown by IHC analyses, periodic HS at 41^{o}C downregulated type II collagen expression on both Day 17 and 24. HS may have increased type II collagen expression on days even earlier than Day 17, as previous studies on gene expression have reported that type II collagen showed a gradual increase since Day 8 [107]. In addition, the possible reasons of observed decrease in collagen type II staining with HS may be two: (1) 41^{o}C may not be the optimized heating temperature for enhancing the chondrogenesis although it proved to be most effective for osteogenesis in the previous study [103]; (2) heating may increase the solubility of collagen type II in the medium. Also, it is not known that the antibody for collagen type II in this study was specific for denatured or native collagen, thus no conclusive remarks can be drawn at this point, on whether this phenomenon with the effects of HS was beneficial or not. Further study will be performed to differentiate between the two. In contrast, chondroitin sulfate proteoglycan (CSPG) staining was more intense in heat shocked pellets than nonheat shocked ones on Day 17 (**Fig. 3.6A**), and CSPG is a major component of aggrecan. Aggrecan was known as the most abundant proteoglycan in cartilage. Thus this supports our hypothesis that HS enhanced the maturation of chondrocytes from hMSCs in pellet culture at early days. Moreover, since type I collagen was regarded as an important ECM molecule during early chondrogenesis [109] and a marker for fibrocartilage [110], we also assessed its protein

expression in this study. Type I collagen appeared to be unchanged during culture and unaffected by HS, and it was expressed substantially less than either type II collagen or aggrecan from our observations (**Fig. 3.5**). Gene expression study also revealed that type I collagen was present throughout the differentiation in hMSC chondrogenic pellet culture [111]. These findings suggest that a fibrocartilage-like phenotype is present in chondrogenic MSC pellet cultures and the overlap regions in the staining patterns of type I and II collagens may indicate that cells were experiencing a gradual transition between fibroblastic and chondrocytic phenotypes.

In order to further investigate if HS may accelerate the maturation process and lead to hypertrophy chondrocyte stage in a much shorter differentiation period, type X collagen expression is currently under evaluation. Type X collagen is considered as the marker for late-stage chondrocyte hypertrophy [71, 112] that is associated with endochondral ossification during skeletal development, in which mature chondrocytes undergo a terminal differentiation process of hypertrophy, mineralization, and apoptosis, and eventually the cartilage is replaced with mineralized bone [109, 113]. This is supported by the observation of a few distinct cells with increased cell size characteristic of hypertrophic chondrocytes in type II collagen staining (**Fig. 3.4**).

In summary, the overall results of this study showed that periodic HS facilitated chondrogenic differentiation of hMSCs when treated for about three weeks. We had previously reported the promotion of osteogenesis in hMSCs by periodic HS [103]. Taken together, these two reports show that HS may be useful for repairing full-thickness joint defects involving both cartilage and bone, such as in the late stage of OA, which requires cartilage, hypertrophic cartilage and bone regeneration from differentiation of implanted hMSCs. The intensity, interval and duration of heat stimulation used in this study can be further optimized to have well-

controlled effects and achieve the desired differentiation results using hMSCs. On the other hand, by improving *in vitro* differentiation protocols with HS, hMSCs can be used to generate constructs with cartilaginous properties that are similar to those produced by mature chondrocytes. Furthermore, 3D hydrogel culture systems may better recapitulate these regulatory mechanisms of *in vivo* chondrogenic differentiation of hMSCs and chondrocyte maturation. Therefore, RAD16-I self-assembling peptide hydrogel used in this study will be further investigated on the histological and immunohistochemical analysis of encapsulated hMSCs. Quantitative analysis such as real-time RT-PCR can be done to verify whether the gene expression of markers relevant to chondrocyte maturation and hypertrophy with the effects of HS is consistent with the biochemical and histological observations of chondrocyte phenotype in this study. Future studies will also evaluate the expression of heat shock proteins (HSP70 etc.) to study the mechanisms of HS-enhanced hMSC chondrogenic differentiation. The *in vitro* hMSC model in this study will guide the design of a thermal treatment protocol to generate a successful bioengineered cartilage from hMSCs for clinical joint repair.

CHAPTER 4 DEVELOPMENT OF A LOW-INTENSITY PULSED ULTRASOUND (LIPUS) SYSTEM FOR THERMAL TREATMENTS OF HUMAN MESENCHYMAL STEM CELLS

4.1 Introduction

Low-intensity pulsed ultrasound (LIPUS) has proven useful for bone fracture healing in both animal models [114-116] and clinical studies [117-119]. Clinical studies demonstrate that LIPUS stimulation with 1.5 MHz frequency, 1 kHz pulses, 20% duty cycle, and 30 mW/cm^2 I_{SATA} (spatial average temporal average) intensity at 20 minutes/day accelerates the fresh fracture healing and resolves the non-unions in bone [120-122]. Thus a commercially available medical device (Exogen) was approved by Food & Drug Administration (FDA) in 1994 using the same US parameters [123]. In addition, for cartilage repair, LIPUS has been shown to promote the repair of damaged cartilage in rabbits [124], and protect cartilage from degeneration in experimental osteoarthritis (OA) of animal models [125-127].

Effects of an ultrasound (US) treatment have also been investigated in cell culture and differentiation, including chondrocytes [128], osteoblasts [129, 130] and mesenchymal stem cells (MSCs) [131-134]. MSCs can be differentiated into osteoblasts, and chondrocytes, and therefore are excellent alternative cell source for the study of LIPUS effects on bone or cartilage regeneration. LIPUS has been demonstrated to enhance the chondrogenic differentiation of MSCs *in vitro* [135]. Direct effects of LIPUS on differentiation of MSCs into osteoblasts *in vitro* have also been studied [136]. Several studies using LIPUS have been reported previously. LIPUS treatment (1.5 MHz, 30 mW/cm^2) at 20 min per day for 2 weeks has been shown to enhance the mineralization in rat osteoblasts [137]. In another study, LIPUS (frequency 1 MHz, duty cycle 20%, pulse repetition frequency (PRF) 1 kHz, intensity 580 mW/cm^2) at 10 min per

day for 1-5 days induced proteoglycan synthesis in bovine chondrocytes [138]. However, the underlying mechanisms for osteogenic or chondrogenic effects of LIPUS remain unclear, and an optimal protocol of US stimulation still needs further investigation. Moreover, US effects in general are composed of thermal and non-thermal effects [139, 140], and non-thermal parts include acoustic streaming (a steady circulation of fluid) and cavitation [141, 142]. Most cell-related ultrasound studies focused on non-thermal stimulations of US , while whether those effects were due to thermal or non-thermal factors was unknown.

Regarding to optimal US parameters, previous studies have found that LIPUS system with different parameters, such as intensity, ultrasound frequency, duty cycle, and pulse repetition frequency (PRF), can have various ultrasonic effects on the cell types tested [136, 143, 144]. Among all these parameters, spatial-averaged temporal-averaged intensity (I_{SATA}) was the focus of many studies [145-147]. Ultrasound frequency, a relatively unimportant parameter of LIPUS (most commonly at 1.5 or 1 MHz), has shown little difference [114, 115]. Different duty cycles have been less investigated as well as PRF. Furthermore, it was known that 1 kHz PRF might be among the best for stimulating osteogenesis of hMSCs in terms of calcium deposition [144]. It was also reported that an optimal intensity of US treatments for hMSC chondrogenesis was 30 mW/cm^2 [148]. Varied US stimulation durations were investigated and 20-minutes daily US treatments seemed more effective for bone [149-151]. Thus designing a custom LIPUS system with optimal US parameters including thermal effects specifically for enhancing bone and cartilage regeneration is the goal of this study.

In summary, since we have shown positive enhancement results from previous studies on heat shock effects on hMSC osteogenesis using incubator heating [103], this study is focused on the development of an optimized custom-made US device with a heating ability to investigate the

thermal and non-thermal effects on hMSC osteogenic differentiation. Non-invasive and easily applicable LIPUS devices may have a promising therapeutic potential to deliver heat to the joints and provide treatments for OA patients during stem cell therapies.

4.2 Materials and Methods

An ultrasound device composed of a 12-well plate and 3×2 transducer matrix was designed to deliver heat for the hMSC osteogenesis (**Figure 4.1**). Plane wave and focused wave transducers (Ultran Group, #WS50-1-P50) elements (1 MHz) were assigned to osteogenic culture wells. In order to find a suitable initial distance between the culture plate and transducers aiming a uniform temperature profile in the well, US intensity simulation using Field II software based on Matlab platform (available at http://field-ii.dk/, developed by Dr. Jørgen Arendt Jensen at the Technical University of Denmark) was performed. The parameters used for focused transducer in the design, were center frequency 1 MHz, diameter 0.5 inch, focal length 2 inches.

The US system was calibrated without cells; intensity distribution was measured using 0.2 mm polyvinylidene fluoride (PVDF) needle hydrophone (Precision Acoustics Ltd., UK). The hydrophone measurements of the relative intensity distributions were performed through the acrylic column (length = 8 cm) filled with distilled water at the distances of 1.8-7.8 cm (increment = 0.2 cm) from the surface of transducer. A multi-channel tone burst pulser/receiver (Ultratek, Concord, CA, model #USB-UT350MT) was used to generate the input signals of which parameters including pulse repetition frequency (PRF), duty cycle can be adjusted through programming with Software Development Kit from Ultratek. In order to briefly validate the heating ability of the US system, the temperature increase induced by US was recorded using the tip of a T type thermocouple (Omega Engineering, Inc., Stamford, CT) put in contact with the bottom of the plastic culture well filled with 1 ml of distilled water, with the plate lid covered.

The ultrasound exposures were administered with the frequency of 1 MHz, duty cycle of 1.5%, and pulse repetition frequency of 1 kHz, and the acrylic column length was 5 cm.

The temperature measurement system in a well of a 12-well plate was set up using 7 pre-calibrated NTC thermistors (#NTSD1XH103FPB30) evenly placed at different spots inside the culture well, and real-time data of the temperature changes were acquired using a DAQ card (National Instruments, Austin, Texas) and displayed using LabVIEW(National Instruments).

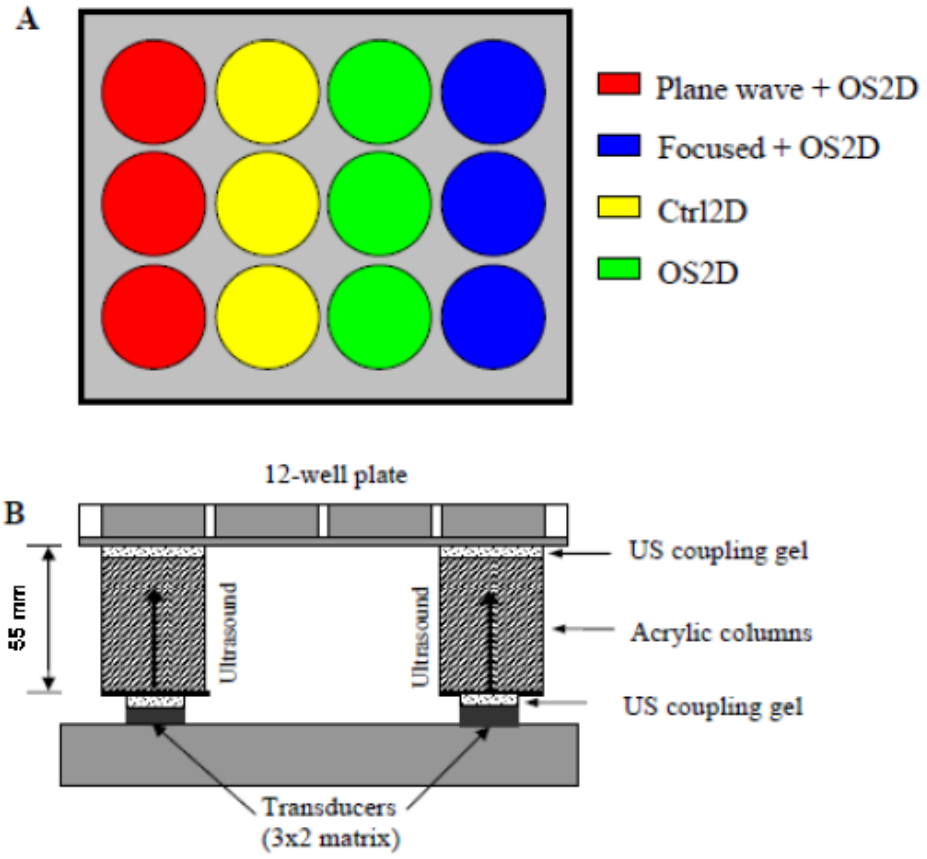

Figure 4.1. Schematic representation of the ultrasound device developed for thermal stimulation during hMSC osteogenic differentiation. **(A)** The plate layout of 12-well plate with four different conditions in triplicates. Three plane wave transducer elements and three focused transducer elements are assigned to osteogenic culture wells **(B)** The cells will be seeded in the plate and located 55 mm above the transducers' surfaces.

4.3 Results

The US intensity distribution was simulated using the parameters described in a previous study [138] as a relatively homogeneous temperature profile was achieved on the whole well area, at the distance they chose between cell culture plate and transducers. Thus based on the comparison of simulation results using focused transducers in the previous study [138] and the design, an initial distance can be chosen in the design. **Figure 4.2(A)&(C)** showed the z-x plane intensity distribution and normalized intensity distribution of the radial plane for the previous study; **Figure 4.2(B)&(D)** was a comparison for the design. The distance of z=55 mm was chosen at which the relative ultrasound intensity to the whole z-x plane intensity field in our transducer resembles that at the distance of z=110 mm chosen in that study. Meanwhile, **Fig. 4.2(C) & (D)** showed respectively the circular focal area for the transducer used in that study and the design.

As shown in **Figure 4.3**, the custom-built LIPUS device for thermal treatments of hMSCs during osteogenesis was developed based on the design in **Figure 4.1**. The measured ultrasound intensity distribution by hydrophone through the well, showed a clear peak at the center of the non-uniform field (**Fig. 4.5(A)**). Hydrophone also verified the formation of a circular focal point at a distance around 4.8 cm from the surface of focused transducer (**Fig. 4.5(B)**).

Figure 4.4 was a screen-shot of temperature measurements in real-time using 7 calibrated thermistors in LabVIEW. Moreover, the feasibility of using this US system for heating was verified by an initial experiment with the frequency of 1 MHz, duty cycle of 1.5%, and pulse repetition frequency of 1 kHz, resulting in a temperature increase of 0.1^{o}C every 3 minutes.

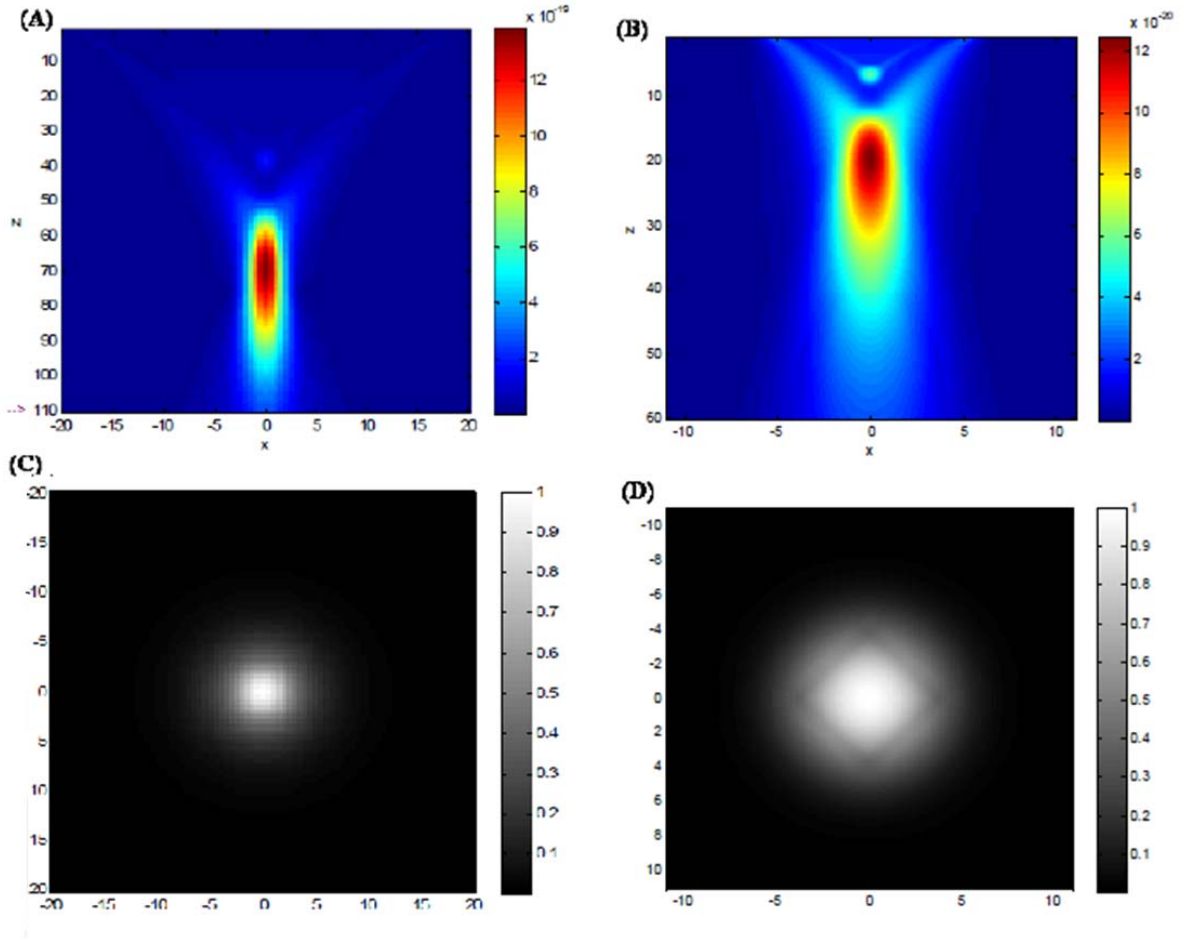

Figure 4.2. Comparison of simulation results using focused transducers in the previous study [138] and the design. **(A)** z-x plane intensity distribution at z=0-110 mm and **(C)** normalized intensity distribution of the radial plane at z = 110 mm away from the surface of the transducer used in the previous study [138]; **(B)** z-x plane intensity distribution at z=0-60 mm and **(D)** normalized intensity distribution of the radial plane at z = 55 mm away from the surface of the transducer used in the design.

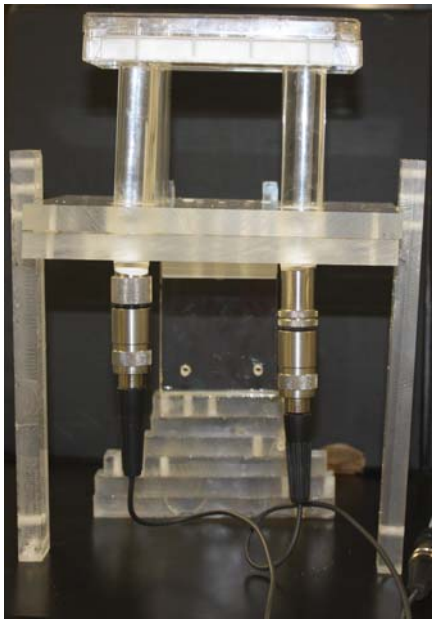

Figure 4.3. The real assembly of the custom LIPUS system composed of both focused and plane wave transducers, acrylic column for ultrasound wave transmission, and 12-well plate for cell seeding. The transducers were connected to and excited by a multi-channel tone burst pulser/receiver where the different parameters (PRF, duty cycle etc.) of input signals can be adjusted.

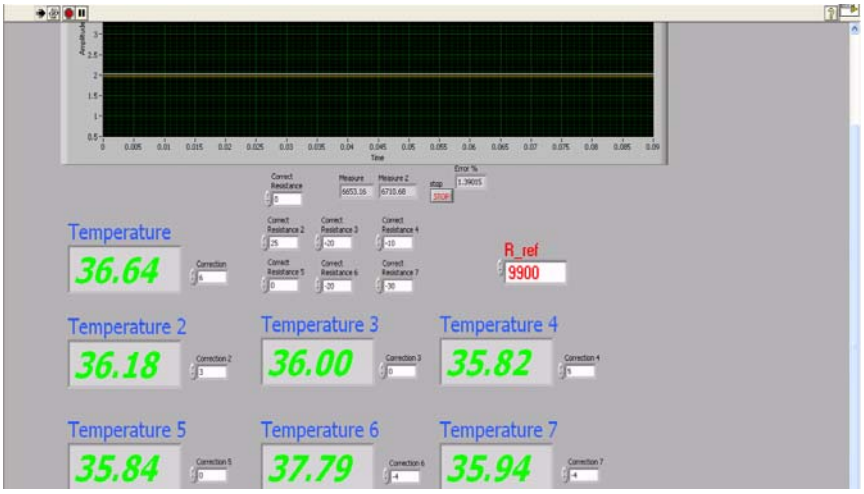

Figure 4.4. The front panel of LabVIEW program displaying the real-time temperature readings simultaneously from the 7 individually calibrated thermistors placed at different locations inside one well of 12-well cell-culture plate.

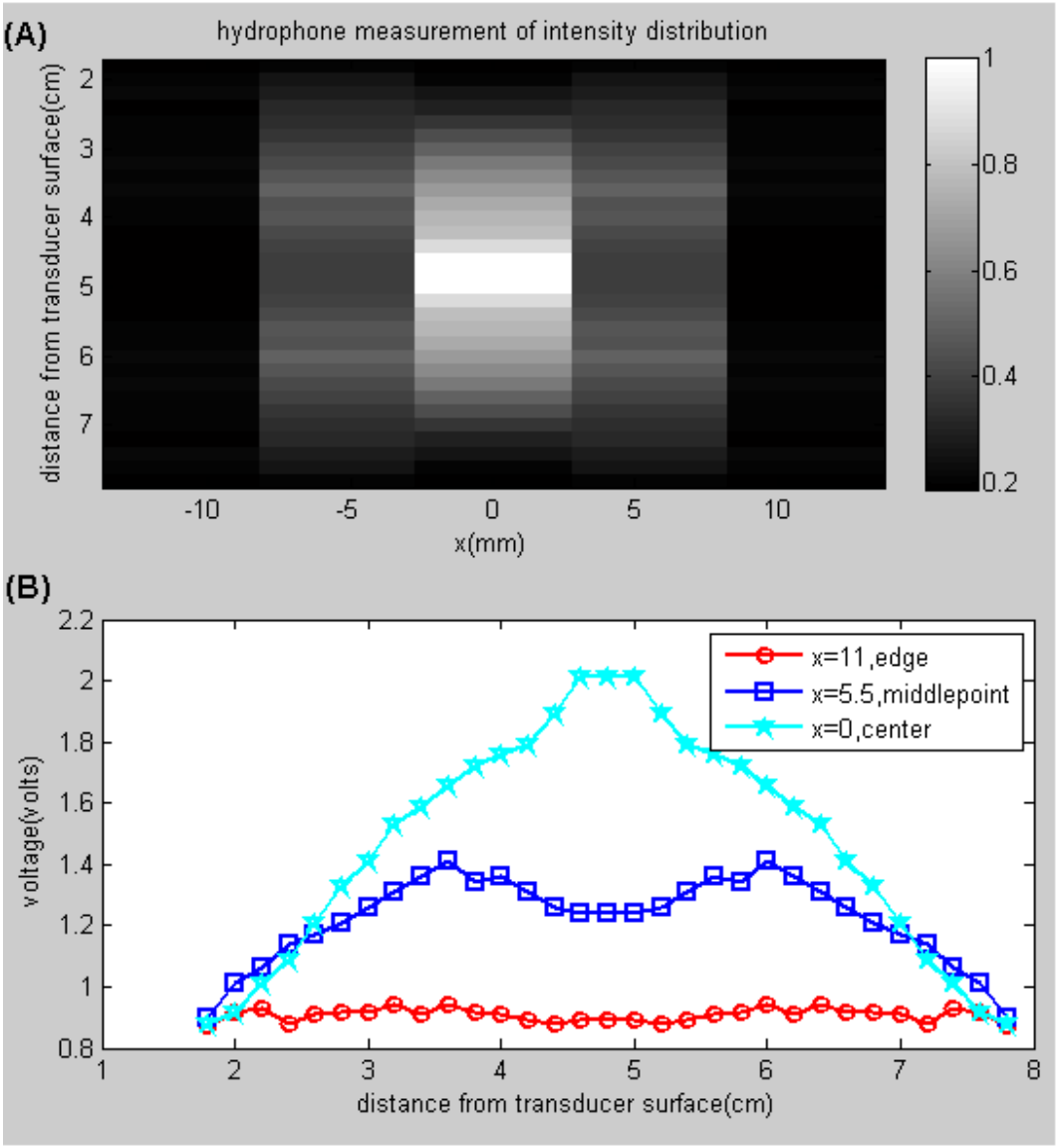

Figure 4.5. US intensity distribution through a well of the 12-well culture plate measured by hydrophone at distances of 1.8-7.8 cm (increment = 0.2 cm) from the transducer's surface. **(A)** A clear intensity peak was shown between distance=4.5 and 5 (cm) at center x=0 by the grayscale image, **(B)** Three individual curves showing the change of voltages (volts) over the measured distances taken at x=0, center, x=5.5cm, middle-point, and x=11cm, edge of the well respectively.

4.4 Conclusion, Discussion and Future Works

The simulation results are useful to guide the device design so that a more defined intensity distribution and evenly distributed temperature profile over a cell culture well can be

achieved. There was a clear intensity peak at the center of the field using a focused ultrasound transducer in the current design from simulation (**Fig. 4.2 (D)**), which was consistent with that observed from the actual measurement (**Fig. 4.5 (A)**). However, due to the limitation of simulation, and simplified conditions and assumptions (e.g., zero attenuation was assumed) used in the simulation, the simulation may not be able to predict an intensity distribution as accurate as that determined in experiments. And with few points roughly measured from hydrophone, it was not possible to have detailed information on the real intensity distribution.

The temperature measurement from multiple well-calibrated thermistors inside the well was taken to balance the variations that possibly exist at different spots of the well due to the ultrasound heating. Thus the average and standard deviation of readings from these points can represent the temperature changes at different time period. To take into account the higher attenuation coefficient of the acrylic material as couplant compared with standard water as propagating medium [152], a shorter distance less than the focal length between the transducer and the 12-well plate may be considered in the future.

Furthermore, the preliminary results from device calibration suggest that focused transducer resulted in a faster temperature rise than plane wave transducer in the well at the same distance away from transducer surface (data not shown), which made possible the control of temperature differently using these two transducers through adjustment of different parameters for excitation.

The goal of using this US system is to control the temperature in the wells from 39 to 41 ^{o}C for 1 hr using focused ultrasound or constant 37 ^{o}C using plane-wave ultrasound. Osteogenic results from US treated samples with or without heating in this setting would decouple the effects of US on osteogenesis between the thermal stimulation and mechanical loading. The

results from thermal treatments of hMSCs by ultrasound can be compared with results in Chapter 2, which is about effects of heat shock by direct incubator heating on hMSC osteogenesis [103].

Further calibration of ultrasound intensity distribution by hydrophone and parameter (intensity, frequency, and duty cycle etc.) optimization of LIPUS system will be done to achieve the desired heating temperature and effects. Further investigation of thermal effects on hMSC osteogenesis via an optimized LIPUS system will be followed. This *in vitro* model for the study of thermal effects on hMSC osteogenesis by US will guide the design of an US device for in vivo thermal treatments in bone and cartilage regeneration.

CHAPTER 5 SUMMARY

Tissue engineering combined with stem cells is an emerging field that offers great promises for tissue regeneration and repair of organ defects resulted from diseases, aging and trauma. Human MSCs from bone marrow can differentiate into osteoblasts and chondrocytes *in vitro* thus have significant implications for their use in bone and cartilage tissue engineering. Well-defined and efficient protocols to enhance maturity and promote specificity of osteogenesis and chondrogenesis of *in vitro* cultured hMSCs become an urgent need.

The mechanisms for the heat-enhanced osteogenesis and overexpression of HSPs during embryonic development are not clear and the thermal regulation of hMSC differentiation is not well studied. In the first part of this study, the direct effects of mild HS on the differentiation of hMSCs into osteoblasts in self-assembling peptide hydrogel and on tissue culture plates were investigated. Periodic 1 h HS at 41°C once a week during osteogenic differentiation significantly enhanced ALP activity and increased the mineralization. It also upregulated osteo-specific genes and HSP70 expression. These results demonstrate that HS induces an earlier osteogenic differentiation of hMSCs and enhances the maturation of osteoblasts differentiated from hMSCs. Therefore, mild HS treatment may be potentially used to enhance the bone regeneration from hMSCs. Our data will guide the design of *in vivo* heating protocols and enable further investigations in thermal treatments of MSC osteogenesis for bone tissue engineering.

In the second part of this study, the objective was to further investigate the effects of periodic HS on hMSC differentiation into chondrocytes in 3D pellet culture and self-assembling peptide hydrogel, PuraMatrix. Similarly, cells were exposed to 1 hr HS at 41 ^{o}C

once a week during chondrogenic differentiation for up to 24 days. Periodic HS increased sGAG synthesis in both 3D pellet and hydrogel cultures in the early stage of chondrogenesis. IHC analyses revealed enhanced aggrecan expression on Day 17. It confirmed that HS induced an earlier chondrogenic differentiation and facilitated the maturation of chondrocytes from hMSCs. However, collagen type II expression was downregulated on Day 24 in chondrogenic pellet culture with HS. The further maturation by HS might lead to hypertrophic chondrocytes in the late stage of chondrogenesis. The decrease of chondrogenic markers at late days may correlate with the phenomena similar to the process during endochondral ossification *in vivo*.

In order to translate these results into clinical useful applications, in the third part of this study, a custom-made LIPUS device with the heating ability was developed to explore the possibility of using ultrasound as a heat delivery tool for future in vivo studies. The goal was to use focused ultrasound transducers to increase temperature while plane-wave ultrasound transducers to maintain 37 ^{o}C. Decoupling of non-thermal effects and thermal effects from US will allow us to compare the US heating results with the direct incubator HS results, so that the efficacy of using US-based HS to stimulate hMSC differentiation can be determined.

Stem cells combined with tissue engineering is a promising technology for regenerative medicine. However a lot of work still needs to be done to explain why the maturation of osteoblasts and chondrocytes differentiated from MSCs is still not optimized and to elucidate the mechanism of MSC differentiation *in vivo*. The significance of studying thermal effects on hMSC osteogenesis and chondrogenesis is to guide the development of a therapeutic thermal treatment protocol to enhance stem cell differentiation during cell

transplantation. Thermal treatments are not expensive and non-invasive. LIPUS may have a promising therapeutic potential as a heat delivery tool to provide treatments for OA patients and facilitate bone and cartilage regeneration.

Appendix A. Protocol of Immunohistochemistry for Collagen Type I&II/ Aggrecan

For Day 1

1. De-paraffinize and rehydrate paraffin-embedded sample sections on the histology slides through citrisolv (3 mins), 100% ethanol (1 min), 95% ethanol (1 min), 70% ethanol (1 min), 50% ethanol (1 min), de-ionized water (1 min).
2. Use water-resistant pen to mark around samples.
3. For collagen type I&II staining, incubate samples in 0.5 mg/ml hyaluronidase in PBS, for 30 mins at 37^{o}C and rinse 2X with PBS. For aggrecan staining, neglect this step and go to step 4 directly.
4. Incubate samples in 0.5N acetic acid for 2 hours at 4 ^{o}C.
5. Rinse 2X with PBS.
6. Incubate samples in 3% H_2O_2 (hydrogen peroxide) in methanol for 10 min at room temperature. Note: Cover samples during incubation so H_2O_2 does not evaporate too quickly.
7. Rinse 2X with PBS.
8. Block samples with blocking solution (10% horse serum for COLI&II, 10% goat serum for aggrecan), and incubate for 20 min at RT.
9. Remove blocking solution but do not rinse.
10. Apply primary antibody or negative control diluted in blocking solution to cover samples and incubate overnight at 4 ^{o}C.
    A. For type I collagen, 1^{o} antibody dilution: 1:5800 (stock concentration 5.8 mg/ml), and negative IgG control antibody dilution: 1: 11000 (stock concentration 11 mg/ml)
    B. For type II collagen, 1^{o} antibody dilution: 1:43 (stock concentration 43 ug/ml), and negative IgG control antibody dilution same as A.
    C. For aggrecan, Anti-chondrotin sulfate (CSPG) 1^{o} antibody dilution: 1:100 (stock concentration 1.6 mg/ml) and negative IgM control antibody dilution: 1: 15.625 (stock concentration 250 ug/ml)

For Day 2

11. Rinse 2X with PBS.
12. Apply biotinylated secondary antibody diluted in blocking solution to cover samples and incubate for 30 min at RT.
    A. For type I&II collagen, biotinylated horse anti-mouse/anti-rabbit IgG(H&L) secondary antibody dilution: 1:50
    B. For aggrecan, biotinylated goat Anti-Mouse IgM secondary antibody dilution: 1:50

    While incubating: Make VECTASTAIN ABC Reagent: 1 drop of Reagent A and 1 drop of Reagent B in 2.5 ml PBS vortex and allow to stand for 30 minutes prior to use.
13. Rinse 2X with PBS.
14. Apply VECTASTAIN ABC Reagent to cover samples and incubate for 30 min at RT.
15. Rinse 2X with PBS.
16. Apply DAB substrate solution to cover samples. 5 min for COLI&II staining, 3 min for aggrecan staining. Immediately remove DAB and rinse 3X with tap water.

A. DAB: In 2.5 ml DI H_2O add 1 drop of Buffer Stock Solution and vortex. Then add 2 drops of DAB Stock Solution and vortex. Then add 1 drop of Hydrogen Peroxide Solution and vortex.

17. Cover samples using Clear-Mount aqueous mounting medium and place in oven at 45 ^{o}C for 45 min.
    Note: All DAB containing solutions must be treated with DAB Neutralizing solution. Dispose of all DAB containing solutions and pipette tips in the appropriate waste containers.

Catalog numbers of materials used in this protocol as belows,

- Type I collagen antibody – Sigma, cat. #C-2456
- Type II collagen antibody – Developmental Studies Hybridoma Bank, cat. #II-II6B3
- Water resistant pen – Vector Laboratories, cat.#H-4000
- Hyaluronidase Type IV-S – Sigma, cat. #H-4272
- VECTASTAIN ABC kit - Vector Laboratories, cat.# PK-6200 (Biotinylated secondary antibody and ABC reagent)
- DAB Substrate kit - Vector Laboratories, cat.# SK-4100
- Hydrogen Peroxide - Fisher Scientific, cat.# H325-100
- Clear-Mount aqueous mounting medium - Electron Microscopy Science, cat.#17985-12

Appendix B. Protocol of DMMB Analysis

Prepare DMMB dye (500 ml, pH 1.5, light sensitive)

- 8 mg DMMB
- 2.5 ml 100% ethanol
- 1 g sodium formate
- 1 ml formic acid

Prepare stock solution chondroitin sulfate C (Sigma C-4384) in a series of concentrations: 0.01 µg/µl, 0.1 µg/µl, 0.25 µg/µl, and 1 µg/µl using DI H_2O

Prepare standards according to the following table:

Standards	µg GAG	Stock Solution	Amt of stock (µl)	Amt of DI H_2O (µl)
1	0	N/A	0	5
2	0.01	0.01 µg/µl	1	4
3	0.02	0.01 µg/µl	2	3
4	0.05	0.01 µg/µl	5	0
5	0.1	0.1 µg/µl	1	4
6	0.2	0.1 µg/µl	2	3
7	0.5	0.1 µg/µl	5	0
8	0.75	0.25 µg/µl	3	2
9	1	0.25 µg/µl	4	1
10	1.25	0.25 µg/µl	5	0
11	2	1 µg/µl	2	3
12	5	1 µg/µl	5	0

In a 96-well plate,

1 For standards, add appropriate volumes of both stock and DI H_2O per well in triplicate.
2 For samples, add 5 µl of sample per well in triplicate.
3 Add 200 µl of DMMB dye to each well.
4 Read absorbance at 595 nm.

Appendix C. Protocol of Sample Preparation for DMMB Assay

Day 1

1. Record the weight of empty microcentrifuge tubes.
2. Record the wet weight of samples including the tubes.
3. Put samples on lyophilizer for overnight drying.

Day 2 Pepsin Digest

1. Prepare pepsin solution.

   Pepsin (4560 units/ml AA) :
   13.22 mg/ml solution in 0.05N Acetic Acid (for pepsin at activity of 345 units/mg solid), for example, weigh 0.0517g pepsin powder in 3.91 ml of Acetic Acid.
   Pepsin - Sigma, cat.# P7000-25G
2. Remove samples from lyophilizer. Record dry weight.
3. Pulverize using 0.5 ml pestle. Add 85 µl 0.05N Acetic Acid. Pulverize more.
4. Add 20 µl pepsin solution. Vortex to mix.
5. Rotate samples at 4^{o}C for 48 hrs.

Day 5

Stop pepsin digestion reaction:
Add 20 µl of 10X TBS #2 and vortex sample. Sample pH should be ~8.0 to neutralize pepsin.
<u>10X TBS #2</u>
1M Tris, 1.5M NaCl
For 100 ml:
12.114 g Tris
8.766 g NaCl
Dissolve in 70 ml sterile water. pH down to 8.0 (starts ~10.5). Fill to 100 ml. Readjust pH to 8.0.

Appendix D. Protocol of Histology Sample Processing

Day 1 Fixation and Dehydration

1. Rinse specimen in PBS
2. Fix samples for 45 minutes in Acid-Formalin at 4 ^{o}C
3. Rinse specimen in PBS for 2X
4. Embed specimen in 2% agarose
5. Transfer to vial and treat with 50% EtOH for 1 hr at 25^{o}C (room temp.)
6. Transfer to 70% EtOH for 1 hr at 25^{o}C
7. Transfer to 95% EtOH for 1 hr at 25^{o}C
8. Transfer to 95% EtOH for 1 hr at 25^{o}C
9. Transfer to 100% EtOH for 1 hr at 25^{o}C
10. Leave specimen at 4^{o}C overnight

Day 2 Clearing and Infiltration:

1. Transfer to 100% CitriSolv for 1 hr at 25^{o}C
2. Transfer to 100% CitriSolv for 1 hr at 55^{o}C
3. Transfer to 1:1 mixture of CitriSolv/Micro-cut Paraffin for 1 hr at 55^{o}C
4. Transfer to 1:1 mixture of CitriSolv/Micro-cut Paraffin for 1 hr at 55^{o}C
5. Transfer to 100% Micro-cut Paraffin for 1 hr at 55^{o}C
6. Transfer to 100% Micro-cut Paraffin overnight at 55^{o}C

Day 3 Embedding:

1. Transfer to 100% Micro-cut Paraffin for 1-2 hrs at 55^{o}C
2. Position specimen in Peel-Away mold with 100% paraffin
3. Allow specimen to harden overnight
4. Specimen may be sectioned the following day

Materials:

CitriSolv – Fisher Scientific, cat. # 22-143-975
Acid-Formalin/ETOH: (to make 100 ml)

1. Absolute Ethanol 70 ml
2. Glacial Acetic Acid 5 ml
3. Formaldehyde (37% stock) 10 ml
4. Distilled water 15 ml

Appendix E. Protocol of Human Mesenchymal Stem Cell Isolation

1. Prepare PBS+2% FBS+1mM EDTA solution. 100 ml is just enough for MSC isolation from10 ml size marrow. Preheat FBS.

2. Make sure bone marrow sample, PBS+2%FBS+1mM EDTA, Ficoll-Paque and centrifuge are all at room temperature.

3. Perform white cell count using 5% acetic acid. Add 50 µl of PBS+2% FBS+1mM EDTA solution, with 50 µl of fresh bone marrow aliquote, then mix with 100 µl of 5% acetic acid, and load about 20 µl into hemacytometer and count. In this case, final concentration need to be multiplied by dilution factor (=4).

4. For 10 ml size bone marrow, the actual total volume would be around 14 ml. So, divide the marrow into 2 50ml conical tubes. And add 50 µl RosetteSep Human Mesenchymal Stem Cell Enrichment Cocktail per ml of bone marrow and mix well. i.e. 350 µl to each tube.

5. Incubate 20 minutes at room temperature. Dispose everything in contact with blood carefully and sterile with 10% bleach.

6. Dilute sample with about same volume of PBS+2% FBS+1mM EDTA solution, e.g. 10 ml/tube for 10 ml marrow case, mix gently.

7. Prepare 2 50 ml conical tubes with 15 ml Ficoll-Paque/tube. Layer the diluted sample on top of Ficoll. Be careful to minimize mixing of Ficoll and sample. Tilt the tube to 45^{o}C, slowly add the sample drop by drop to form a layer on top.

8. Centrifuge at 300×g for 25 minutes. Set the centrifuge to brake off. (decel->0). Walk slowly to avoid moving the tubes.

9. Remove the enriched cells from the Ficoll-Paque: plasma interface, by inserting rubber-top pasteur pipet at the level of interface, and slowly moving it along the circular wall of the tube. Be sure not to touch the red pellet at the bottom. It is advisable to remove some of the Ficoll-Paque and a bit of upper plasma layer in order to ensure complete recovery of the desired cells.

10. Wash enriched cells with 5X the volume of PBS+2% FBS+1mM EDTA solution. Spin 300×g for 10 minutes (brake can be on).

11. Remove the supernatant and resuspend cells in 1 ml of MSCGM/tube. Perform a cell count again. Take 10 µl of cell suspension, mix with 10 µl of 5% acetic acid, load into hemacytometer and count. Dilution factor =2.

12. Seed cells into 1 T-75 flask finally for 10 ml size marrow. 12 ml of MSCGM was supplemented.

Ordering information:

- Fresh whole bone marrow, 10 ml – AllCells, LLC, cat.#ABM001

- RosetteSep Human Mesenchymal Stem Cell Enrichment Cocktail – Stemcell Technologies, cat.#15128
- Ficoll-Paque PLUS - Stemcell Technologies, cat.#07907

Appendix F. Protocol of Surface Marker Staining for FACS

1. Trypsinize the MSCs from the flasks. Number of flasks has been pre-calculated to acquire enough cells for the samples.
2. Resuspend cells using MSCGM in 50 ml conical tubes.
3. Filter the cell suspension into new 50 ml conical tubes through cell strainer caps.
4. Spin the cell suspension at 150×g for 5 minutes.
5. Carefully remove the supernatant and re-suspend the pellet in an appropriate volume of MSCGM. Count cells and then add appropriate volume of MSCGM to reach a concentration of 1 million cells/ml.
6. Distribute about 0.5 million cells per FACS tube in a volume of 500 µl per tube. Same condition has 3 triplicate tubes.
7. Add primary antibodies (FITC or PE-conjugated) to surface markers CD×× or negative IgG control antibodies (BD Biosciences), 10 µl for each. Depending on the labels of the tubes, one tube can be a combination of two antibodies with different dyes.
8. Incubate for 20 minutes on a shaker at RT to prevent aggregation.
9. Washing 2X:
    - add 2 ml of MSCGM
    - centrifuge the tube at 150 g for 5 minutes
    - pipet off the supernatant

    Then add 500 µl of MSCGM per tube. Use samples for FACS analysis.

Appendix G. Incubator Heating Calibration Curve

The thermocouple was measuring the temperature cells experienced when they were put in an incubator pre-calibrated at 41°C.

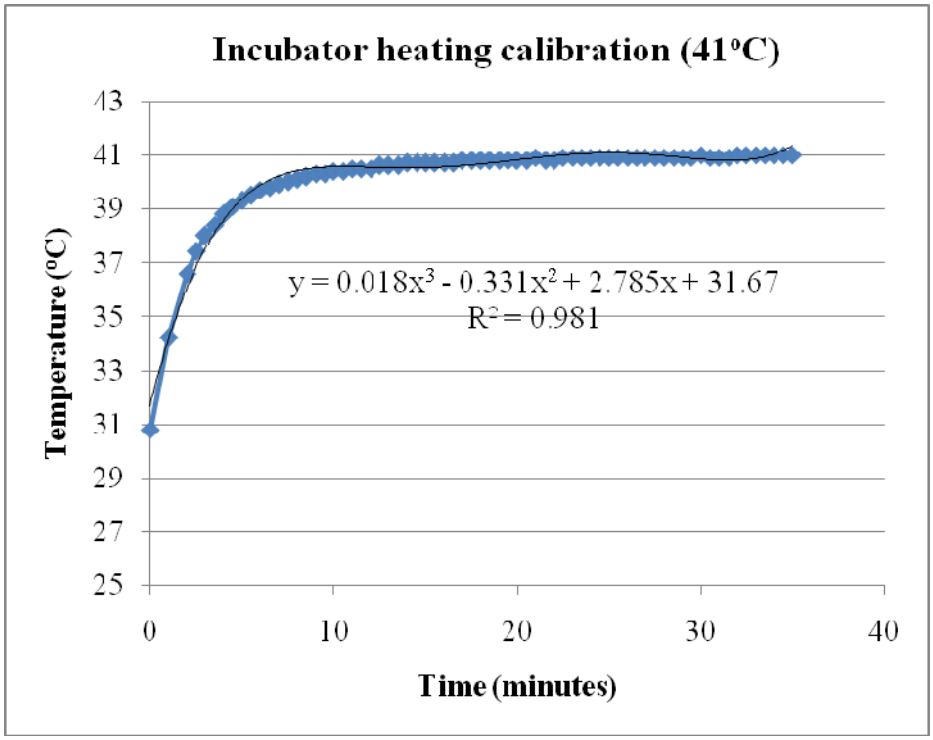

Appendix H. Protocol of Von Kossa Staining

1. Prepare a 2% (w/v) solution of silver nitrate in water. Make up only what is needed since the shelf life of the solution is approximately one week.
2. Rinse culture 2X with cold Tyrode's balanced salt solution.
3. Fix cultures with 10% buffered formalin phosphate for 30 minutes. All steps involving formalin must be carried out in a fume hood.
4. Rinse cultures 2X with distilled water.
5. Add 2% silver nitrate to cover the cells; place the dishes or flasks in dark for 10 minutes.
6. Rinse 3X with distilled water. Leave the water from the final rinse on the culture dish.
7. With water still covering the cells, expose the cultures to bright light for 15 minutes. Use a white background beneath the dishes to help reflect the light.
8. Remove the water covering the cells, then rinse 2X with distilled water.
9. Dehydrate with 100% ethanol; remove the ethanol after 1 minute, and then allow the cultures to air dry.

Appendix I. Protocol of SEM

The samples were 3D hydrogel samples in Lab-Tek chambered coverglass.

1) Fix cells in 4% glutaraldehyde. Note: need transfer pipets, work in fume hood.
Add fixing solution into each well of chamber, close the cap, put the chamber in a 10 cm petri dish, and seal with parafilm around (to prevent the dirt comes in). Then put the solution buffer and petri dish both in the refridge ($4^{o}C$) overnight.

2) On the next day, open the petri dish in fume hood. Open the cap of chamber in dish, and rinse 5X with (glass) distill water using transfer pipets. Remember to leave a little water inside, to prevent sample drying. After rinsing, add more water into each well.

3) After that, take the chamber to benchtop. No need for fume hood. Then take 4 sample holders (baskets) to hold one piece of sample in each basket. The piece of sample was cut along with the surrounding area of coverglass. And the sample was placed carefully by a tweezer. Close the caps of the 4 baskets, and put in a clean glass container. And start dehydrating the samples in a series of ethanol, 25%, 50%, 70%, 80%, 90%, 100%, 100%. Note: each solution was prepared in a 50 ml conical tube to 50 ml in total.

4) Take the whole container with the last change of ethanol to critical point dry room, use the machine according to the instructions. Turn on the power, the light, and put 4 baskets one by one next to each other in the liquid CO2 container. Rise 7 times and 3-5 min each time.

5) Then go to SEM room, tape the SEM pin, and put sample facing up. And then plug the pins into the holes and start gold/carbon sputtering following the instructions there.

6) Before starting SEM machine, turn on chiller, gas tank, and then turn on the key, turn on voltage, and power. Place the samples inside the machine. Then start searching for samples and taking pictures.

Appendix J. Protocol of ALP Assay

For samples in 24-well plate,

1. Rinse with PBS first
2. Extract samples with digestion buffer (300 µl 0.5% Triton X-100) by homogenizing with pipette (tip cut). For hydrogel samples, sonication for 10 minutes was added afterwards.
3. Samples were then vortexed.
4. Place 0.5 ml Alkaline Buffer into 15 ml centrifuge tubes for each sample as well as (+), (-), (blank)
5. Place 0.5 ml Stock Substrate solution (SSS) into each tube
6. Place tubes in 37^{o}C water bath for 2 minutes (bring vortexer, samples, ddH_2O and timer to water bath)
7. Vortex samples and let them settle down for a while.
8. Start timer, @30 seconds place 100 µl of first sample into 15 ml tube, @ 1 min, place 100 µl of second sample into 15 ml tube, @ 1:30 place 100 µl of third sample into 15 ml tube, …continue…until the last sample. Note: less than 30 samples should be used.
9. Place 100 µl of ddwater into 15 ml tube (blank)
10. For first of run only, place 100 µl of Shrimp Alkaline Phosphatase Substrate from (+) into 15 ml tube (+), also place 100 µl of Shrimp Alkaline Phosphatase Substrate from (-) into 15 ml tube (-)
11. @15 min after first sample add 1 ml of 1N NaOH into first sample tube, continue for each time interval for each sample. Note: Alkali stops reaction and develops color which is stable several hours.
12. Prepare standards in 15 ml tubes according to following chart:

p-Nitrophenol concentration (nmol/ml)	Volume (ml) of diluted p-nitrophenol solution (100 nmol/ml)	Volume (ml) of 0.02N NaOH
9	0.1	1.0
18	0.2	0.9
36	0.4	0.7
54	0.6	0.5
72	0.8	0.3
90	1.0	0.1

Note: Prepare 100 nmol/ml solution of p-nitrophenol by combining 100 µl of 10 mM p-nitrophenol standard solution with 9.9 ml 0.02N NaOH.

13. Place 300 µl of standards to wells in triplicate (invert tube to mix)

14. Place 300 µl of samples to wells in triplicate (invert tube to mix). Be careful about bubbles as Triton X-100 is a detergent.

15. Read the absorbance at 405 nm.

Reagents used in this assay, as below:

- Alkaline Buffer Solution – Sigma, cat. #A9226
- Phosphatase Substrate – Sigma, cat.#P5744-25CAP
    - Substrate Stock Solution (SSS): Dissolve 40 mg capsule (contents only- rinse capsule out with pipet) in 10 ml ddH_2O
- p-Nitrophenol Standard Solution – Sigma, cat. #N7660-100ML
- Shrimp Alkaline Phosphatase Stock Solution
    - Pipette 5 µl Shrimp Alkaline Phosphatase in 250 µl SAP Dilution Buffer in 1.5 ml tube
    - Pipette 5 µl of this solution into 1 ml Digestion Buffer (ex. Triton X-100) into 2 each 1.5 ml tubes labeled (+) and (-)
    - Place tube (-) in 65^{o}C water bath for 10 min

Appendix K. Protocol of Calcium Deposition Assay

For cells in 24-well plate,

1. Aspirate or pipette out all culture medium from each well of 24-well culture plate that contains induced or control cells to be tested.
2. Rinse the cells 2X with PBS. Add 500 µl of PBS to the side of each well, being careful to not dislodge the cells. Aspirate off the PBS and re-rinse.
3. Aspirate the second wash and add 125 µl of 0.5N HCl to each well.
4. Scrape the cells off of the surface using a cell scraper and transfer the cells and HCl to a 1.5 ml polypropylene microcentrifuge tube with a tight fitting cap.
5. Add an additional 125 µl of 0.5N HCl to each well to recover any cells remaining in the well, and transfer this to the appropriate tube.
6. Samples may be capped tightly and stored at -20 ^{o}C for one month if they are not to be tested immediately.
7. Extract the calcium from the cells by shaking the tubes on an orbital shaker for 4 hours at 4 ^{o}C. If using frozen samples, allow extra time for samples to thaw.
8. Centrifuge the sample tubes at 500g for 2 minutes.
9. Carefully collect the supernatant with extracted calcium, without disrupting the pellet, and transfer to a new tube.
10. Following the instructions provided in the Stanbio Laboratory Calcium (CPC) Liquicolor kit (Fisher Scientific, Stanbio cat. #0150-250), prepare a standard curve with the calcium standard and determine the amount of calcium in each control and osteo-induced sample.
11. 3 µl of sample vs. 300 µl of assay reagent (1:100 ratio for sample to reagent) for 96-well plate is used for each calcium determination. Assay reagent was mixed by equal volume of two solutions provided in the kit, and distributed by multipipettor after adding samples. Absorbance was read at 550 nm.
12. Unused sample extract may be re-frozen for future re-assay. If the reading was out of range, the sample can be diluted with ddwater in a total volume of 3 µl (e.g. 1 µl of sample +2 µl of ddwater) and re-assayed again.

Appendix L. Protocol of Real-time RT-PCR

For cells in 24-well plate,

Part 1 RNA isolation:

1. Aspirate or pipette the medium out.
2. Add 750 µl of TRIzol reagent per well.
3. Collect each sample in individual 1.5 ml microcentrifuge tubes. For 2D samples, collect them directly after waiting for several minutes. For 3D hydrogel samples, pipette up and down several times before collecting into tubes. No visible gel pieces should be seen afterwards.
4. Add 250 µl of chloroform per sample into appropriate tubes. Mix well by inverting tubes.
5. Centrifuge at maximum speed (16,×××g) for 15 minutes at 4 ^{o}C
6. During centrifugation, prepare labeled columns for each sample. The columns were placed on Qiagen vacuum pump without closing caps. Remember to clean the surface with ethanol first to eliminate RNase.
7. After centrifugation, several layers were formed. Top: water phase, which contains RNA. Middle: protein & DNA, appear white. Bottom: Trizol, appear pink. Take the top liquid phase carefully, without touching anything from middle layer, then put in another set of clean microcentrifuge tubes.
8. Add 500 µl of 75% ethanol to those tubes, as the supernatant collected normally ranges from 300 µl ~ 500 µl. Then mix well.
9. Pour the samples one by one into the columns. Then follow the instructions from Qiagen RNeasy Mini kit. Lysis RLT buffer was not used. Briefly, steps are as follows,
    - Apply the vacuum until samples go through.
    - Add 700 µl of buffer RW1. Vacuum.
    - Add 500 µl of buffer RPE. Vacuum.
    - Add 500 µl of buffer RPE again. Vacuum.
    - Place columns into 2 ml new tubes. Centrifuge at maximum speed for 1 minute to get rid of excess fluid. Discard the tubes.
10. Place columns in 1.5 ml tubes. Add 30 µl of RNase-free water into the center of tubes. Centrifuge at maximum speed for 1 minute.
11. Then add 1.2 µl DNase+RNase Inhibitor (3:1 ratio) concentrated solution into each tube. Prepare the solution for all samples together and then divide. Or DNase could be added

into the water to elute RNA at the step above. Pipette the samples out and transfer into PCR strips.

12. Then use preset program 3715755 in PCR machine. Heated at 37 ^{o}C for 15 minutes, and 75 ^{o}C for 5 minutes. After that, store the strip in -80 ^{o}C freezer.

Part 2 cDNA synthesis:

1. To convert 10 µl of RNA, 4 µl of dNTP Mix and 2 µl of Oligo dT primer were needed. Prepare enough volume of dNTP Mix and Oligo dT primer (2:1 ratio) for all samples together. And add 18 µl of supplemented dNTP Mix to each sample that contains 30 µl of RNA.
2. After that, the steps as below,
    - The 48 µl of mixture was heated at 70 ^{o}C for 3 minutes. Use preset 703 program on PCR machine.
    - Place on ice for 1 minute.
3. Then add remaining RT reagents, 2:1:1 ratio for 10X RT buffer, Reverse Transcriptase, RNase Inhibitor. For 10 µl of RNA, 2 µl of 10X RT buffer, 1 µl of Reverse Transcriptase, 1 µl of RNase Inhibitor were needed. So, prepare RT mix (3 components as above) for all samples together. And add 12 µl of RT mix to each sample.
4. Use preset program RT on the PCR machine. (42 ^{o}C for 1 hr, 95 ^{o}C for 10 min)

    After cDNA synthesis, the volume of each sample was doubled (~60 µl).

Part 3 Regular PCR and gel electrophoresis:

1. 1.5 µl of cDNA and 14 µl of primer mix were used for each sample. Use preset program 5235 on the PCR machine. For 1 reaction, 2 µl of primer (1 µM) + 9 µl of DNase/RNase-free water + 3 µl of 5X master mix makes a total of 14 µl of primer mix.
2. Make agarose gel. Add 60 µl of EB+ 75 ml of 1X TAE buffer + 1.6 g agarose gel powder for 2 gels, into a flask. And heat with microwave for 2 minutes, at 70% power level 7. Prepare dam and tray for 2 gels. Once the microwave stops, pour the gel in and insert the combs. Wait for 20 minutes at least until the gel becomes white. Unplug the combs, and seal the unused gel in bags to prevent drying.
3. For gel electrophoresis, distribute a small drop of 15 µl of DNA loading dye one by one onto a new strip of PCR tubes, and then load the sample with dye into each tube. Add enough 1X TAE buffer in the electrophoresis machine, put gel on top of the tray in the buffer. The last column of wells in the gel was for DNA ladder. Cut the unnecessary part of gels.

4. Start loading samples and DNA ladder. DNA ladder was 4 µl / well. Samples were around 15 µl / well. After loading all, put on the cap of electrophoresis unit, let it run for 10~15 minutes at 98 V or watch the blue line run to about center of the gel and stop.

Part 4 Real-time PCR:

1. Prepare diluted 1 µM primer from 10 µM with DNase/RNase-free water.
2. For each well of 96-well PCR plate, 25 µl of reaction volume was used. It consists of 3 µl of primer (1 µM), 2 µl of cDNA, 7.5 µl of water, 12.5 µl of 2X SYBR dye. Prepare cDNA mix (cDNA+water) altogether for the wells of same sample, different primers. Add 3 µl of primer to each well first and each row has the same one primer that represents one gene. Add cDNA mix from one sample in duplicate wells for each primer. Finally distribute 12.5 µl of SYBR dye/well separately into each well.
3. The thermal profile preset in the machine: 95 ^{o}C for 10 mins, followed by 45 cycles at 95 ^{o}C for 15s, 55 ^{o}C for 35s, and 72 ^{o}C for 35s.

Catalog numbers for reagents or supplies used in this protocol:

- TRIzol Reagent – Invitrogen, cat. #15596-018
- RNeasy Mini kit – Qiagen, cat.#74104
- Cells-to-cDNA II kit - Ambion, cat.#AM1722
- SYBR Green PCR Master Mix – Ambion, cat.#4309155

Appendix M. Protocol of Western Blot

Preparation: prepare enough **transfer buffer** (2 Liters for 4 gels) and put in refridge (4^oC) one day ahead. Run protein assay and calculate **total protein concentrations** and volumes to be loaded into each lane to make total protein equal.

[Day 1]
Electrophoresis

1. Thaw samples on ice, thaw protein standards, prepare 1x running buffer from 10 x. Boil water.
2. Assemble the electrophoresis machine, rinse each part with ddwater, put on a clean tray, put ready gel on ice, cut gel bag with blade, cut along black edge, peel off tape, take out the comb, rinse off bubbles in the wells. Rinse gel with ddwater, do the same for another gel, then hold two gels and adhere to the rack, close the unit. Prepare another unit for 4-gel system, and then put 1x running buffer inside the unit. Check if the system leaks for couple of minutes.
3. Start preparing sample loading buffer, 50 ul of **2-Mecaptomethanol** + 950 ul sample loading buffer, enough for 4 gels. 2-Mecaptomethanol should be opened in fume hood. Mix and vortex, then prepare individual sample tubes, label the tubes and put in certain sequence, load sample loading buffer in each tube first based on calculations, (prepare 1.1x of extra volume) and add same volume of samples as buffer(1:1 ratio) accordingly. Also, dilute pure protein controls with ddwater to the known quantity, and mix with sample buffer too. Vortex all samples together.
4. Boil the protein samples in tightly closed tubes for 5 mins at least, cool down in RT, and start loading samples to each well based on calculations using special gel loading tips. Prevent overflow from one well to another, try to load slowly. Load in certain sequence according to the template, and put protein standard for **10ul** next to the last sample, always load from left to right (for opposite side, left side is on the right). Make sure to differentiate the 4 gels (gel1-4). Fill the tank with more 1x running buffer outside the unit up to the designated level.
5. Put on the cover, match the color of electrodes, set constant voltage to **150V**, run, watch the blue line go to the bottom of the gel, stop it. Usually for 150V, it takes 50 minutes-1 hr to finish.

Transfer

1. Disassemble the gel (details as below), remember the label of each gel when detaching, and put in corresponding gel box. Wet the membrane with 100% methanol, (PVDF membrane is folded and cut, 1 piece is good for 2 gels) after that collect 100% methanol to a 50ml tube **ASAP** to prevent evaporation, label well and it can be reused next time. Let gel be in equilibrium with transfer buffer for 20 mins, at the same time, also soak 8 fiber pads/ 8 filter papers/ 4 membranes in transfer buffer.
   Note: About disassembling the gel, cut along the white edges, take the plastic off, cut off the wells, the gel will fall onto the box when touching the transfer buffer prepared ahead in boxes. Throw glass in glass container.
2. Wash everything for transfer machine with ddwater, start assembling the sandwich, rinse the electrophoresis machine with tap water to wash off the ions, and dry.

3. Assemble the sandwich in the following way, black side at the bottom, fiber pad-> filter paper-> gel-> membrane -> filter paper-> fiber pad, use three fingers to hold the gel, keep wet in transfer buffer all times when assembling. For gel, put one side down then slowly put the whole once and for all, do not move once attached. Use tweezer to make the edges smooth, and make sure no bubbles. Put the membrane with tweezer on top using similar techniques. Hold one corner with finger, and then smooth out the membrane by tweezer. Prepare another sandwich similarly. Put the sandwiches in a way that **black side leans on black side.** Pour all the transfer buffers into the tank, put a stir bar and an ice pack. Fill the tank to just lower than the edges. Run for **30V**, 16hrs (**960** mins), need to also put transfer buffer into empty biohazard bottle after running overnight.

[Day 2]
Blocking, Antibodies and Detection

1. Make 1x TBS from 10x TBS, and then add 1ml of 10% **tween-20** per 100ml of 1x TBS to make 1x TBS-T, 3% (3g/100ml) of non-fat dry milk is used to make blotto from TBS-T. Disassemble the sandwich (rinse fiber pad, throw filter paper and gel, keep membrane, cut the membrane smaller by the blade). Put 10-12 ml of blotto in each box ahead in order to cover the membrane. To save antibodies, 8 ml can be used if the membrane is cut small. Use tweezer to hold membrane and put in the box of blotto according to the labels, **with the protein side on top** (usually need to invert it if membrane is on top of gel). Put the boxes on the shaker for slow speed shaking, block for 1 hr.
2. Prepare primary antibody diluted in blotto, (no need to rinse after blocking) then discard the blocking solution and change to antibody solution, put on shaker for 1hr
3. Wash the membrane in 1x TBS-T for 3x, each time for 5 mins on shaker. Use more volume to wash.
4. Prepare secondary antibody diluted in blotto, incubate for 1 hr on shaker.
5. Wash with 1x TBS-T twice for 5 mins/time on shaker, **wash the box** after 2nd wash, and then wash with 1x **TBS** instead of TBS-T for the last wash.
6. Keep membrane in the last wash of TBS, prepare TMB solution, 10 ml/box, according to instructions for the detection reagent. Transfer membrane to new box used for substrate with corresponding labels, add TMB solution from side, swing the box back and forth by hand, and shake for **10-15 mins** until all bands show up. Stop reaction by ddwater, and **collect the substrate waste in 50ml tube and dispose.** Dry the membrane overnight by hanging inside the Styrofoam box, and then scan it the next day.

Buffers used in Western Blotting:

1. 10x Tank Buffer (Running buffer, 4^{o}C, warm before use)
   15 g Tris
   72 g Glycine
   5 g SDS
   Add ddwater to 500 ml
2. Transfer buffer (do not adjust pH, 4 ^{o}C, use cold)
   3.03 g Tris (25 mM)
   14.4 g Glycine (192 mM)
   200 ml methanol (20% v/v)

Add ddwater to 1L

3. 10x TBS (Tris-buffered Saline, 4 ^{o}C, 2-3 years)
   12.1 g Tris (100 mM)
   87.5 g NaCl
   Adjust to pH7.2 with conc. HCl (6N)
   Add ddwater to 1L

Note: need to use **electrophoresis grade** Glycine and SDS.

Ordering information and antibody dilutions:

- HSP27 (G3.1) antibody (1:500 dilution) – Enzo Life Sciences, cat. #ADI-SPA-800-F
- HSP70/HSP72 (C92F3A-5) (1:500 dilution) – Enzo Life Sciences, cat. # ADI-SPA-810-F
- Goat anti-mouse IgG (HRP conjugate) secondary antibody (1:1000 dilution) - Enzo Life Sciences, cat. # ADI-SAB-100-J
- HSP70/HSC70 antibody (W27) (1:500 dilution) – Santa Cruz Biotechnology, cat. #sc-24
- HSP 90α/β antibody (F-8) (1:500 dilution) – Santa Cruz Biotechnology, cat. #sc-13119
- Actin antibody, clone C4 (1:1000 dilution) – Millipore, cat. #MAB1501
- TMB substrate kit - Vector Laboratories, cat.# SK-4400
- Laemmli Sample Buffer - Bio-Rad, cat. #161-0737
- Glycine - Sigma-Aldrich, cat.# G8898-1KG
- Blotting-Grade Blocker- Bio-Rad, cat. #170-6404
- Ready Gel Tris-HCl Gel - Bio-Rad, cat. #161-1155
- 2-Mercaptoethanol- Bio-Rad, cat. #161-0710
- methanol – Fisher Scientific, cat. #A412P-4
- Kaleidoscope Prestained Standards - Bio-Rad, cat. #161-0324
- Immun-Blot PVDF Membrane - Bio-Rad, cat. #162-0175
- Thick Blot Paper - Bio-Rad, cat. #170-3932
- Fiber Pads - Bio-Rad, cat. #170-3933

Appendix N. Protocol of Safranin O Staining

1. Deparaffinize pellet sections in xylene (3×3 min), 100% ethanol (2×3 min), 95% ethanol (2×3 min) then 70% ethanol (1×3 min)
2. Stain in Weigert's iron hematoxylin (Sigma, cat.#HT1079-1SET) for 4 minutes, then destain in fresh acid alcohol (1 ml concentrated HCl in 100 ml 70% ethanol) and rinse in tap water
3. Stain in 0.02% aqueous fast green FCF (Sigma, cat.#F7258-25G) for 3 minutes, then wash in 1% acetic acid for 30 seconds
4. Stain in 0.1% aqueous Safranin-O (Sigma, cat.#HT904-8FOZ) for 5 minutes
5. Dehydrate in 95% ethanol (2×5 min), 100% ethanol (3×5 min), then xylene (3×5 min)
6. Mount sections in synthetic resin
7. Proteoglycans will stain red, cytoplasm will stain gray green and nuclei will stain black

Appendix O. C Programming Code for Ultrasound Pulser/Receiver

```
// PRF1000.cpp : Defines the entry point for the console application.
//
#include "stdafx.h"
#include "stdio.h"
#include "USBUTSDK.h"
int main(int argc, char* argv[])
{
   USBUTParms(INITIALIZE,    0, 0, 0);    // initialize the device
   USBUTParms(SETPULSEVOLTAGE,        0, 0, 0);    // Power: 300 volts
   USBUTParms(SETADTRIGGERSOURCE,  0, 1, 0);        //Set the trigger source to software
trigger
   USBUTParms(SETCHANNEL,            0, 0, 0);    // transmit chan: 1; receiver chan: 1
   USBUTParms(SETTONEBURSTFREQUENCY,            0, 1000, 0);    // pulse frequency to 1
MHz
   USBUTParms(SETPULSEWIDTH,            0, 30, 0);    // pulse cycles: 15 full cycles
   USBUTParms(SETPRF,                0, 1000, 0);    // PRF to 1000 Hz
   printf("Pulsing... Hit any key to stop. ");
   getchar();
   USBUTParms(SETPRF,                0, 0, 0);    // PRF to 0 Hz
   return 0;
}
```

Appendix P. Matlab Code for Ultrasound Intensity Simulation

```
clear all;
field_init(0);
% Create a piston transducer with an 12.7 mm diameter and divided
% into 0.2 mm mathematical elements
% Set initial parameters
R=12.7/2/1000; % Radius of transducer
ele_size=0.2/1000; % Size of mathematical elements
% Define the transducer
% Th=xdc_piston(R,ele_size); % plane wave unfocused
% Create a concave, round transducer with an 13 mm diameter and
% a focal radius of 17.78 mm (0.7 inch) (range 0.6-0.8 inch,i.e.15.24-20.32 mm) and divided it
into 0.2 mm mathematical
% elements
% focused,spherical,
% Set initial parameters
  Rfocal=50.8/1000; % Focal radius of transducer
% Define the transducer
  Th=xdc_concave(R,Rfocal,ele_size);
% Show the transducer surface
% show_apo(Th);
% show_xdc(Th);
% Transducer parameters
f0=1e6; % Transducer center frequency [Hz]
fs=100e6; % Sampling frequency [Hz]
c=1540; % Speed of sound [m/s]
lamda=c/f0; % Wavelength [m]
% Set the sampling frequency
set_sampling(fs);
% Generate aperture for emission
emit_aperture=Th;
% Set the impulse response and excitation of the emit aperture
impulse_response=sin(2*pi*f0*(0:1/fs:2/f0));
impulse_response=impulse_response.*hanning(max(size(impulse_response)))';
xdc_impulse(emit_aperture,impulse_response);
excitation=sin(2*pi*f0*(0:1/fs:2/f0));
xdc_excitation(emit_aperture,excitation);
% xdc_focus(Th,0,[0 0 5]/1000);%???
% Calculate the field to see the effect
% p_max=[];
% for z=1:20
% [h,t]=calc_hp(Th,[0 0 z]/1000);
% % figure
% % plot((0:length(h)-1)/fs+t,h)
% % ylabel('Pressure')
```

```
% % xlabel('Time [s]')
%
% p_max=[p_max max(h)];
% end
%
% figure
% plot(p_max)
%[x,y]=meshgrid(-11:0.1:11,-11:0.1:11);

%for z=20:20
%points=[x(:) y(:) z*ones(size(x(:)))]/1000;
%[h,t]=calc_hp(Th,points);
%p_max=reshape(max(h),size(x));
%p_max=p_max.^2;
%p_max=p_max/max(p_max(:));
%figure
%imagesc(-11:0.1:11,-11:0.1:11,p_max)
%colorbar
%end
[x,z]=meshgrid(-11:0.1:11,1:0.2:20);%mm
points=[x(:) zeros(size(x(:))) z(:)]/1000;%mm -> m
[hp,start_t] = calc_hp(Th,points);
a=reshape(max(hp),size(x));
a=a.^2;
[x,z]=meshgrid(-11:0.1:11,21:0.2:30);%mm
points=[x(:) zeros(size(x(:))) z(:)]/1000;%mm -> m
[hp,start_t] = calc_hp(Th,points);
b=reshape(max(hp),size(x));
b=b.^2;
[x,z]=meshgrid(-11:0.1:11,31:0.2:40);%mm
points=[x(:) zeros(size(x(:))) z(:)]/1000;%mm -> m
[hp,start_t] = calc_hp(Th,points);
c=reshape(max(hp),size(x));
c=c.^2;
figure
imagesc(-11:0.1:11,1:0.2:40,[a;b;c])
colorbar
xlabel('x');
ylabel('z');
% Release the aperture
xdc_free(Th);
```

Appendix Q. ANOVA Test for DMMB Assay Samples

Example 1: Day 10 pellet culture samples for DMMB (GAG quantification) assay

	Sample 1	**Sample 2**	**Sample 3**	**Sample 4**
Control	210.9219	241.9667	423.4417	292.1101
Chon	149.6817	161.1144	167.6305	159.4756
HS+Chon	254.065	177.1463	236.3396	215.9553

Step 1 One-way ANOVA: (using Matlab)

```
>> Y=[210.9219, 241.9667, 423.4417, 292.1101;149.6817, 161.1144, 167.6305,
159.4756;254.065, 177.1463, 236.3396, 215.9553]
Y =
  210.9219  241.9667  423.4417  292.1101
  149.6817  161.1144  167.6305  159.4756
  254.0650  177.1463  236.3396  215.9553
>> Y=transpose(Y)
Y =
  210.9219  149.6817  254.0650
  241.9667  161.1144  177.1463
  423.4417  167.6305  236.3396
  292.1101  159.4756  215.9553
>> p=anova1(Y)
p =
    0.0298<0.05
```

>> Thus at least one of the three conditions (Control, Chon or HS+Chon) is significantly different than the other.

ANOVA Table

Source	SS	df	MS	F	Prob>F
Columns	35248.3	2	17624.2	5.32	0.0298
Error	29796.1	9	3310.7		
Total	65044.4	11			

Further, to verify that the significance exists between Chon & HS+Chon,

Step 2 One-way ANOVA (between Chon & HS+Chon)

```
Y=[149.6817, 161.1144, 167.6305, 159.4756;254.065, 177.1463, 236.3396, 215.9553]
Y =
  149.6817  161.1144  167.6305  159.4756
  254.0650  177.1463  236.3396  215.9553
>> Y=transpose(Y)
Y =
  149.6817  254.0650
  161.1144  177.1463
  167.6305  236.3396
  159.4756  215.9553
>> p=anova1(Y)
p =
```

0.0110 <0.05

>> When only two conditions are compared, the one-way ANOVA result is the same as Student's t-test result. P<0.05 indicates that there is a significance between Chon & HS+Chon. It is consistent with the p value found using Student's t-test.

ANOVA Table

Source	SS	df	MS	F	Prob>F
Columns	7540.2	1	7540.17	13.14	0.011
Error	3442.2	6	573.71		
Total	10982.4	7			

Example 2: Day 17 & 24 hydrogel culture samples for DMMB (GAG quantification) assay

	Day 17	**Day 24**
Control	59.65816 63.00622 97.28347	28.97447 65.13809 47.05628
Chon	341.1971 447.5939 583.1837	545.5797 426.4785 669.7729
HS+Chon	1099.91 827.8413 1144.105	578.564 551.5497 530.4102

Step 1 Two-way ANOVA: (using Matlab)

>> Z= [59.65816, 63.00622, 97.28347, 28.97447, 65.13809, 47.05628; 341.1971, 447.5939, 583.1837, 545.5797, 426.4785, 669.7729; 1099.911, 827.8413, 1144.105, 578.564, 551.5497, 530.4102]

Z =

1.0e+003 *

0.0597	0.0630	0.0973	0.0290	0.0651	0.0471
0.3412	0.4476	0.5832	0.5456	0.4265	0.6698
1.0999	0.8278	1.1441	0.5786	0.5515	0.5304

>> Z= transpose (Z)

Z =

1.0e+003 *

0.0597	0.3412	1.0999
0.0630	0.4476	0.8278
0.0973	0.5832	1.1441
0.0290	0.5456	0.5786
0.0651	0.4265	0.5515
0.0471	0.6698	0.5304

>> t= anova2 (Z, 3)

t =

0.0000	0.0140	0.0010

ANOVA Table

Source	SS	df	MS	F	Prob>F
Columns	1616567.5	2	808283.7	80.58	0
Rows	82723.6	1	82723.6	8.25	0.014
Interaction	262424.8	2	131212.4	13.08	0.001
Error	120373.4	12	10031.1		
Total	2082089.3	17			

>> The first p = 0 suggests that the difference is very significant due to the different conditions (Control, Chon or HS+Chon); the second p = 0.014 <0.05 suggests that the difference is also significant due to the different culture days (Day 17 or Day 24); the third p = 0.001<0.005 suggests that there is an interaction between factors A and B (A: different conditions/treatment, B: different culture days).

Further, to confirm that the significance exists between Chon & HS+Chon,
Step 2 One-way ANOVA (between Chon & HS+Chon)
X=[341.1971, 178.1436, 447.5939, 906.2358, 598.8576, 583.1837;1099.911, 808.9253, 827.8413, 1163.537, 1144.105, 1218.189]
X =
1.0e+003 *
0.3412 0.1781 0.4476 0.9062 0.5989 0.5832
1.0999 0.8089 0.8278 1.1635 1.1441 1.2182
>> X=transpose(X)
X =
1.0e+003 *
0.3412 1.0999
0.1781 0.8089
0.4476 0.8278
0.9062 1.1635
0.5989 1.1441
0.5832 1.2182
>> p=anova1(X)
p =
0.0017<0.005
>> One-way ANOVA result is the same as Student's t-test result. P<0.005 indicates that there is a significance between Chon & HS+Chon. It is consistent with the p value found using Student's t-test.

ANOVA Table

Source	SS	df	MS	F	Prob>F
Columns	857229.5	1	857229.5	18.14	0.0017
Error	472530.4	10	47253		
Total	1329759.9	11			

Bibliography

[1] S. C. Cowin, Doty,S.B., *Tissue Mechanics*. New York: Springer, 2006.

[2] F. J. Hughes, *et al.*, "Effects of growth factors and cytokines on osteoblast differentiation," *Periodontology 2000,* vol. 41, pp. 48-72, 2006.

[3] J. J. Mao, "Stem-cell-driven regeneration of synovial joints," *Biology of the Cell,* vol. 97, pp. 289-301, May 2005.

[4] R. Lanza, Gearhart,J.,Hogan,B.,et al., *Essentials of Stem Cell Biology*. San Diego: Elsevier, 2006.

[5] C. A. Vacanti, "History of tissue engineering and a glimpse into its future," *Tissue Engineering,* vol. 12, pp. 1137-1142, May 2006.

[6] A. I. Caplan, "MESENCHYMAL STEM-CELLS," *Journal of Orthopaedic Research,* vol. 9, pp. 641-650, Sep 1991.

[7] C. P. Ye, *et al.*, "Culture media conditioned by heat-shocked osteoblasts enhances the osteogenesis of bone marrow-derived mesenchymal stromal cells," *Cell Biochem Funct,* vol. 25, pp. 267-76, May-Jun 2007.

[8] F. P. Barry and J. M. Murphy, "Mesenchymal stem cells: clinical applications and biological characterization," *International Journal of Biochemistry & Cell Biology,* vol. 36, pp. 568-584, Apr 2004.

[9] N. W. Marion and J. J. Mao, "Mesenchymal stem cells and tissue engineering," in *Stem Cell Tools and Other Experimental Protocols*. vol. 420, ed San Diego: Elsevier Academic Press Inc, 2006, pp. 339-361.

[10] M. F. Pittenger, *et al.*, "Multilineage potential of adult human mesenchymal stem cells," *Science,* vol. 284, pp. 143-147, Apr 1999.

[11] Friedens.Aj, *et al.*, "OSTEOGENESIS IN TRANSPLANTS OF BONE MARROW CELLS," *Journal of Embryology and Experimental Morphology,* vol. 16, pp. 381-&, 1966.

[12] Friedens.Aj, *et al.*, "DEVELOPMENT OF FIBROBLAST COLONIES IN MONOLAYER CULTURES OF GUINEA-PIG BONE MARROW AND SPLEEN CELLS," *Cell and Tissue Kinetics,* vol. 3, pp. 393-&, 1970.

[13] R. Lanza, Langer,R.,Vacanti,J., *Principles of Tissue Engineering*. San Diego: Elsevier, 2007.

[14] A. Alhadlaq and J. J. Mao, "Mesenchymal stem cells: Isolation and therapeutics," *Stem Cells and Development,* vol. 13, pp. 436-448, Aug 2004.

[15] M. Schindler, *et al.*, "Living in three dimensions - 3D nanostructured environments for cell culture and regenerative medicine," *Cell Biochemistry and Biophysics,* vol. 45, pp. 215-227, 2006.

[16] S. G. Zhang, *et al.*, "SPONTANEOUS ASSEMBLY OF A SELF-COMPLEMENTARY OLIGOPEPTIDE TO FORM A STABLE MACROSCOPIC MEMBRANE," *Proceedings of the National Academy of Sciences of the United States of America,* vol. 90, pp. 3334-3338, Apr 1993.

[17] H. Misawa, *et al.*, "PuraMatrix (TM) facilitates bone regeneration in bone defects of calvaria in mice," *Cell Transplantation,* vol. 15, pp. 903-910, 2006.

[18] T. C. Holmes, *et al.*, "Extensive neurite outgrowth and active synapse formation on self-assembling peptide scaffolds," *Proceedings of the National Academy of Sciences of the United States of America,* vol. 97, pp. 6728-6733, Jun 2000.

[19] C. E. Semino, *et al.*, "Entrapment of migrating hippocampal neural cells in three-dimensional peptide nanofiber scaffold," *Tissue Engineering,* vol. 10, pp. 643-655, Mar-Apr 2004.
[20] J. Kisiday, *et al.*, "Self-assembling peptide hydrogel fosters chondrocyte extracellular matrix production and cell division: Implications for cartilage tissue repair," *Proceedings of the National Academy of Sciences of the United States of America,* vol. 99, pp. 9996-10001, Jul 2002.
[21] C. E. Semino, *et al.*, "Functional differentiation of hepatocyte-like spheroid structures from putative liver progenitor cells in three-dimensional peptide scaffolds," *Differentiation,* vol. 71, pp. 262-270, Jun 2003.
[22] S. Wang, *et al.*, "Three-dimensional primary hepatocyte culture in synthetic self-assembling peptide hydrogel," *Tissue Engineering Part A,* vol. 14, pp. 227-236, Feb 2008.
[23] M. E. Davis, *et al.*, "Injectable self-assembling peptide nanofibers create intramyocardial microenvironments for endothelial cells," *Circulation,* vol. 111, pp. 442-450, Feb 2005.
[24] D. A. Narmoneva, *et al.*, "Endothelial cells promote cardiac myocyte survival and spatial reorganization - Implications for cardiac regeneration," *Circulation,* vol. 110, pp. 962-968, Aug 2004.
[25] K. Hamada, *et al.*, "Spatial distribution of mineralized bone matrix produced by marrow mesenchymal stem cells in self-assembling peptide hydrogel scaffold," *Journal of Biomedical Materials Research Part A,* vol. 84A, pp. 128-136, Jan 2008.
[26] H. J. Mauck RL, Tuan RS (2008). *ENHANCED CHONDROGENESIS AND DEVELOPMENT OF MECHANICAL PROPERTIES OF HUMAN MESENCHYMAL STEM CELLS SEEDED IN A SELF-ASSEMBLING PEPTIDE HYDROGEL*
[27] K. R. Diller, "Stress protein expression kinetics," *Annual Review of Biomedical Engineering,* vol. 8, pp. 403-424, 2006.
[28] L. Wieten, *et al.*, "Cell stress induced HSP are targets of regulatory T cells: A role for HSP inducing compounds as anti-inflammatory immuno-modulators?," *Febs Letters,* vol. 581, pp. 3716-3722, Jul 2007.
[29] S. K. Calderwood, *et al.*, "Extracellular heat shock proteins in cell signaling," *Febs Letters,* vol. 581, pp. 3689-3694, Jul 2007.
[30] S. A. Shui C, "Mild heat shock induces proliferation, alkaline phosphatase activity, and mineralization in human bone marrow stromal cells and Mg-63 cells in vitro.," *J Bone Miner Res. ,* vol. 16, pp. 731-41, April 2001 2001.
[31] K. M. Nørgaard R, Rattan SI., "Heat shock-induced enhancement of osteoblastic differentiation of hTERT-immortalized mesenchymal stem cells.," *Ann N Y Acad Sci. ,* vol. 1067, pp. 443-7, 2006 May 2006.
[32] V. B. Kraus, "Pathogenesis and treatment of osteoarthritis," *Medical Clinics of North America,* vol. 81, pp. 85-&, Jan 1997.
[33] Z. Q. Shen FH, Lv Q, Choi L, Balian G, Li X, Laurencin CT., "Osteogenic differentiation of adipose-derived stromal cells treated with GDF-5 cultured on a novel three-dimensional sintered microsphere matrix.," *Spine J.,* vol. 6, pp. 615-23, 2006 Nov-Dec 2006
[34] Y. R. V. Shih, *et al.*, "Growth of mesenchymal stem cells on electrospun type I collagen nanofibers," *Stem Cells,* vol. 24, pp. 2391-2397, Nov 2006.
[35] H. K. Kim, *et al.*, "Injectable In Situ-Forming pH/Thermo-Sensitive Hydrogel for Bone Tissue Engineering," *Tissue Engineering Part A,* vol. 15, pp. 923-933, Apr 2009.

[36] J. L. Moreau and H. H. K. Xu, "Mesenchymal stem cell proliferation and differentiation on an injectable calcium phosphate - Chitosan composite scaffold," *Biomaterials,* vol. 30, pp. 2675-2682, May 2009.
[37] C. Chun, *et al.*, "The use of injectable, thermosensitive poly(organophosphazene)-RGD conjugates for the enhancement of mesenchymal stem cell osteogenic differentiation," *Biomaterials,* vol. 30, pp. 6295-6308, Nov 2009.
[38] I. Kratchmarova, *et al.*, "Mechanism of divergent growth factor effects in mesenchymal stem cell differentiation," *Science,* vol. 308, pp. 1472-1477, Jun 2005.
[39] V. David, *et al.*, "Mechanical loading down-regulates peroxisome proliferator-activated receptor gamma in bone marrow stromal cells and favors osteoblastogenesis at the expense of adipogenesis," *Endocrinology,* vol. 148, pp. 2553-2562, May 2007.
[40] H. Ogawa, "[Effects of the localized thermal enhancement on new bone formation following mechanical expansion of the rat sagittal suture]," *Nippon Kyosei Shika Gakkai Zasshi,* vol. 49, pp. 485-96, 1990 1990.
[41] M. Brookes, *et al.*, "VASCULAR SEQUELAE OF EXPERIMENTAL OSTEOTOMY," *Angiology,* vol. 21, pp. 355-&, 1970.
[42] K. A. Takahashi, *et al.*, "Hyperthermia for the treatment of articular cartilage with osteoarthritis," *International Journal of Hyperthermia,* vol. 25, pp. 661-667, 2009.
[43] J. R. Doyle and B. W. Smart, "STIMULATION OF BONE GROWTH BY SHORT-WAVE DIATHERMY," *Journal of Bone and Joint Surgery-American Volume,* vol. 45, pp. 15-24, 1963.
[44] V. Richards and R. Stofer, "THE STIMULATION OF BONE GROWTH BY INTERNAL HEATING," *Surgery,* vol. 46, pp. 84-96, 1959.
[45] H. Brodin, "Longitudinal bone growth, the nutrition of the epiphyseal cartilages and the local blood supply; an experimental study in the rabbit," *Acta orthopaedica Scandinavica. Supplementum,* vol. 20, pp. 1-92, 1955 1955.
[46] K. Trieb, *et al.*, "Effects of hyperthermia on heat shock protein expression, alkaline phosphatase activity and proliferation in human osteosarcoma cells," *Cell Biochemistry and Function,* vol. 25, pp. 669-672, Nov-Dec 2007.
[47] E. Genove, *et al.*, "The effect of functionalized self-assembling peptide scaffolds on human aortic endothelial cell function," *Biomaterials,* vol. 26, pp. 3341-3351, Jun 2005.
[48] http://www.engineeringtoolbox.com/young-modulus-d_417.html.
[49] J. P. Winer, *et al.*, "Bone Marrow-Derived Human Mesenchymal Stem Cells Become Quiescent on Soft Substrates but Remain Responsive to Chemical or Mechanical Stimuli," *Tissue Engineering Part A,* vol. 15, pp. 147-154, Jan 2009.
[50] S. G. Zhang, *et al.*, "SELF-COMPLEMENTARY OLIGOPEPTIDE MATRICES SUPPORT MAMMALIAN-CELL ATTACHMENT," *Biomaterials,* vol. 16, pp. 1385-1393, Dec 1995.
[51] M. A. Bokhari, *et al.*, "Enhancement of osteoblast growth and differentiation in vitro on a peptide hydrogel - polyHIPE polymer hybrid material," *Biomaterials,* vol. 26, pp. 5198-5208, Sep 2005.
[52] A. Dickhut, *et al.*, "Chondrogenesis of mesenchymal stem cells in gel-like biomaterials in vitro and in vivo," *Frontiers in Bioscience,* vol. 13, pp. 4517-4528, May 2008.
[53] I. E. Erickson, *et al.*, "Differential Maturation and Structure-Function Relationships in Mesenchymal Stem Cell- and Chondrocyte-Seeded Hydrogels," *Tissue Engineering Part A,* vol. 15, pp. 1041-1052, May 2009.

[54] R. Yoshimi, *et al.*, "Self-Assembling Peptide Nanofiber Scaffolds, Platelet-Rich Plasma, and Mesenchymal Stem Cells for Injectable Bone Regeneration With Tissue Engineering," *Journal of Craniofacial Surgery,* vol. 20, pp. 1523-1530, Sep 2009.
[55] C. L. Lim, *et al.*, "Human thermoregulation and measurement of body temperature in exercise and clinical settings," *Annals Academy of Medicine Singapore,* vol. 37, pp. 347-353, Apr 2008.
[56] N. Jaiswal, *et al.*, "Osteogenic differentiation of purified, culture-expanded human mesenchymal stem cells in vitro," *Journal of Cellular Biochemistry,* vol. 64, pp. 295-312, Feb 1997.
[57] J. Goldstein, *et al.*, *Scanning Electron Microscopy and X-Ray Microanalysis*, 3 ed., 2003.
[58] C. K. Hee, *et al.*, "Influence of three-dimensional scaffold on the expression of osteogenic differentiation markers by human dermal fibroblasts," *Biomaterials,* vol. 27, pp. 875-884, Feb 2006.
[59] A. Hirata, *et al.*, "Localization of Runx2, Osterix, and Osteopontin in Tooth Root Formation in Rat Molars," *Journal of Histochemistry & Cytochemistry,* vol. 57, pp. 397-403, Apr 2009.
[60] S. A. Johnsen, *et al.*, "Opposing roles of Osterix and TGF beta inducible early gene in osteoblast differentiation downstream of Cbfa1/Runx2," *Journal of Bone and Mineral Research,* vol. 17, pp. S129-S129, Sep 2002.
[61] Y. Cao, *et al.*, "Osterix, a transcription factor for osteoblast differentiation, mediates antitumor activity in murine osteosarcoma," *Cancer Research,* vol. 65, pp. 1124-1128, Feb 2005.
[62] H. Nakamura, *et al.*, "LOCALIZATION OF CD44, THE HYALURONATE RECEPTOR, ON THE PLASMA-MEMBRANE OF OSTEOCYTES AND OSTEOCLASTS IN RAT TIBIAE," *Cell and Tissue Research,* vol. 280, pp. 225-233, May 1995.
[63] M. S. Friedman, *et al.*, "Osteogenic differentiation of human mesenchymal stem cells is regulated by bone morphogenetic protein-6," *Journal of Cellular Biochemistry,* vol. 98, pp. 538-554, Jun 2006.
[64] B. Kern, *et al.*, "Cbfa1 contributes to the osteoblast-specific expression of type I collagen genes," *Journal of Biological Chemistry,* vol. 276, pp. 7101-7107, Mar 2001.
[65] S. Even-Ram, *et al.*, "Matrix control of stem cell fate," *Cell,* vol. 126, pp. 645-647, Aug 2006.
[66] S. Kostenko and U. Moens, "Heat shock protein 27 phosphorylation: kinases, phosphatases, functions and pathology," *Cellular and Molecular Life Sciences,* vol. 66, pp. 3289-3307, Oct 2009.
[67] G. Turturici, *et al.*, "Hsp70 localizes differently from chaperone Hsc70 in mouse mesoangioblasts under physiological growth conditions," *Journal of Molecular Histology,* vol. 39, pp. 571-578, Dec 2008.
[68] A. S. Sreedhar, *et al.*, "Hsp90 isoforms: functions, expression and clinical importance," *Febs Letters,* vol. 562, pp. 11-15, Mar 2004.
[69] B. Hilscher and W. Hilscher, "KINETICS OF GAMETOGENESIS .2. COMPARATIVE AUTORADIOGRAPHIC STUDIES OF OOGONIA AND MULTIPLYING PROSPERMATOGONIA OF WISTAR RAT," *Cell and Tissue Research,* vol. 190, pp. 61-68, 1978.

[70] N. Vanmuylder, *et al.*, "Heat shock protein HSP86 expression during mouse embryo development, especially in the germ-line," *Anatomy and Embryology,* vol. 205, pp. 301-306, Jul 2002.
[71] G. van Osch, *et al.*, "Cartilage repair: past and future - lessons for regenerative medicine," *Journal of Cellular and Molecular Medicine,* vol. 13, pp. 792-810, May 2009.
[72] C. Vinatier, *et al.*, "Cartilage and bone tissue engineering using hydrogels," *Bio-Medical Materials and Engineering,* vol. 16, pp. S107-S113, 2006.
[73] I. L. Kim, *et al.*, "Hydrogel design for cartilage tissue engineering: A case study with hyaluronic acid," *Biomaterials,* vol. 32, pp. 8771-8782, Dec 2011.
[74] J. Raghunath, *et al.*, "Advancing cartilage tissue engineering: the application of stem cell technology," *Current Opinion in Biotechnology,* vol. 16, pp. 503-509, Oct 2005.
[75] R. E. Miller, *et al.*, "Effect of self-assembling peptide, chondrogenic factors, and bone marrow-derived stromal cells on osteochondral repair," *Osteoarthritis and Cartilage,* vol. 18, pp. 1608-1619, Dec 2010.
[76] C. Chung and J. A. Burdick, "Engineering cartilage tissue," *Advanced Drug Delivery Reviews,* vol. 60, pp. 243-262, Jan 2008.
[77] S. Wakitani, *et al.*, "MESENCHYMAL CELL-BASED REPAIR OF LARGE, FULL-THICKNESS DEFECTS OF ARTICULAR-CARTILAGE," *Journal of Bone and Joint Surgery-American Volume,* vol. 76A, pp. 579-592, Apr 1994.
[78] L. A. Solchaga, *et al.*, "Hyaluronan-based polymers in the treatment of osteochondral defects," *Journal of Orthopaedic Research,* vol. 18, pp. 773-780, Sep 2000.
[79] X. Z. Zhou, *et al.*, "Mesenchymal stem cell-based repair of articular cartilage with polyglycolic acid-hydroxyapatite biphasic scaffold," *International Journal of Artificial Organs,* vol. 31, pp. 480-489, Jun 2008.
[80] X. D. Guo, *et al.*, "Repair of full-thickness articular cartilage defects by cultured mesenchymal stem cells transfected with the transforming growth factor beta(1) gene," *Biomedical Materials,* vol. 1, pp. 206-215, Dec 2006.
[81] S. Wakitani, *et al.*, "Human autologous culture expanded bone marrow mesenchymal cell transplantation for repair of cartilage defects in osteoarthritic knees," *Osteoarthritis and Cartilage,* vol. 10, pp. 199-206, Mar 2002.
[82] S. Wakitani, *et al.*, "Autologous bone marrow stromal cell transplantation for repair of full-thickness articular cartilage defects in human patellae: Two case reports," *Cell Transplantation,* vol. 13, pp. 595-600, 2004.
[83] C. J. Centeno, *et al.*, "Increased Knee Cartilage Volume in Degenerative Joint Disease using Percutaneously Implanted, Autologous Mesenchymal Stem Cells," *Pain Physician,* vol. 11, pp. 343-353, May-Jun 2008.
[84] C. K. Abrahamsson, *et al.*, "Chondrogenesis and Mineralization During In Vitro Culture of Human Mesenchymal Stem Cells on Three-Dimensional Woven Scaffolds," *Tissue Engineering Part A,* vol. 16, pp. 3709-3718, Dec 2010.
[85] P. W. Kopesky, *et al.*, "Controlled Delivery of Transforming Growth Factor beta 1 by Self-Assembling Peptide Hydrogels Induces Chondrogenesis of Bone Marrow Stromal Cells and Modulates Smad2/3 Signaling," *Tissue Engineering Part A,* vol. 17, pp. 83-92, Jan 2011.
[86] H. A. Awad, *et al.*, "Chondrogenic differentiation of adipose-derived adult stem cells in agarose, alginate, and gelatin scaffolds," *Biomaterials,* vol. 25, pp. 3211-3222, Jul 2004.

[87] R. L. Mauck, *et al.*, "Regulation of cartilaginous ECM gene transcription by chondrocytes and MSCs in 3D culture in response to dynamic loading," *Biomechanics and Modeling in Mechanobiology,* vol. 6, pp. 113-125, Jan 2007.
[88] D. R. Wagner, *et al.*, "Hydrostatic pressure enhances chondrogenic differentiation of human bone marrow stromal cells in osteochondrogenic medium," *Annals of Biomedical Engineering,* vol. 36, pp. 813-820, May 2008.
[89] R. L. Mauck, *et al.*, "Chondrogenic differentiation and functional maturation of bovine mesenchymal stem cells in long-term agarose culture," *Osteoarthritis and Cartilage,* vol. 14, pp. 179-189, Feb 2006.
[90] Y. Arai, *et al.*, "Adenovirus vector-mediated gene transduction to chondrocytes: In vitro evaluation of therapeutic efficacy of transforming growth factor-beta 1 and heat shock protein 70 gene transduction," *Journal of Rheumatology,* vol. 24, pp. 1787-1795, Sep 1997.
[91] T. Kubo, *et al.*, "Expression of transduced HSP70 gene protects chondrocytes from stress," *Journal of Rheumatology,* vol. 28, pp. 330-335, Feb 2001.
[92] L. Grossin, *et al.*, "Gene transfer with HSP 70 in rat chondrocytes confers cytoprotection in vitro and during experimental osteoarthritis," *Faseb Journal,* vol. 20, pp. 65-75, Jan 2006.
[93] S. Etienne, *et al.*, "Local induction of heat shock protein 70 (Hsp70) by proteasome inhibition confers chondroprotection during surgically induced osteoarthritis in the rat knee," *Bio-Medical Materials and Engineering,* vol. 18, pp. 253-260, 2008.
[94] H. Tonomura, *et al.*, "Glutamine protects articular chondrocytes from heat stress and NO-induced apoptosis with HSP70 expression," *Osteoarthritis and Cartilage,* vol. 14, pp. 545-553, Jun 2006.
[95] L. Grossin, *et al.*, "Induction of heat shock protein 70 (Hsp70) by proteasome inhibitor MG 132 protects articular chondrocytes from cellular death in vitro and in vivo," *Biorheology,* vol. 41, pp. 521-534, 2004.
[96] R. Terauchi, *et al.*, "Hsp70 prevents nitric oxide-induced apoptosis in articular chondrocytes," *Arthritis and Rheumatism,* vol. 48, pp. 1562-1568, Jun 2003.
[97] T. Hojo, *et al.*, "Effect of heat stimulation on viability and proteoglycan metabolism of cultured chondrocytes: preliminary report," *Journal of orthopaedic science : official journal of the Japanese Orthopaedic Association,* vol. 8, pp. 396-9, 2003 2003.
[98] H. Tonomura, *et al.*, "Effects of heat stimulation via microwave applicator on cartilage matrix gene and HSP70 expression in the rabbit knee joint," *Journal of Orthopaedic Research,* vol. 26, pp. 34-41, Jan 2008.
[99] H. Yamaoka, *et al.*, "Cartilage tissue engineering chondrocytes embedded in using human auricular different hydrogel materials," *Journal of Biomedical Materials Research Part A,* vol. 78A, pp. 1-11, Jul 2006.
[100] J. D. Kisiday, *et al.*, "Effects of dynamic compressive loading on chondrocyte biosynthesis in self-assembling peptide scaffolds," *Journal of Biomechanics,* vol. 37, pp. 595-604, May 2004.
[101] P. W. Kopesky, *et al.*, "Self-Assembling Peptide Hydrogels Modulate In Vitro Chondrogenesis of Bovine Bone Marrow Stromal Cells," *Tissue Engineering Part A,* vol. 16, pp. 465-477, Feb 2010.
[102] R. Miller, Grodzinsky, A., Vanderploeg, E., Kopesky, P., and E. Florine, Barrett, M., Ferris, D., Kisiday, J., and Frisbie, D., "Self-assembling peptide heals rabbit defects in

vivo.," *In: Proceedings of the 2009 OARSI World Congress on Osteoarthritis,Montreal, Canada,September 10–13, 2009*.
[103] J. Chen, Shi,Z.D., Ji,X., Morales,J., Zhang,J., Kaur,N., Wang,S.. "Enhanced Osteogenesis of Human Mesenchymal Stem Cells by Periodic Heat Shock in Self-assembling Peptide Hydrogel.," *Tissue Eng Part A,* vol. 19, 2013.
[104] A. M. Mackay, *et al.*, "Chondrogenic differentiation of cultured human mesenchymal stem cells from marrow," *Tissue Engineering,* vol. 4, pp. 415-428, Win 1998.
[105] W. Q. Lin, *et al.*, "Patterns of hyaluronan staining are modified by fixation techniques," *Journal of Histochemistry & Cytochemistry,* vol. 45, pp. 1157-1163, Aug 1997.
[106] J. U. Yoo, *et al.*, "The chondrogenic potential of human bone-marrow-derived mesenchymal progenitor cells," *Journal of Bone and Joint Surgery-American Volume,* vol. 80A, pp. 1745-1757, Dec 1998.
[107] F. Barry, *et al.*, "Chondrogenic differentiation of mesenchymal stem cells from bone marrow: Differentiation-dependent gene expression of matrix components," *Experimental Cell Research,* vol. 268, pp. 189-200, Aug 2001.
[108] M. B. Mueller, *et al.*, "Hypertrophy in Mesenchymal Stem Cell Chondrogenesis: Effect of TGF-beta Isoforms and Chondrogenic Conditioning," *Cells Tissues Organs,* vol. 192, pp. 158-166, 2010.
[109] L. Quintana, *et al.*, "Morphogenetic and Regulatory Mechanisms During Developmental Chondrogenesis: New Paradigms for Cartilage Tissue Engineering," *Tissue Engineering Part B-Reviews,* vol. 15, pp. 29-41, Mar 2009.
[110] K. Pelttari, *et al.*, "Premature induction of hypertrophy during in vitro chondrogenesis of human mesenchymal stem cells correlates with calcification and vascular invasion after ectopic transplantation in SCID mice," *Arthritis and Rheumatism,* vol. 54, pp. 3254-3266, Oct 2006.
[111] F. Mwale, *et al.*, "Limitations of using aggrecan and type X collagen as markers of chondrogenesis in mesenchymal stem cell differentiation," *Journal of Orthopaedic Research,* vol. 24, pp. 1791-1798, Aug 2006.
[112] M. B. Mueller and R. S. Tuan, "Functional characterization of hypertrophy in chondrogenesis of human mesenchymal stem cells," *Arthritis and Rheumatism,* vol. 58, pp. 1377-1388, May 2008.
[113] A. F. Steinert, *et al.*, "Hypertrophy is induced during the in vitro chondrogenic differentiation of human mesenchymal stem cells by bone morphogenetic protein-2 and bone morphogenetic protein-4 gene transfer," *Arthritis Research & Therapy,* vol. 11, 2009.
[114] L. R. Duarte, "THE STIMULATION OF BONE-GROWTH BY ULTRASOUND," *Archives of Orthopaedic and Trauma Surgery,* vol. 101, pp. 153-159, 1983.
[115] S. J. Wang, *et al.*, "LOW-INTENSITY ULTRASOUND TREATMENT INCREASES STRENGTH IN A RAT FEMORAL FRACTURE MODEL," *Journal of Orthopaedic Research,* vol. 12, pp. 40-47, Jan 1994.
[116] A. A. Pilla, *et al.*, "Non-invasive low-intensity pulsed ultrasound accelerates bone healing in the rabbit," *Journal of orthopaedic trauma,* vol. 4, pp. 246-53, 1990 1990.
[117] J. D. Heckman, *et al.*, "ACCELERATION OF TIBIAL FRACTURE-HEALING BY NONINVASIVE, LOW-INTENSITY PULSED ULTRASOUND," *Journal of Bone and Joint Surgery-American Volume,* vol. 76A, pp. 26-34, Jan 1994.

[118] S. D. Cook, *et al.*, "Acceleration of tibia and distal radius fracture healing in patients who smoke," *Clinical Orthopaedics and Related Research,* pp. 198-207, Apr 1997.
[119] K. S. Leung, *et al.*, "Complex tibial fracture outcomes following treatment with low-intensity pulsed ultrasound," *Ultrasound in Medicine and Biology,* vol. 30, pp. 389-395, Mar 2004.
[120] W. Klug, *et al.*, "SCINTIGRAPHIC CONTROL OF BONE-FRACTURE HEALING UNDER ULTRASONIC STIMULATION - AN ANIMAL EXPERIMENTAL-STUDY," *European Journal of Nuclear Medicine,* vol. 11, pp. 494-497, 1986.
[121] T. K. Kristiansen, *et al.*, "Accelerated healing of distal radial fractures with the use of specific, low-intensity ultrasound - A multicenter, prospective, randomized, double-blind, placebo-controlled study," *Journal of Bone and Joint Surgery-American Volume,* vol. 79A, pp. 961-973, Jul 1997.
[122] S. Takikawa, *et al.*, "Low-intensity pulsed ultrasound initiates bone healing in rat nonunion fracture model," *Journal of Ultrasound in Medicine,* vol. 20, pp. 197-205, Mar 2001.
[123] N. M. Pounder and A. J. Harrison, "Low intensity pulsed ultrasound for fracture healing: A review of the clinical evidence and the associated biological mechanism of action," *Ultrasonics,* vol. 48, pp. 330-338, Aug 2008.
[124] S. D. Cook, *et al.*, "Improved cartilage repair after treatment with low-intensity pulsed ultrasound," *Clinical Orthopaedics and Related Research,* pp. S231-S243, Oct 2001.
[125] K. Naito, *et al.*, "Low-Intensity Pulsed Ultrasound (LIPUS) Increases the Articular Cartilage Type II Collagen in a Rat Osteoarthritis Model," *Journal of Orthopaedic Research,* vol. 28, pp. 361-369, Mar 2010.
[126] M. H. Huang, *et al.*, "Effects of sonication on articular cartilage in experimental osteoarthritis," *Journal of Rheumatology,* vol. 24, pp. 1978-1984, Oct 1997.
[127] M. H. Huang, *et al.*, "Ultrasound effect on level of stress proteins and arthritic histology in experimental arthritis," *Archives of Physical Medicine and Rehabilitation,* vol. 80, pp. 551-556, May 1999.
[128] C. M. Korstjens, *et al.*, "Low-intensity pulsed ultrasound affects human articular chondrocytes in vitro," *Medical & Biological Engineering & Computing,* vol. 46, pp. 1263-1270, Dec 2008.
[129] K. Naruse, *et al.*, "Distinct anabolic response of osteoblast to low-intensity pulsed ultrasound," *Journal of Bone and Mineral Research,* vol. 18, pp. 360-369, Feb 2003.
[130] S. M. Z. Uddin, *et al.*, "Low-Intensity Amplitude Modulated Ultrasound Increases Osteoblastic Mineralization," *Cellular and Molecular Bioengineering,* vol. 4, pp. 81-90, Mar 2011.
[131] K. Naruse, *et al.*, "Anabolic response of mouse bone-marrow-derived stromal cell clone ST2 cells to low-intensity pulsed ultrasound," *Biochemical and Biophysical Research Communications,* vol. 268, pp. 216-220, Feb 2000.
[132] K. Sena, *et al.*, "Low-intensity pulsed ultrasound (LIPUS) and cell-to-cell communication in bone marrow stromal cells," *Ultrasonics,* vol. 51, pp. 639-644, Jul 2011.
[133] H. J. Lee, *et al.*, "Low-intensity ultrasound inhibits apoptosis and enhances viability of human mesenchymal stem cells in three-dimensional alginate culture during chondrogenic differentiation," *Tissue Engineering,* vol. 13, pp. 1049-1057, May 2007.

[134] H. J. Lee, *et al.*, "Low-intensity ultrasound stimulation enhances chondrogenic differentiation in alginate culture of mesenchymal stem cells," *Artificial Organs,* vol. 30, pp. 707-715, Sep 2006.
[135] D. Schumann, *et al.*, "Treatment of human mesenchymal stem cells with pulsed low intensity ultrasound enhances the chondrogenic phenotype in vitro," *Biorheology,* vol. 43, pp. 431-443, 2006.
[136] S. R. Angle, *et al.*, "Osteogenic differentiation of rat bone marrow stromal cells by various intensities of low-intensity pulsed ultrasound," *Ultrasonics,* vol. 51, pp. 281-288, Apr 2011.
[137] A. Suzuki, *et al.*, "Daily low-intensity pulsed ultrasound-mediated osteogenic differentiation in rat osteoblasts," *Acta Biochimica Et Biophysica Sinica,* vol. 41, pp. 108-115, Feb 2009.
[138] M. Kopakkala-Tani, *et al.*, "Ultrasound stimulates proteoglycan synthesis in bovine primary chondrocytes," *Biorheology,* vol. 43, pp. 271-282, 2006.
[139] D. Dalecki, "Mechanical bioeffects of ultrasound," *Annual Review of Biomedical Engineering,* vol. 6, pp. 229-248, 2004.
[140] B. H. Min, *et al.*, "Low intensity ultrasound as a supporter of cartilage regeneration and its engineering," *Biotechnology and Bioprocess Engineering,* vol. 12, pp. 22-31, Jan-Feb 2007.
[141] J. H. Cui, *et al.*, "Effects of low-intensity ultrasound on chondrogenic differentiation of mesenchymal stem cells embedded in polyglycolic acid: An in vivo study," *Tissue Engineering,* vol. 12, pp. 75-82, Jan 2006.
[142] H. Park, *et al.*, "Indirect low-intensity ultrasonic stimulation for tissue engineering," *Journal of tissue engineering,* vol. 2010, p. 973530, 2010 2010.
[143] M. A. Buldakov, *et al.*, "Influence of changing pulse repetition frequency on chemical and biological effects induced by low-intensity ultrasound in vitro," *Ultrasonics Sonochemistry,* vol. 16, pp. 392-397, Mar 2009.
[144] S. Marvel, *et al.*, "The Development and Validation of a LIPUS System With Preliminary Observations of Ultrasonic Effects on Human Adult Stem Cells," *Ieee Transactions on Ultrasonics Ferroelectrics and Frequency Control,* vol. 57, pp. 1977-1984, Sep 2010.
[145] T. Iwashina, *et al.*, "Low-intensity pulsed ultrasound stimulates cell proliferation and proteoglycan production in rabbit intervertebral disc cells cultured in alginate," *Biomaterials,* vol. 27, pp. 354-361, Jan 2006.
[146] J. G. R. Li, *et al.*, "Optimum intensities of ultrasound for PGE(2) secretion and growth of osteoblasts," *Ultrasound in Medicine and Biology,* vol. 28, pp. 683-690, May 2002.
[147] M. Saito, *et al.*, "Intensity-related differences in collagen post-translational modification in MCM-E1 osteoblasts after exposure to low- and high-intensity pulsed ultrasound," *Bone,* vol. 35, pp. 644-655, Sep 2004.
[148] K. Ebisawa, *et al.*, "Ultrasound enhances transforming growth factor beta-mediated chondrocyte differentiation of human mesenchymal stem cells," *Tissue Engineering,* vol. 10, pp. 921-929, May 2004.
[149] P. A. Nolte, *et al.*, "Low-intensity pulsed ultrasound in the treatment of nonunions," *Journal of Trauma-Injury Infection and Critical Care,* vol. 51, pp. 693-702, Oct 2001.
[150] P. A. Nolte, *et al.*, "Low-intensity ultrasound stimulates endochondral ossification in vitro," *Journal of Orthopaedic Research,* vol. 19, pp. 301-307, Mar 2001.

[151] H. Fujioka, *et al.*, "Ultrasound treatment of nonunion of the hook of the hamate in sports activities," *Knee Surgery Sports Traumatology Arthroscopy*, vol. 12, pp. 162-164, Mar 2004.
[152] E.A.Ginzel and R.K.Ginzel, "ULTRASONIC PROPERTIES OF A NEW LOW ATTENUATION DRY COUPLANT ELASTOMER," April, 1994.